EARLY TRIASSIC ECHINOIDS OF THE WESTERN UNITED STATES: THEIR IMPLICATIONS FOR PALEOECOLOGY AND THE HABITABLE ZONE HYPOTHESIS FOLLOWING THE PERMO-TRIASSIC MASS EXTINCTION

by
Jenna J. Rolle

A Thesis Submitted in
Partial Fulfillment of the
Requirements for the Degree of

Masters of Science
in Geosciences

at
The University of Wisconsin-Milwaukee
August 2014

ABSTRACT

EARLY TRIASSIC ECHINOIDS OF THE WESTERN UNITED STATES:
THEIR IMPLICATIONS FOR PALEOECOLOGY
AND THE HABITABLE ZONE HYPOTHESIS FOLLOWING THE
PERMO-TRIASSIC MASS EXTINCTION

by
Jenna J. Rolle

The University of Wisconsin-Milwaukee, 2014
Under the Supervision of Margaret L. Fraiser, PhD

Confronted with global climate change and ocean acidification, our collective knowledge of ecosystem response during times of environmental crisis in Earth's ancient past may provide insights towards combating ecological degradation in modern oceans. Early Triassic marine environments were characterized by oceanic warming due in part to elevated levels of atmospheric CO_2 and periodic intervals of localized anoxia, resulting in an overall restructuring of faunal dominance, distribution, and biodiversity. Re-assembly of ecological communities during the Early Triassic are largely unknown; however, a previous paleoecological study by Tyler Beatty *et al.* (2008), suggests that post-extinction recovery length was minimized in shallow marine habitable zones. To further expand upon the investigations of Beatty *et al.*, I used Early Triassic echinoids as a case study for understanding paleoecology on the eastern margin of Panthalassa. I hypothesized that amidst the deleterious environmental conditions of the Early Triassic, echinoids thrived within the habitable zone as an abundant member of the Modern Fauna.

Early Triassic echinoids of the western United States appear exclusively within shallow marine shelves, all of which contain evidence of frequent storm

activity. Echinoids co-occur with bivalves, brachiopods, gastropods, and other echinoderms, indicating that these habitats were well oxygenated enough to support paleocommunities of considerable diversity. The oceans of the Early Triassic provide only an approximate analogue for modern oceans; however, analysis of Early Triassic ecosystems via quantification of echinoid abundance and paleoecology may help reveal important patterns necessary in understanding the rapidly shifting ecosystems of our modern, warming oceans.

TABLE OF CONTENTS

LIST OF FIGURES

LIST OF TABLES

ACKNOWLEDGEMENTS

Foremost, I am deeply grateful to my advisor, Dr. Margaret Fraiser, without her steadfast encouragement, superlative wisdom, and diligent effort, the actuality of this thesis would not have been possible. I would like to thank my committee members, Dr. Stephen Dornbos and Dr. Mark Harris, whose expertise, guidance, and dedication to students' success have broadened my academic capacities.

To my field assistant, Erin Wagner, thank you for your tireless physical and mental exertions in the field and for your patience and companionship throughout our extensive, often frenzied, travels.

The Wisconsin Geological Society and Department of Geosciences at UW-Milwaukee provided funding for this project, for which I am truly appreciative. Moreover, my attendance at the World Summit on P-Tr Mass Extinction in Wuhan, China would not have been possible without the finances donated by my extraordinary friends and family.

I owe particular gratitude to my parents, to whom I am eternally indebted for their enduring patience, compassion, and support. To my fiancé, who vanquishes discouragement with incomparable grace and empathy and relishes any opportunity to instruct me in the utilities of Adobe products. Finally, to my office mates and friends who provide inspiration, excite creativity, and indulge my curiosity for the natural world, I share my accomplishments with all of you, as they are truly a reflection of our solidarity.

1. Introduction

The Permo-Triassic mass extinction (PTME) was the largest biotic crisis of the Phanerozoic (Fig. 1) (Raup, 1979; Raup and Sepkoski, 1982; Erwin, 1994; Erwin, 1996; Erwin, 2000; Bambach *et al.*, 2004), eliminating at least 78% of marine genera (Raup, 1979; Alroy *et al.*, 2008). Although it is debated whether the crisis represents one event or two successive events (Clapham *et al.*, 2009; Song *et al.*, 2013), numerous factors associated with rapid climate change led to a devastating deterioration of global ecosystems (Erwin, 1994; Erwin, 1996; Wignall and Twitchett, 2002; Bottjer *et al.*, 2008; Clapham *et al.*, 2009). The extinction and post-extinction intervals were characterized by increased atmospheric CO_2 levels and elevated global temperatures (Joachimski *et al.*, 2012; Sun *et al.*, 2012; Song *et al.*, 2012a), fluctuations of the oxygen minimum zone (Algeo *et al.*, 2010; Brennecka *et al.*, 2011), as well as surface ocean acidification (Knoll *et al.*, 1996; Kidder and Worsley, 2004; Wignall *et al.*, 2009). Multiple lines of direct and indirect evidence, including ichnofossil (Zonneveld *et al.*, 2010) and isotopic data (Grice *et al.*, 2005; Song *et al.*, 2012a), suggest that deep-water anoxia and euxinic shallow waters facilitated a delay in post-extinction faunal recovery and prevented marine recovery (Knoll *et al.*, 2007; Beatty *et al.*, 2008). In all, these hypoxic marine conditions persisted for the entirety of the Griesbachian (252.6 – 251.2 MY) around most of the world (Kidder and Worsley, 2004) and continued in pulses throughout the Smithian (251.2 – 250.6 MY) and Spathian (250.6 – 247.2 MY) (Lehrmann *et al.*, 2006).

The Permo-Triassic mass extinction and its aftermath were marked by a drastic ecological shift in which the Modern Fauna replaced the Paleozoic Fauna (Raup and Sepkoski, 1982). The Paleozoic Fauna refers to organisms such as brachiopods and

crinoids who dominated the marine realm in abundance prior to the PTME (Sepkoski *et al.*, 1981; Raup and Sepkoski, 1982; Clapham *et al.*, 2006; Stanley, 2007; Fraiser and Bottjer, 2007b); however, post-extinction fossil assemblages indicate a rapid replacement of the Paleozoic Fauna by bivalves, gastropods, and echinoids, organisms referred to as the Modern Fauna (Fig. 2) (Sepkoski *et al.*, 1981; Raup and Sepkoski, 1982; Clapham *et al.*, 2006; Stanley, 2007; Fraiser and Bottjer, 2007b). Further, the shift in environmental conditions following the Permo-Triassic mass extinction created settings more amenable to microbial reef proliferation as opposed to metazoan reefs composed of hard corals and skeletonized sponges (Fagerstrom, 1987; Hallam and Wignall, 1997; Pruss and Bottjer, 2004; Pruss and Bottjer, 2005). Due to the disappearance of metazoan reefs and subsequent replacement by microbial reefs following the PTME, the Early Triassic has been termed a "reef gap" (Fagerstrom, 1987; Hallam and Wignall, 1997; Pruss and Bottjer, 2004; Pruss and Bottjer, 2005). The prolonged aftermath was characterized by a complete restructuring of many components of the marine ecosystem, including; loss of ecologically critical taxa (Droser *et al.*, 2000) and a simplified palaeoecology reminiscent of earlier eras of geological time (Bottjer *et al.*, 1996; Bambach *et al.,* 2004; Wagner *et al.,* 2007). Low taxonomic diversity, inactive utilization of ecospace, taxa adapted to reduced levels of oxygen, diminished body size, and the re-appearance of microbial hardened substrates make marine conditions of the Early Triassic comparable to those of the Late Cambrian (Bottjer *et al.*, 1996; Fraiser and Bottjer, 2005a). The presence of microbial mats, stromatolites, and thrombolites during the Early Triassic reef gap suggests overall decreases in bioturbation and low abundance of mat grazing organisms (Flügel, 2002; Pruss and Bottjer, 2004; Sheehan and Harris, 2004; Mata and Bottjer, 2009).

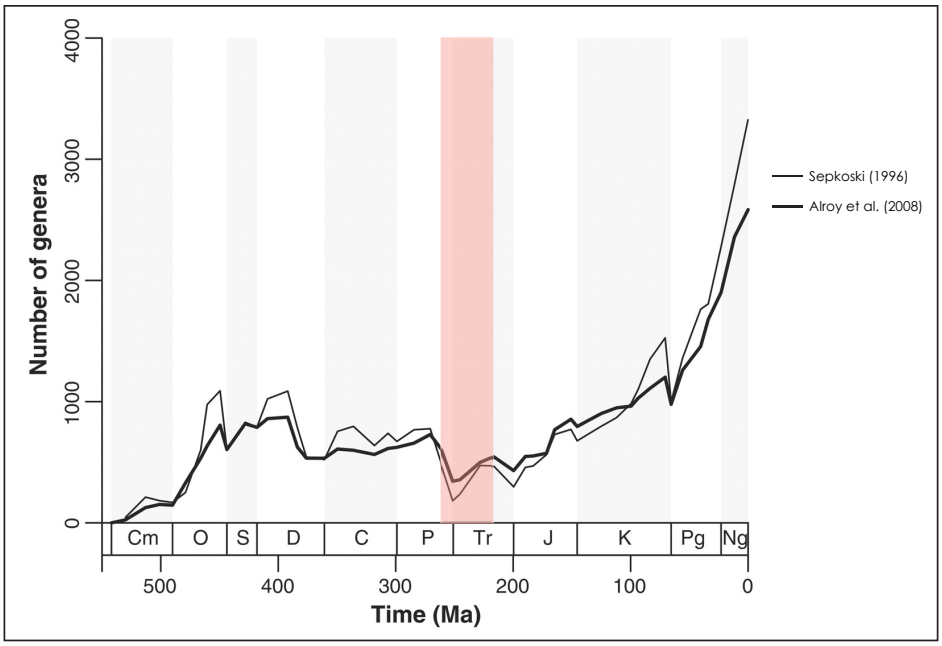

Figure 1 Genus-level diversity curves of both Sepkoski (1996) and Alroy *et al.* (2008). The red, shaded area highlights the rapid loss of genera at the Permo-Triassic boundary, as well as the prolonged recovery following the extinction event(s). Modified from Alroy *et al.* (2008).

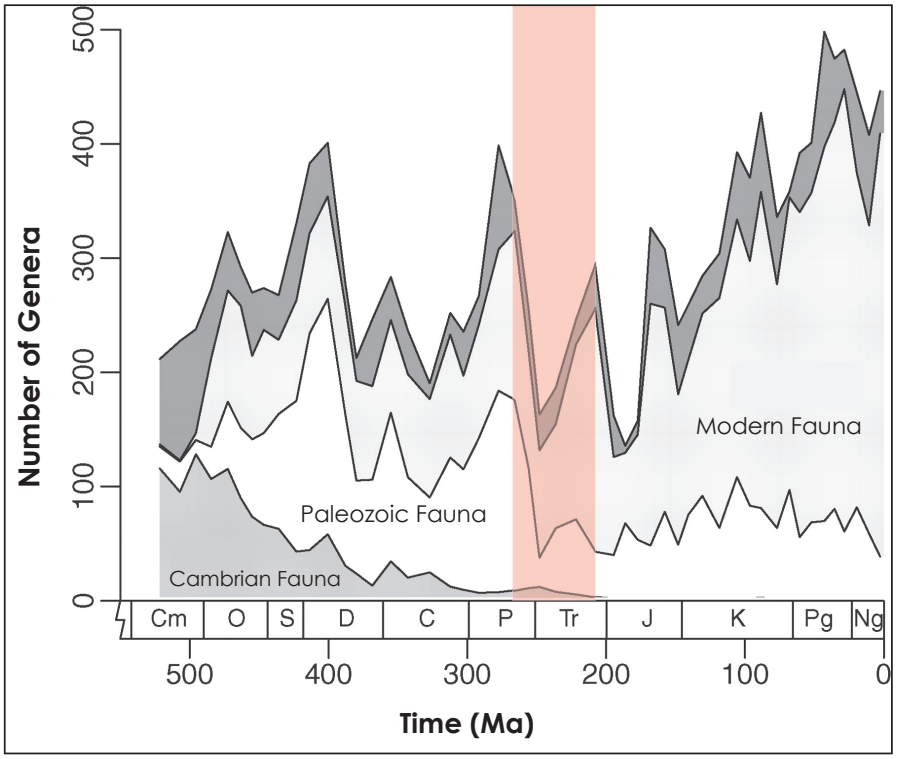

Figure 2 Normalized diversity curve displaying the trends of the three marine evolutionary faunas. The unlabeled area of the curve represents genera not assigned to any particular fauna. The red, shaded area highlights the rapid shift from the Paleozoic Fauna to the Modern Fauna following the PTME. Modified from Alroy *et al.* (2010).

Even with the ever-increasing and interrelating investigation and modeling of Early Triassic ecosystems, livable environments and recovery patterns following the Permo-Triassic mass extinction remain largely unknown. Estimates of the delay in biotic recovery following the mass extinction range from 500 Ka to 6 Ma (Hallam, 1991; Erwin, 1994; Erwin, 1996; Fraiser and Bottjer, 2005b; Fraiser and Bottjer, 2007b; Fraiser and Bottjer, 2009a; Lehrmann *et al.*, 2006; Bottjer *et al.*, 2008; Chen and Benton, 2012; Hofmann *et al.*, 2013a).

Though multiple lines of empirical evidence indicate that environmental stresses such as anoxia, euxinia, and hypercapnia suppressed post-extinction recovery globally, the severity and duration of such stresses were undoubtedly variable throughout the globe. For example, the frequency of fluctuations in oxygen levels for any given location may have occurred on the magnitude of decades to millennia, or as daily pulsations and isolated upwelling of anoxic or dysoxic waters (Tyson and Pearson, 1991; Wallace and Wirick, 1992; Beatty *et al.*, 2008). Hofmann *et al.* (2013) suggest that low diversity of benthic organisms and the dominance of disaster taxa during the Early Triassic reflects the intensity of the PTME rather than the persistence of environmental stresses. Even though environmental stresses during the Early Triassic were neither uniformly distributed nor uniformly persistent, suggesting that the low diversity and diminished complexity characterized by Early Triassic paleocommunities reflects the consequences of the intensity of the Permo-Triassic extinction event solely (e.g. Hofmann *et al.*, 2013a) rather than a combined interplay of environmental and ecological factors seems overly simplistic given the multitude of factors known to affect modern ecosystems.

Given that paleoenvironments were neither uniformly affected in magnitude nor duration by any known environmental pressure, it follows that recovery and restructuring patterns for Early Triassic fauna varied spatially and temporally (Pruss *et al.*, 2006; Algeo *et al.*, 2011; Clapham *et al.*, 2013). Although, globally, the Early Triassic was characterized by delayed recovery, faunal recovery varied regionally based upon fluctuations in O_2 and CO_2 levels, sedimentation rates, as well as the composition and distribution of various macrofauna (Clapham *et al.*, 2013; Algeo *et al.*, 2011; Pruss *et al.*, 2006). Moreover, extinction pressures and recovery patterns were experienced differently between benthic and pelagic zones. Organisms living within the pelagic realm were likely less vulnerable to deep-water anoxia and euxinia, as well as periodic upwelling of such volatile waters, as compared to benthic organisms (Tyson and Pearson, 1991; Wallace and Wirick, 1992; Grice *et al.*, 2005; Kump *et al.*, 2005; Beatty *et al.*, 2008; Brayard *et al.*, 2009; Grasby and Beauchamp, 2009; Song *et al.*, 2012b). Therefore, delayed recovery would be expected for benthic, shelf-dwelling, paleocommunities as long as local, anoxic conditions persisted.

Remarkably, ichnofossil assemblages from the northwestern margin of Pangaea suggest that, despite enduring ecological stresses, post-extinction recovery length may have been minimized in well-oxygenated, shallow marine habitable zones (Fig. 3)(Beatty *et al.*, 2008). The habitable zone as described by Beatty *et al.* (2008) is a nearshore, benthic region typically situated on a broad, shallow continental shelf (Fig. 3). Often, these zones are found in large embayments distanced from deep, anoxic or dysoxic water, thus providing a refuge for benthic organisms where environmental extinction pressures diminished. Beatty *et al.* (2008) propose that these spatially

isolated environments were capable of retaining sufficient life-sustaining levels of wave-generated oxygen that was likely provided by frequent storm activity and are primarily located within lower shoreface facies and offshore transition zones (Fig. 3). Wallace and Wrick (1992) observed that breaking waves in 38 meters of water maintain the potential of generating oxygen-supersaturated conditions up to depths of at least 19 meters and that the oxygen-rich conditions created by large breaking-wave events could remain for weeks. If similar rules apply, oxygen saturation within the habitable zone would have reached its greatest depth and degree after a storm event, even with reduced concentration and diffusion of atmospheric oxygen (Beatty *et al.*, 2008).

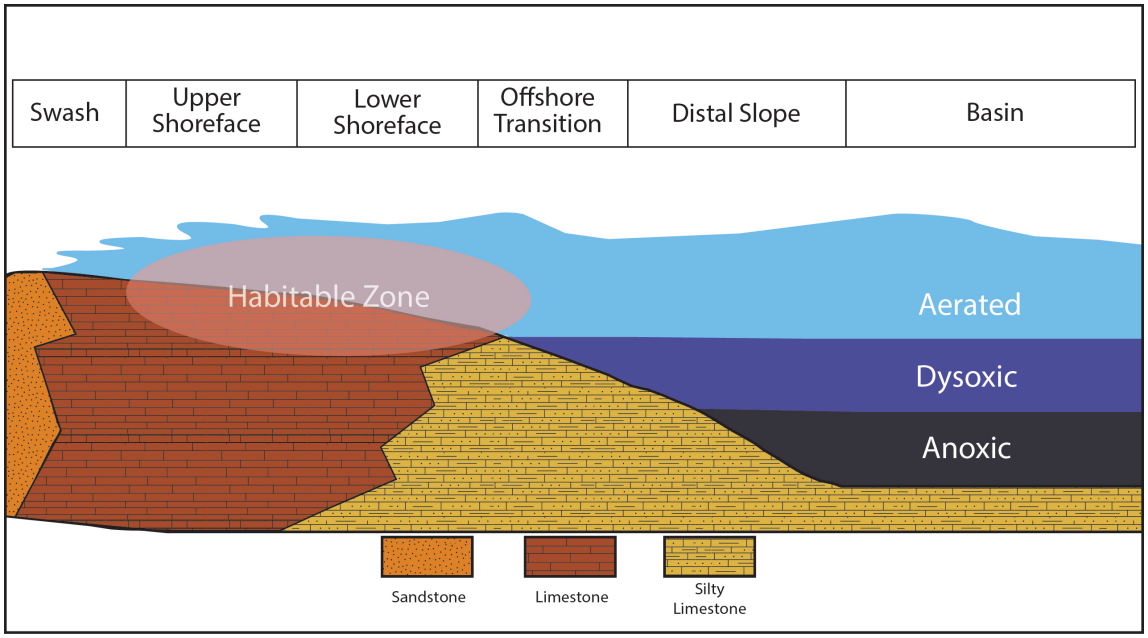

Figure 3 Schematic cross section of a typical shoreline from northwest Pangea. The habitable zone is depicted with respect to shoreface position and species diversity. Lithologies are based upon those observed in the Lower Triassic strata of the western United States. Based on Beatty *et al.*, 2008.

1.1 Previous Work

As reported by Durham *et al.* (1966), *Miocidaris*, a genus of regular echinoid belonging to the family *Miocidaride*, was not only one of the few taxa to survive the PTME event, but the only genus of regular echinoid reported to persist from the Paleozoic into later geological time (Fig. 4) (Durham *et al.*, 1966). *Miocidaris* appears to be globally dispersed throughout the entirety of the Triassic and persisted into the Lower Jurassic of France (de Brun *et al.*, 1919). This particular, persisting genus evolved and diversified as slow moving, low-level epifaunal grazers who were facultative omnivores, feeding upon detritus and algae (Döderlein, 1887; Smith and Hollingworth, 1990). Morphologically distinct, the body composition of *Miocidaris* was comprised of two columns of interambulacral plates interlocked between each of five columns of ambulacral plates (Fig. 5) (Durham *et al.*, 1966). This highly organized body plan displays stark divergence from the contrasting and highly variable interamubulacral plate patterns of Paleozoic echinoids (Durham *et al.*, 1966; McKinney, 1988; Erwin, 2000).

Lenticidaris, a genus of regular echinoid also belonging to the family *Miocidaridae*, has been documented in the Lower Triassic Virgin Limestone Member of Utah during the Spathian of the Early Triassic, and appears, at least temporally, later than *Miocidaris* (Kier, 1968). Apart from chronological dissimilarity, *Lenticidaris* differs from *Miocidaris* only in that *Lenticidaris*'s apical surface may have been more flexible than its predecessors', and its spines lack the cortex layer present within *Miocidaris* spines (Kier, 1968).

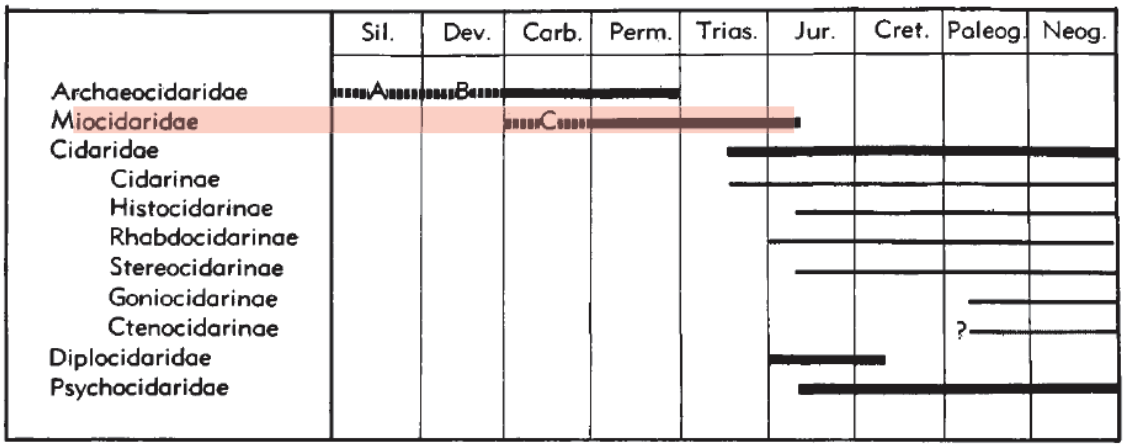

Figure 4 Stratigraphic distribution of cidaroid family and subfamily assemblages. The red, shaded area highlights the family, *Miocidaridae*, to which the genus *Miocidaris* belonged. The genetic stock from which the family *Cidaridae* arose was like supplied by *Miocidaridae* as opposed to that of the family *Lenticidaridae*, thus *Lenticidaridae's* exclusion from the figure. Modified from Fell, (1966).

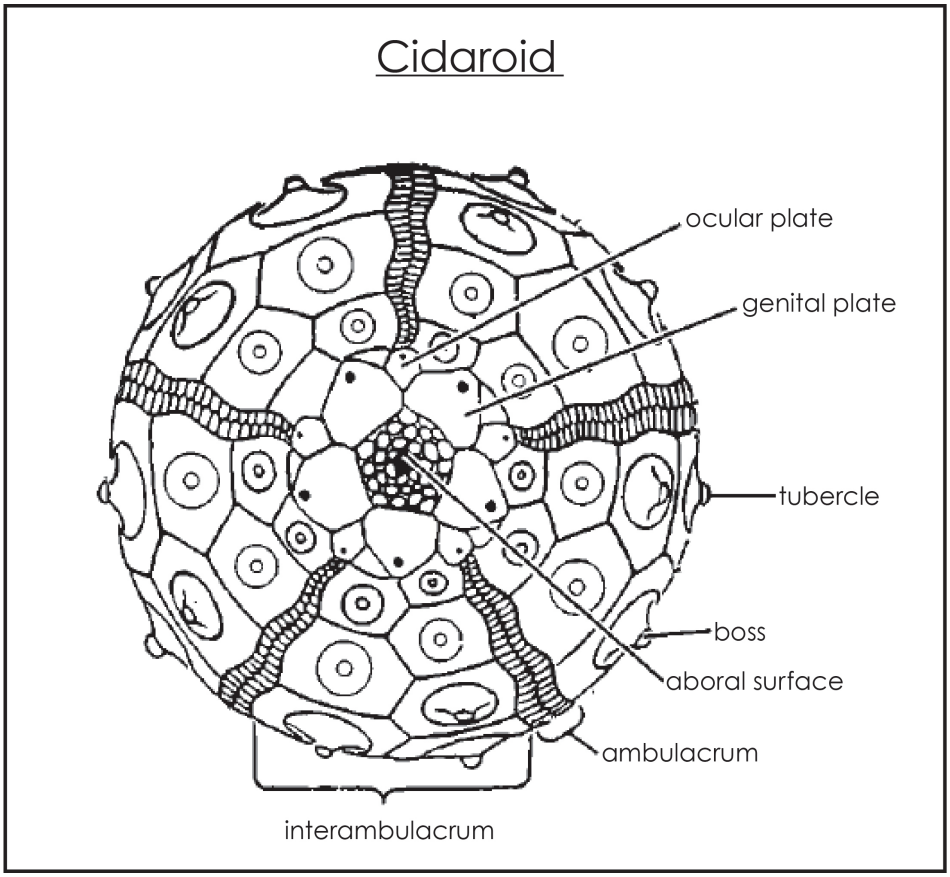

Figure 5 Morphological features of cidaroid echinoids. Modified from Fell, (1966).

As an added detriment to paleontologists attempting to analyze an incomplete fossil record, the imbricated tests of echinoids disarticulate rapidly upon death (Smith and Hollingworth, 1990). The disarticulation of echinoids post-mortem owes, in part, to the shallow, wave-dominated environments in which they have evolved and diversified where preservation is disfavored by active erosion (Smith, 1984; Barnes, 1989; Moffat and Bottjer, 1999). Moreover, the preservation potential for regular echinoids varies greatly dependent upon plate test rigidity and the degree to which test plates are locked together by connective tissue (Smith, 1984; Moffat and Bottjer, 1999). Ambulacral plates are rarely preserved in the fossil record and as a result, the morphological features necessary for examining disparities in echinoid taxonomy are extremely limited. Echinoid spines provide limited morphological information and, thus, have restricted taxonomic utility. In Kier's (1965) assessment of early echinoids, he states that any improvement in the method of food gathering, locomotion, and, perhaps, respiration would be reflected in a structural change of ambulacra, corresponding to a change in the usage of tubefeet. Unfortunately, those studying Early Triassic echinoid paleoecology are forced to make inferences based almost entirely upon spine debris (e.g. Moffat and Bottjer, 1999; Twitchett and Oji, 2005; Mata and Woods, 2008). However, despite their lack of information regarding evolutionary trends, echinoid spines can provide useful information in regards to depositional setting, post-mortem transportation, and regional population abundance.

Previous studies of Early Triassic benthic marine invertebrate survivors have revealed that faunal assemblages belonging to shallow shelf environments generally contain communities with low diversity; opportunistic and disaster taxa and

organisms adapted to oxygen-depleted waters, like *Claraia* and *Lingula* (Rodland and Bottjer, 2001) in high abundance (Fraiser and Bottjer, 2007a). Further, many Early Triassic assemblages deposited after the initial pulse of extinction contain short-lived Permian survivors such as rhynchonelliform brachiopods that, in comparison to the bivalve *Claraia*, have poor regulation of metabolic oxygen consumption (Clapham *et al.*, 2013). The temporal and spatial distribution of organisms without specialized low-oxygen adaptations such as rhychonelliform brachiopods, gastropods, and echinoids provide insights into the variability of anoxic conditions, ocean acidification, and warming throughout the Early Triassic and how those deleterious factors influenced regional recovery. Additionally, some organisms, including echinoids, of the Early Triassic display a distinct reduction in overall body size in comparison to their Paleozoic ancestors and Modern descendants (Schubert and Bottjer, 1995; Rodland and Bottjer, 2001; Fraiser and Bottjer, 2004; Fraiser and Bottjer, 2005b; Payne *et al.*, 2006), termed the Lilliput Effect (Urbanek, 1993; Harries and Knorr, 2009). Documentation of the Lilliput Effect is widespread during the immediate PTME aftermath (Newell, 1952; Schubert and Bottjer, 1995; Twitchett, 2007) and likely reflects the effects of marine anoxia, nutrient limitations, and acidification on organismal metabolism and ecology (Twitchett, 2007).Accordingly, the decreased body size of echinoids and associated biota during the Early Triassic further indicates that environmental limitations such as oxygen and nutrient availability affected not only survivorship, but also species' specific biology, behavior, and paleoecological role (Twitchett, 2007).

Rodland and Bottjer (2001) and Boyer *et al.* (2004) positively identified

echinoid spines in the Dinwoody Formation of southwestern Montana and western Wyoming. An echinoid spine bed from the Spathian Virgin Limestone Member of Nevada was described by Moffat and Bottjer (1999) indicating echinoid proliferation into the Smithian and Spathian. The echinoid spine beds at this locality, Lost Cabin Springs, were deposited in a distal carbonate shelf setting where echinoid spines are the only macroscopic features present (Moffat *et al.*, 1999). Additionally, as described by Mata and Woods (2008), echinoid debris dominates the fossil composition of the Lower Member of the Union Wash Formation in southeastern California. The Union Wash Formation was deposited as a transgressive-regressive sequence on a mixed carbonate-siliciclastic shelf located along the western edge of Pangaea during the Smithian and Spathian of the Early Triassic (Mata *et al.*, 2008), correlating with the strata of the Moenkopi Formation and Virgin Limestone Member. The regular echinoid, *Miocidaris*, was distributed globally throughout the Early Triassic and has been documented in the Early Triassic strata of North America, Asia, and Europe (Paleobiology Database (PBDB), 7/1/2013).

1.2 Scientific Significance

Paleoecological studies of the PTME and Early Triassic are fundamental not only to our understanding of recovery and restructuring following Earth's largest mass extinction, but also our collective knowledge of ecosystem response during times of environmental crisis, past and present. Confronted with global climate change and ocean acidification (Hughes, 2000; Doney *et al.*, 2009), gaining insights into the mechanisms used by ancient, marine organisms faced with environmental

collapse and ecological restructuring is essential to our understanding of present-day and future ecological degradation. Even though the oceans of the Early Triassic provide only an approximate analogue for modern oceans, analysis of Early Triassic paleoecology may reveal important, reoccurring, evolutionary patterns related to rapidly shifting environments and ecosystem response. The aims of this paleoecological study are: 1) to test the environmentally controlled model of a shallow-marine habitable zone as described by Beatty *et al.* (2008); and 2) to use echinoids as a case study for Early Triassic benthic paleoecology on the eastern margin of Panthalassa. This research is one of the first studies to apply and test the habitable zone hypothesis (Beatty *et al.*, 2008) not only within paleoenvironments that contain macrofossils, as opposed to ichnofossils solely, but also within paleoenvironments outside arctic paleolatitudes (e.g. Schaefer, 2012).

The habitable zone hypothesis (Beatty *et al.*, 2008), as of yet, applies only regionally and has not undergone rigorous testing. Given that the data presented in this study are constrained to the eastern margin of Panthalassa, testing the habitable zone hypothesis provides the benefit of a localized constraint. Moreover, the localized test parameters of the habitable zone hypothesis have the potential to reveal local, paleoecological mechanisms that may have been masked by the generalized test parameters of globally averaged data sets.

I hypothesize that habitable zones were present within the Early Triassic shallow-marine shelves of the western United States. The working hypothesis is that these habitable zones provided sufficiently oxygenated refuges from the post-extinction pressures of dysoxia and anoxia to allow establishment of a relatively

diverse benthic community; the highest diversity and abundance of benthic marine organisms should be located within habitable zone environments as characterized by Beatty *et al.* (2008). Furthermore, given the apparent, yet limited, presence of echinoid spines and test material within Lower Triassic strata (Kier, 1968; Boyer *et al.*, 2004), I hypothesize that amidst the deleterious environmental conditions of the Early Triassic, regional echinoid populations thrived within the habitable zone, allowing them to transition from a diverse member of the Paleozoic Fauna into an abundant member of the Modern Fauna.

Evidence of echinoid survival has been documented in the Dinwoody, Thaynes, and Moenkopi Formations of the western U.S. (Kier, 1968; Moffat and Bottjer, 1999; Rodland and Bottjer, 2001; Boyer *et al.*, 2004; Fraiser and Bottjer, 2004; Mata and Woods, 2008; Fraiser and Bottjer, 2009); however, relatively little is known of echinoid paleoecology or echinoid diversity during the Early Triassic. Thus, the data collected from the Lower Triassic strata of the western U.S. will provide the foundation of regional echinoid paleoecology in the following ways: 1) Quantification of echinoid abundance relative to other members of the Early Triassic paleocommunity; and 2) Interpretations of environmental contexts based upon analysis of measured sections and how depositional environments relate to the habitable zone hypothesis. The enduring echinoids of the extinction aftermath are evolutionarily significant because it is from their genetic stock that all post-Paleozoic echinoids arose (Kier, 1968). Therefore, focused research within the Lower Triassic strata of the western United States may provide insight into the adaptations that permitted echinoid survival into later geological time in regional and, perhaps, global contexts (Durham *et al.*, 1966).

2. Geologic Setting and Methods

The aftermath of the Permo-Triassic mass extinction has been recorded in Greisbachian, Smithian, and Spathian age strata located within the present-day western United States (Figs. 6 & 7) (Newell and Kummel, 1942; Kummel, 1943; Kummel, 1954; Paull and Paull, 1983; Paull and Paull, 1994; Carr and Paull, 1983; Paull *et al.*, 1989; Rodland and Bottjer, 2001; Fraiser and Bottjer, 2007a). Strata in this region were deposited discontinuously during the Late Permian through the Middle Triassic along the eastern margin of the Panthalassa Ocean near 35°N paleolatitude (Fig. 8a) (Paull and Paull, 1983; Paull et al., 1989; Paull and Paull, 1994a; Fraiser and Bottjer, 2007a).

The Lower Triassic Dinwoody Formation of Wyoming and southern Montana unconformably overlies the Middle Permian Phosphoria and Park City Formations and records the northeastern-most extent of the widespread and rapid Griesbachian transgression onto the Wyoming shelf (Schock, 1981; Paull and Paull, 1983; Paull and Paull, 1986; Schubert and Bottjer, 1995; Rodland and Bottjer, 2001). The Dinwoody basin remained a sublet basin through the Early Triassic with an overall pattern of three transgressions and a final regression through to the Late Triassic (Fig. 9) (Paull and Paull, 1994a; Paull and Paull, 1994b; Boyer *et al.*, 2004). The earliest deposition of Griesbachian strata is dominated by laminated mudstone, with increasing levels of silt during regression, followed by an increase to limestone upsection (Schock, 1981; Paull and Paull, 1983; Paull and Paull, 1986; Schubert and Bottjer, 1995; Rodland and Bottjer, 2001; Boyer *et al.*, 2004). The Woodside Formation, which is synonymous with the Red Peak Formation, intertongues along the north and eastern regions of the

Dinwoody basin (Fig. 6) (Paull et al., 1989). The Woodside and Red Peak Formations contain high amounts of terrigenous silts and sandstones transported westward into the basin and, thus, have a distinct lithologies and red colorations (Kummel, 1954; Paull and Paull, 1983; Paull et al., 1989). The Dinwoody Formation reaches its maximum thickness in southeastern Idaho where it is conformably overlain by the Thaynes Formation (Boutwell, 1907; Kummel, 1954; Paulls *et al.* 1989). The contact between the Dinwoody and Thaynes Formations, identified by the appearance of an ammonoid-bearing, *Meekoceras*, limestone interval, defines the top of the Griesbachian and Dienerian and the base of the Smithian (Newell and Kummel, 1942; Kummel, 1943; Kummel, 1954; Paull and Paull, 1983; Paull *et al.*, 1989).

Deposition of the Thaynes Formation began in the second transgression during the Smithian and continued through the third, final transgression from the Spathian until the end of the Early Triassic (Paull *et al.*, 1989; Boyer *et al.*, 2004). The majority of the Thaynes Formation directly overlies the intertonguing Woodside and Red Formations and only in its northwestern extent does it overly the Dinwoody Formation directly (Fig. 6) (Paull *et al.*, 1989). The Thaynes has a larger proportion of limestone lithologies in comparison to the mud-rich Dinwoody Formation below (Paull *et al.*, 1989).

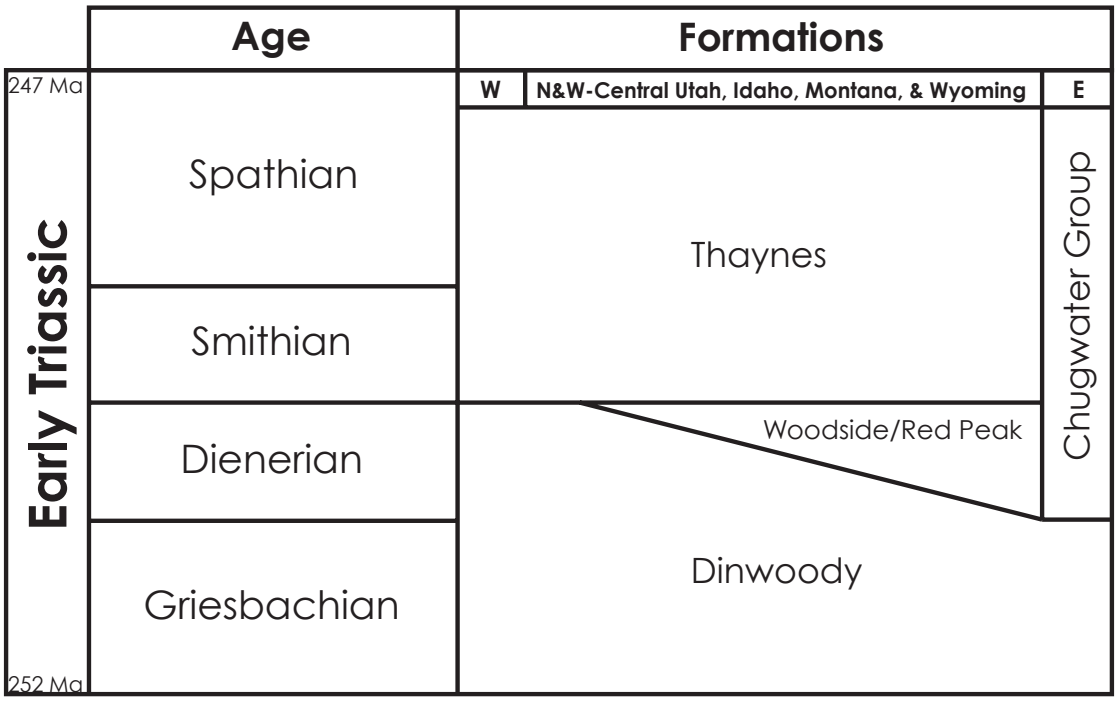

Figure 6 Geological time scale and schematic, spatial orientation of Lower Triassic strata of the Dinwoody Basin. The Dinwoody and Thaynes Formations were examined in this study. Modified from Paull *et al.* (1989) and Boyer *et al.* (2004).

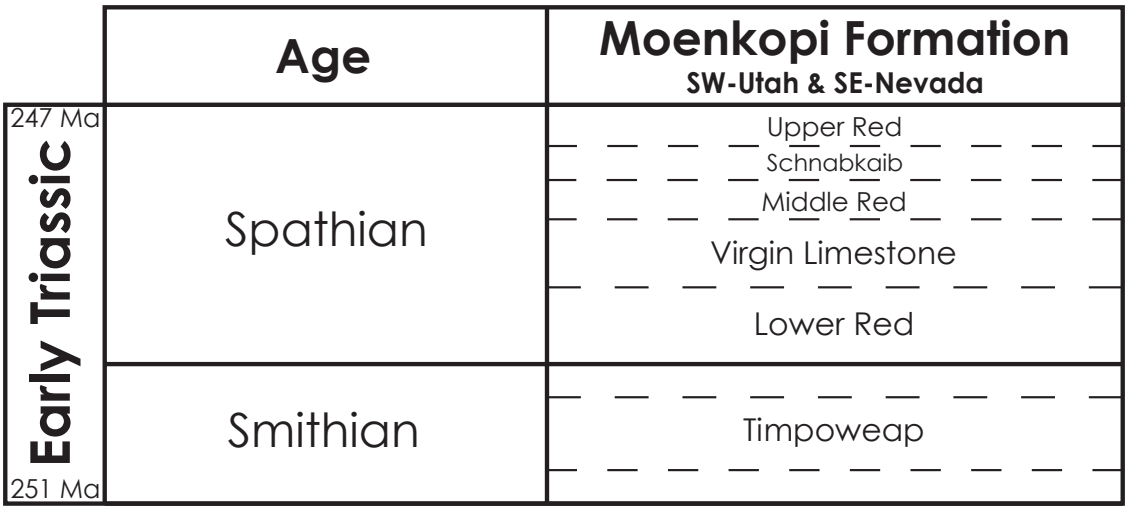

Figure 7 Temporal distribution and general stratigraphy of the Lower Triassic strata of the Moenkopi Formation. The Virgin Limestone Member was examined in this study. Modified from Boyer *et al.* (2004).

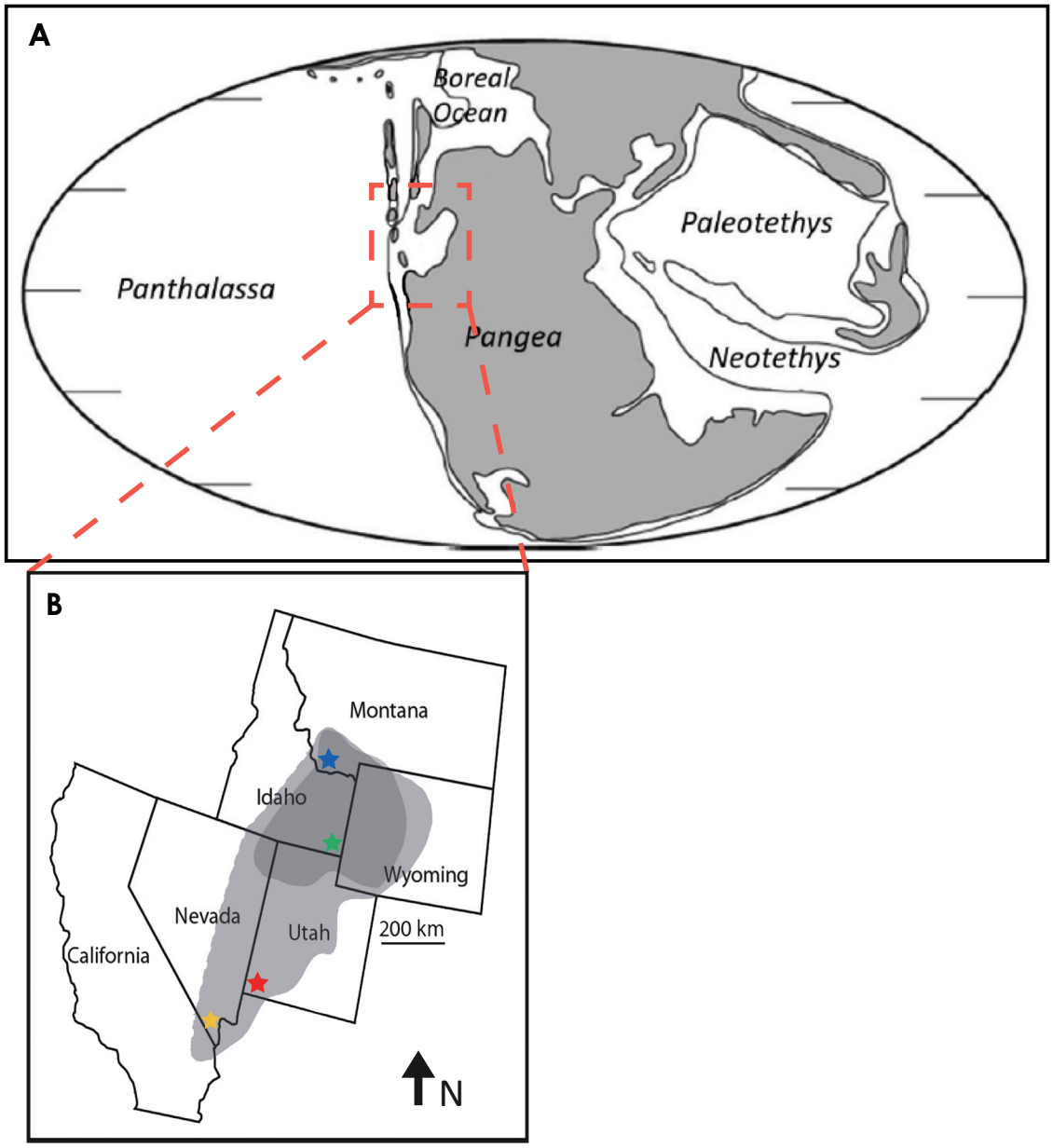

Figure 8 Paleogeography and localities of Lower Triassic strata examined in this study. (A) Paleogeography of the Early Triassic (approximately 252 Ma). Study area located on the northwestern margin of Pangea outlined by orange box. (2) Lower Triassic strata exposed in present-day, western United States. Dark grey shading indicates outcrop exposures of the Dinwoody Formation. Light grey shading indicates outcrop exposures of the Thaynes Formation in the North and analogous strata in the South (e.g. Moenkopi Formation). Starred locations indicate outcrop exposures where echinoid remains have been positively identified. Blue: Hidden Pasture and Blacktail Creek; Green: Montpelier Canyon and Bear Lake; Red: White Hills; Yellow: Lost Cabin Springs. Modified from Scotese (1994), Fraiser and Bottjer (2007) Fraiser and Bottjer (2009).

The Thaynes Formation is equivalent to the Moenkopi Formation (Fig. 7) (e.g. Boyer *et al.*, 2004). The Moenkopi represents both the second and third, Smithian and Spathian, respectively, regional transgressions in the southwestern U.S. (Dean, 1981; Boyer *et al.* 2004). The Virgin Limestone Member in southwestern Utah and southern Nevada represents the Spathian portion of the Moenkopi Formation examined in this study (Kummel, 1954; Reif and Slatt, 1979; Boyer *et al.* 2004). The third trangressive event (Spathian) resulted in the most extensive shallow seaway in the western United States during the Early Triassic (Carr and Paull, 1983). The Moenkopi Formation is composed largely of limestone lithologies.

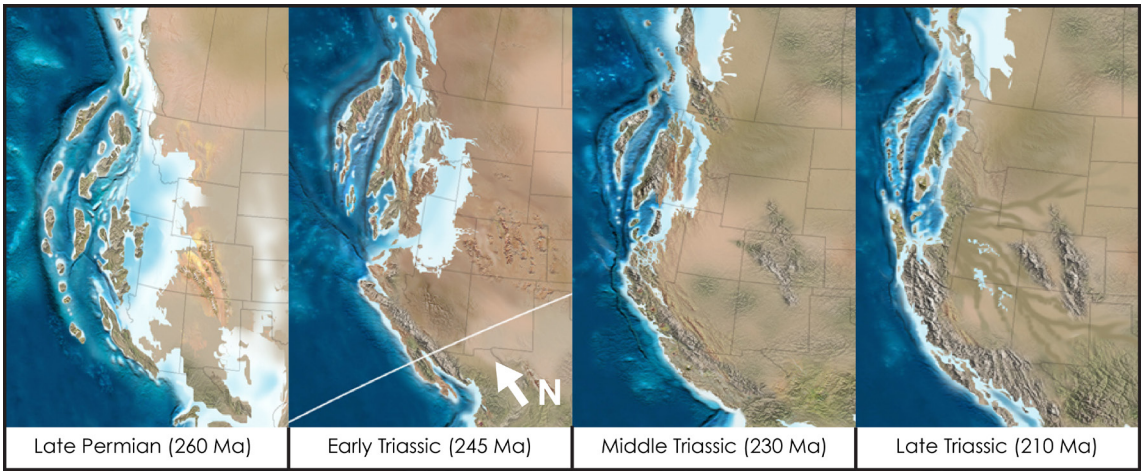

Figure 9 Sequential, reconstructed images of western North American paleogeography spanning 50 million years from the Late Permian until the Late Triassic. Modified from Blakely: http://cpgeosystems.com/paleomaps.html (2010).

Greisbachian age strata and the associated fauna were examined at two sites in southern Montana (Hidden Pasture and Blacktail Creek) (Appendix A & B), and one site in eastern Idaho (Bear Lake) (Fig. 8b) (Appendix C). Smithian and Spathian age strata and the associated faunas of the Dinwoody Basin are represented by the Thaynes Formation at Hidden Pasture, MT and Montpellier, Idaho (Fig. 8b) (Appendix B &

D). The examined strata of the Moenkopi Formation, the Virgin Limestone Member of White Hills, Utah and Lost Cabin Springs, Nevada (Fig. 8b) (Appendix E & F), are contemporaneous to the Thaynes Fm. of the Dinwoody Basin, but were deposited along the Panthalassan shoreline southwest of the basin.

Fieldwork was conducted May to June 2013 in southwestern Montana, southeastern Idaho, southwestern Utah, and southern Nevada (Fig. 8b) (Appendix A-F). Stratigraphic columns were measured and fossils were collected at two sections each of the Dinwoody Formation, the Thaynes Formation, and the Virgin Limestone Member. A total of 1130 m of section were measured in the Lower Triassic strata; each measured section was at least 2-3km apart so as to gain a lateral perspective of environments and paleoecology. To determine the abundance of echinoids relative to other marine benthic invertebrates, 85 hand samples were collected preferentially from 16 echinoid-bearing beds (determined by field observation of spine and test material), but neighboring beds where echinoid debris was not readily visible were also sampled. On average, 12 kg of limestone was sampled from each field site.

Thin sections were made for 25 samples from 25 distinct, separate beds collected from the Dinwoody Fm., Thaynes Fm., and Virgin Limestone Member of the Moenkopi Fm. Nine samples were analyzed from the Dinwoody Fm., seven from the Thaynes Fm., and nine from the Virgin Limestone Member, thus providing an even temporal survey of the Early Triassic. The majority of the sampled beds are of wackestone and packstone lithologies. Point counts in thin sections were performed to determine the proportion of fossil material relative to matrix (e.g. calcite cement, spar, quartz, micrite, intraclasts), as well as the proportion of echinoid material relative to that of other taxa (Fig. 10)

(Appendix G-K). Counts were made using Flügel's (1982) solid grain point-counting method using a Zeiss Axioskop 40 microscope and mechanical stepping stage.

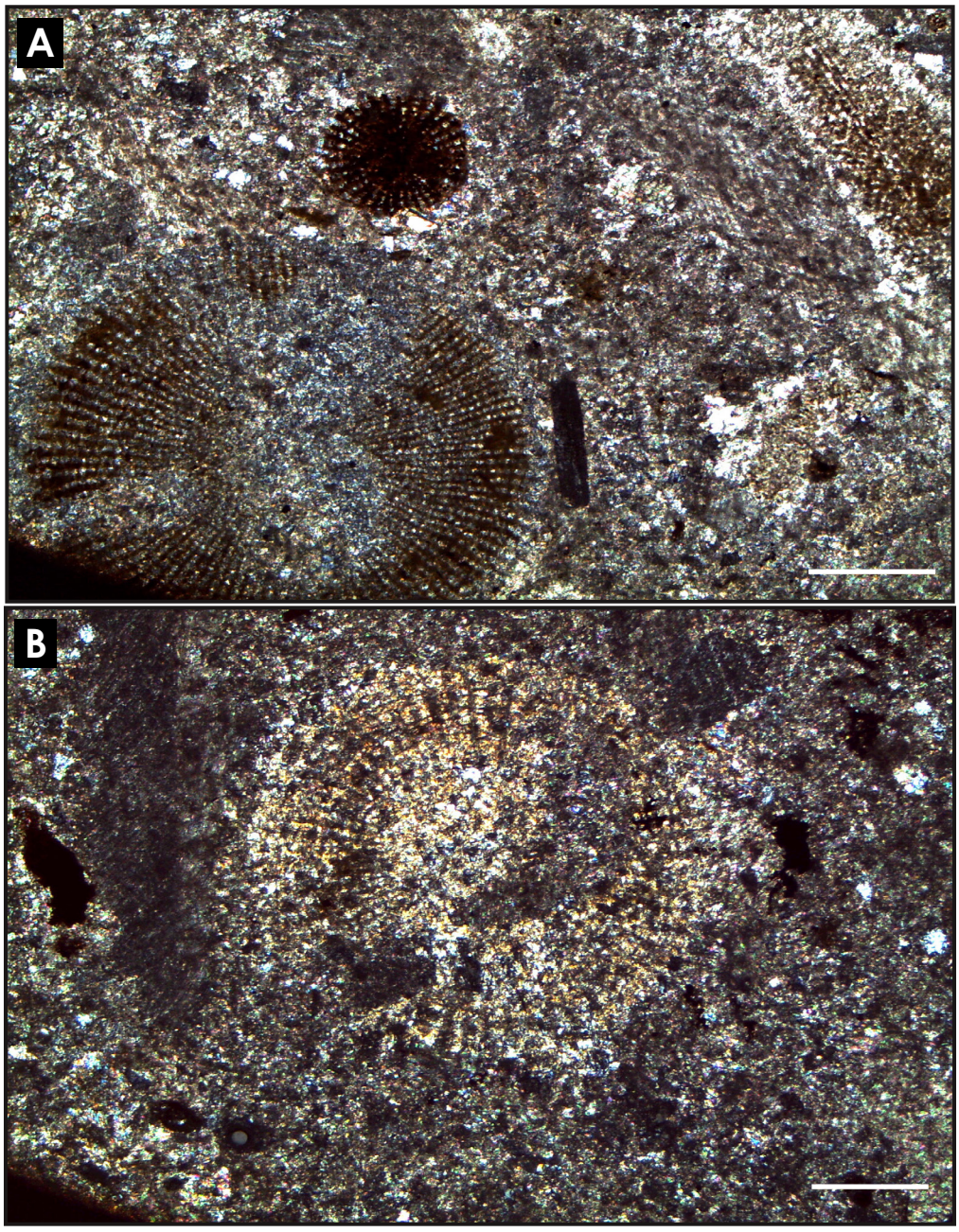

Figure 10 (A) Photomicrograph of three echinoid spines in a micritic matrix from the Dinwoody Fm. at Hidden Pasture, MT. Spines in the lower, left corner are cross-sections whereas the spine in the upper, right corner is a longitudinal section. Spines have been recrystallized and phosphatized. (B) Photomicrograph of an echinoid spine from the Dinwoody Fm. at Blacktail Creek, MT in a micritic matrix displaying full birefringence. Pictured echinoids (A and B) likely belong to the genus *Miocidaris*. Both scale bars are 250μm.

At least 300 points at 1 mm increments were counted per thin section and only material (e.g. fossils, matrix, and grains) that fell directly beneath the cross hairs was counted (Payne *et al.*, 2006; Jacobsen *et al.*, 2011). One-mm increments were chosen so as to accommodate the largest grain fraction present in the analysis (*sensu* Van der Plas and Tobi, 1965).When the same fossil, matrix, or grain appeared under consecutive cross hairs, it was counted again to quantify proportions as accurately as possible.

Point count data of Early Triassic echinoids and associated taxa were analyzed with the paleontological statistic software PAST (Hammer and Harper, 2001). Ecological metrics including Shannon Index (*H'*), Simpson Index (*1-D*), and evenness (H'/H_{max}) were used to quantify echinoid abundance and overall paleoecology of the Greisbachian, Smithian, and Spathian in eastern Panthalassa. The estimates of biodiversity herein will be measures of alpha diversity, as each bed at a given locality was considered a sample of a single community (Kidwell and Flessa, 1996). The Shannon Index (*H'*) is a measure of order or disorder of a system (Shannon, 1948); in terms of an ecological study, order is characterized by the number of individuals in each group of organisms per sample (Shannon and Weaver, 1949; Fraiser and Bottjer, 2007a). The Simpson's Index (*1-D*) quantifies the diversity, or dominance, of a sample, taking into account the number of different groups of taxa (e.g. genus) present and the abundance of organisms in each group (Simpson, 1949). Simpson's Index (*1-D*) measures the probability that two randomly selected individuals from a sample will belong to the same group (Simpson, 1949; Fraiser and Bottjer, 2007a). Evenness values (H'/H_{max}) measure how similar the abundances of different groups of organisms are

while normalizing for species richness and are calculated using the Shannon Index paired with the number of groups examined (Shannon and Weaver, 1949; Hammer and Harper, 2008). These metrics provide varying ways of determining which taxonomic groups are numerically dominant in each thin section and, in turn, each corresponding bed (Fraiser and Bottjer, 2007a). As previous paleoecological studies have demonstrated, determining which taxa are ecologically dominant, or rather, determining the most abundant members of a community, may be more important than analysis of species richness alone (Fraiser and Bottjer, 2005b). Determining ecological dominance within a community provides an understanding of both short-term and long-term fluctuations in community structure resulting from changes in energy flow and species composition (Grime, 1997; Symstad *et al.*, 1998; Downing and Leibold, 2002; Fraiser and Bottjer, 2005b). Accordingly, clarifying echinoid abundance in Early Triassic paleocommunities allows us to better understand their importance in community structure following the Permo-Triassic mass extinction. A two-sample Z test and t-test were performed to determine if fluctuations in echinoid abundance and faunal composition throughout the sampled beds at a given locality were statistically significant (Appendix L-Q). Rarefaction curves based upon point count data were produced for each bed to ensure paleoecological analyses were representative of the paleocommunities (Appendix R-V).

To test the habitable zone hypothesis, lithologies and sedimentary structures were documented in the field and in the laboratory to determine in which environments fossil accumulations occurred. Particular care was taken to note beds in which echinoid debris was found, as well as all accompanying and neighboring

faunas. At each field location, sections were measured at the meter scale from the earliest depositions of Lower Triassic strata until the strata could no longer be traced. Measurements of strike, dip and thickness were taken using a Brunton compass and Jacob's staff. Lithologies were determined using the Dunham classification system as follows: Mudstone (M), wackestone (W), packstone (P), and grainstone (G). Semi-quantitative measurements of ichnofabric were documented for each bed using the 1 through 5 ichnofabric index (ii) scale for shelf environments as described by Bottjer and Droser (1991). Field measurements for each section were used to construct stratigraphic columns of which meter-scale changes in lithologies, visible sedimentary structures, and fossil accumulations are indicated.

3. Results: Stratigraphic Analysis

3.1 Blacktail Creek, Montana

The 60 m-thick Blacktail Creek section contains the basal portion of the Dinwoody Formation and records a shallowing-upwards succession from distal ramp mudstone and siltstone to fossiliferous, lower-shoreface packstone. The base of the Griesbachian age strata at Blacktail Creek lies above the chert-rich strata of the Middle Permian Phosphoria Formation separated by a 15 m covered interval and contains 20 m of *Claraia*-bearing siltstones (Figs. 11 & 12).

Echinoid debris appears 35 m from the base of the section in concurrence with a lithological change from mudstone to silt-rich wackestone. The change in lithology and the appearance of echinoids are accompanied by a change in faunal composition from predominately bivalves to linguid brachiopods and microgastropods. Echinoid debris continually appears through a 10 m interval that is largely covered but contains discontinuous outcroppings and float of wackestone (Fig. 11). Thin section samples from these wackestone beds contain skeletal fragments that have been highly micritized.

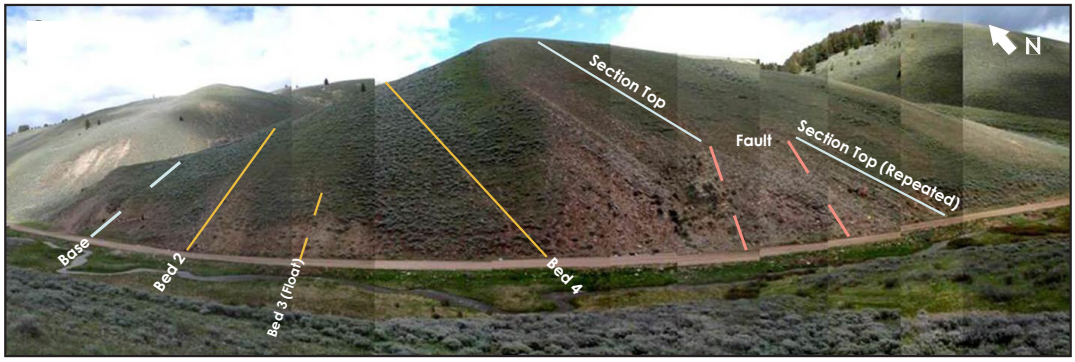

Figure 11 The entire exposure of the incomplete Dinwoody Formation at Blacktail Creek, Montana. Because the base of the Dinwoody Fm. is not exposed at this site, the dotted line indicates the approximate location of the base of the Dinwoody and base from which the measured section begins. Echinoid debris was found in beds highlighted in yellow. Photomosaic modified from Schaefer (2012, unpublished manuscript).

Skeletal debris increases 45 m above the base of the section producing packstone lithologies abundant with echinoid spines, rhynchonelliform brachiopods, and bivalves. Echinoid spines, through largely fragmented, are readily visible and abundant on bedding planes in association with brachiopod fragments through 5 m of limestone (Figs. 13 & 14). The disappearance of echinoid debris coincides with the final change in lithology from packstone to siltstone that occurs 50 m above the base of the section. The siltstone continues for 10 m and contains bivalves such as *Promyalina*, *Eumorphotis*, and *Unionites* as well as trace fossils such as *Diplocraterion*. Calcite replacement and slickensides also become prevalent within these beds indicating substantial faulting which is further confirmed by a repeated interval towards the top of the section (Fig. 11).

Overall, the echinoid-bearing beds at Blacktail Creek preserve little to no signs of sedimentary structures; however, bed 4 shows some evidence of vertical bioturbation with an estimated ii of 3.

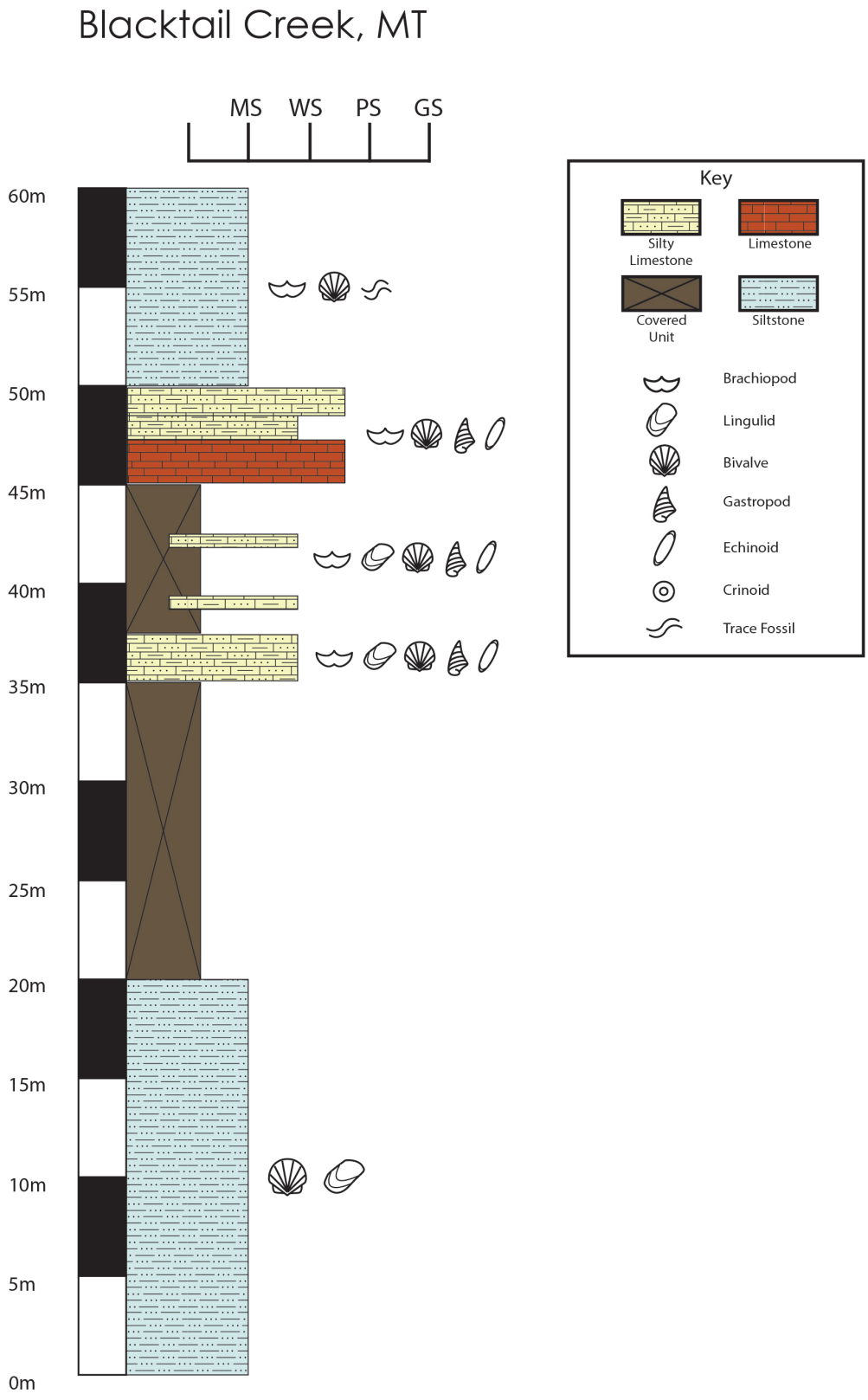

Figure 12 Stratigraphic column for Blacktail Creek, Montana highlighting the faunal composition of beds analyzed in thin section. Paleoecological analysis was performed for all beds containing echinoids.

Figure 13 Assemblage of echinoid spines and external mold of a rhynchonelliform brachiopod located 35 m from the base of the Dinwoody Formation at Blacktail Creek, Montana. Camera lens for scale.

Figure 14 Assemblage of bivalve and echinoid spine debris located 45 m from the base of the Dinwoody Formation at Blacktail Creek, Montana. Circled echinoid spine has spine insertion preserved intact. Camera lens for scale.

3.2 Hidden Pasture, Montana

The measured section at Hidden Pasture, Montana contains the entirety of the Dinwoody Formation from base to top, the entirety of the intertonguing Woodside Formation, and a considerable portion of the Thaynes Formation (Figs. 15 &16). In total, 545 meters of Lower Triassic strata where measured at this locality. The basal strata of the Dinwoody Formation at Hidden Pasture consist of thinly laminated, silty, mudstone with *Claraia* occurrences ranging from sparse to dense accumulations upsection, much like the basal Dinwoody strata at Blacktail Creek.

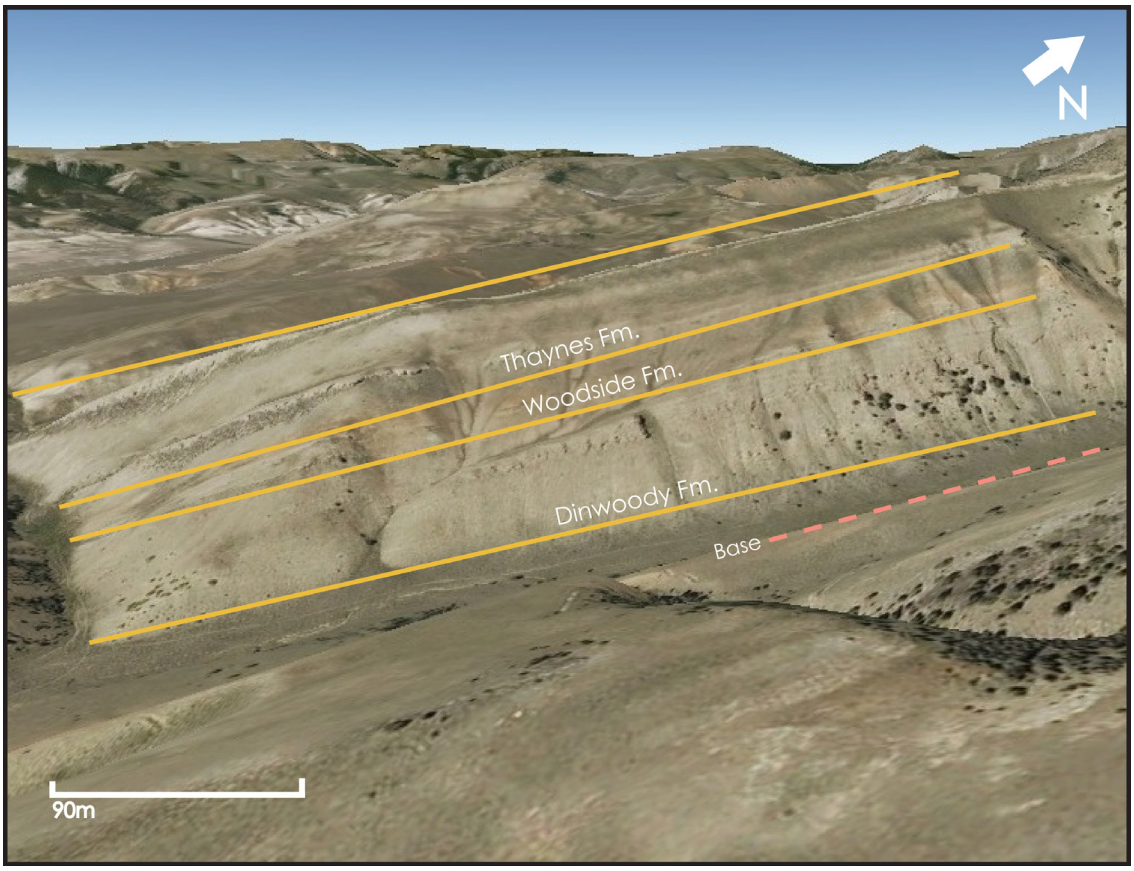

Figure 15 Google satellite map of Hidden Pasture, Montana. The measured base of the section relative to the full measured interval is indicated in red. Relative locations of the Dinwoody, Woodside, and Thaynes boundaries are indicated in yellow.

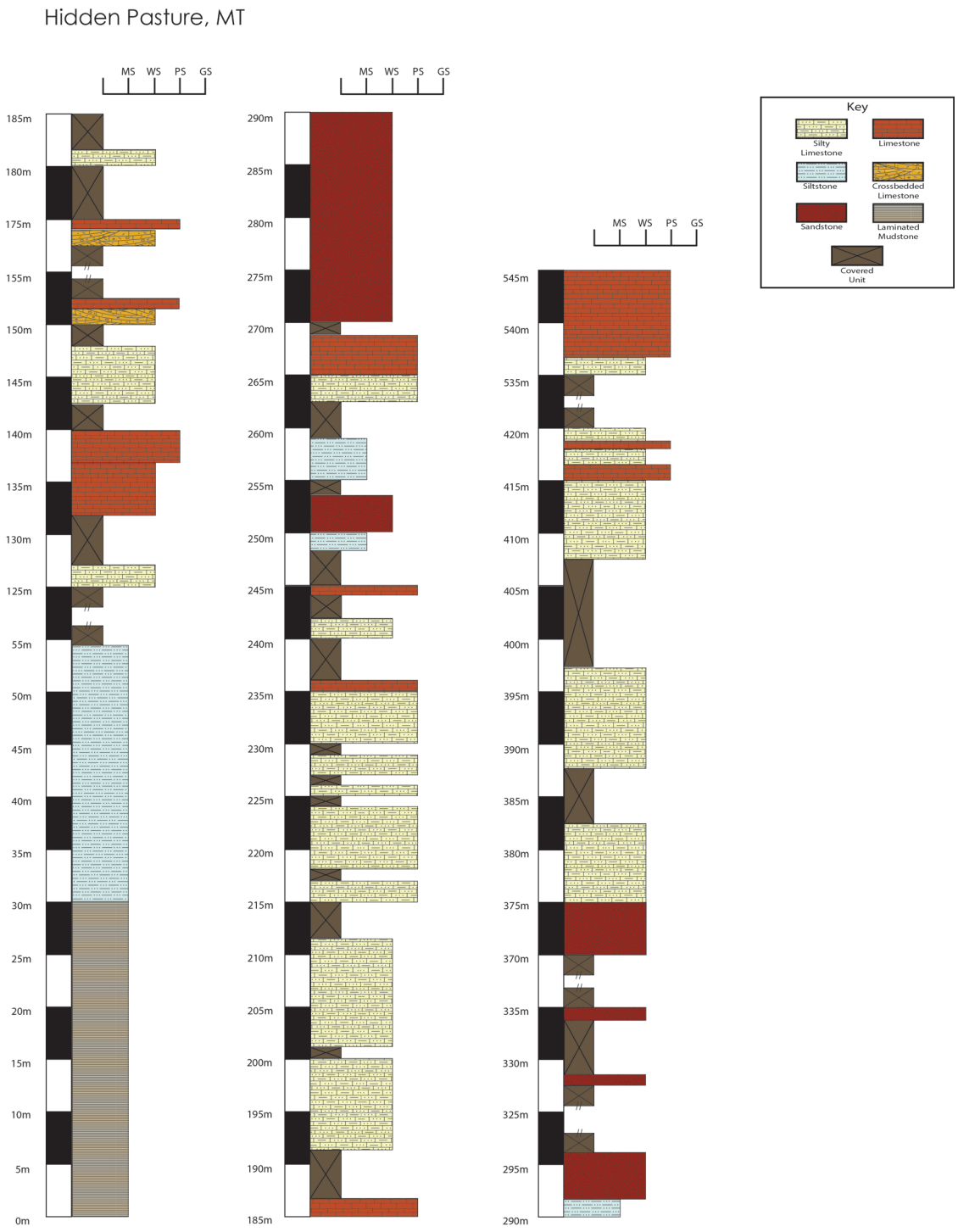

Figure 16 Stratigraphic column for Hidden Pasture, Montana.

Following a covered interval, the lithologies change to fossiliferous limestone 125 m above the base of the section. Three limestone beds extend vertically for 15 m and contain echinoids, bivalves, mircogastropods, and lingulid brachiopods (Figs. 17 & 18). A bed of silty wackestone appears from 142 m to 147 m containing mainly bivalves and less abundantly crinoids, followed by 2.5 m of alternating and cross-bedded packstone and silt-rich wackestone. Another 2.5 m section of alternating and cross-bedded packstone and silt-rich wackestone appears above a 20 m covered interval 172 m from the base of the section (Fig. 19). The bioclasts found within the packstone ledges are largely fragmented, but thin section analysis revealed the presence of echinoids, bivalves, crinoids, microgastropods, and lingulid brachiopods (see Results: Paleoecological Analysis). Hummocky cross-bedding from wave-ripples are visible within the alternating beds of packstone and silt-rich wackestone (Fig. 20). The packstone ledges at 172 m record the last occurrence of echinoid debris found within the Dinwoody Formation at Hidden Pasture.

From 180 m to 270 m, alternating beds of wackestone and packstone continue with increasing amounts of silt upsection. The bedding planes of wackestone and packstones within this interval contain an abundance of trace fossils, including *Arenicolites* and *Rhizocarallium*, as well as bivalves and lingulid brachiopods and numerous bedding planes contain wrinkle structures. At 270 m above the base of the section the lithology changes significantly to sandstone marking the boundary between the underlying Dinwoody Formation and the intertonguing Woodside Formation (Figs. 15 & 16).

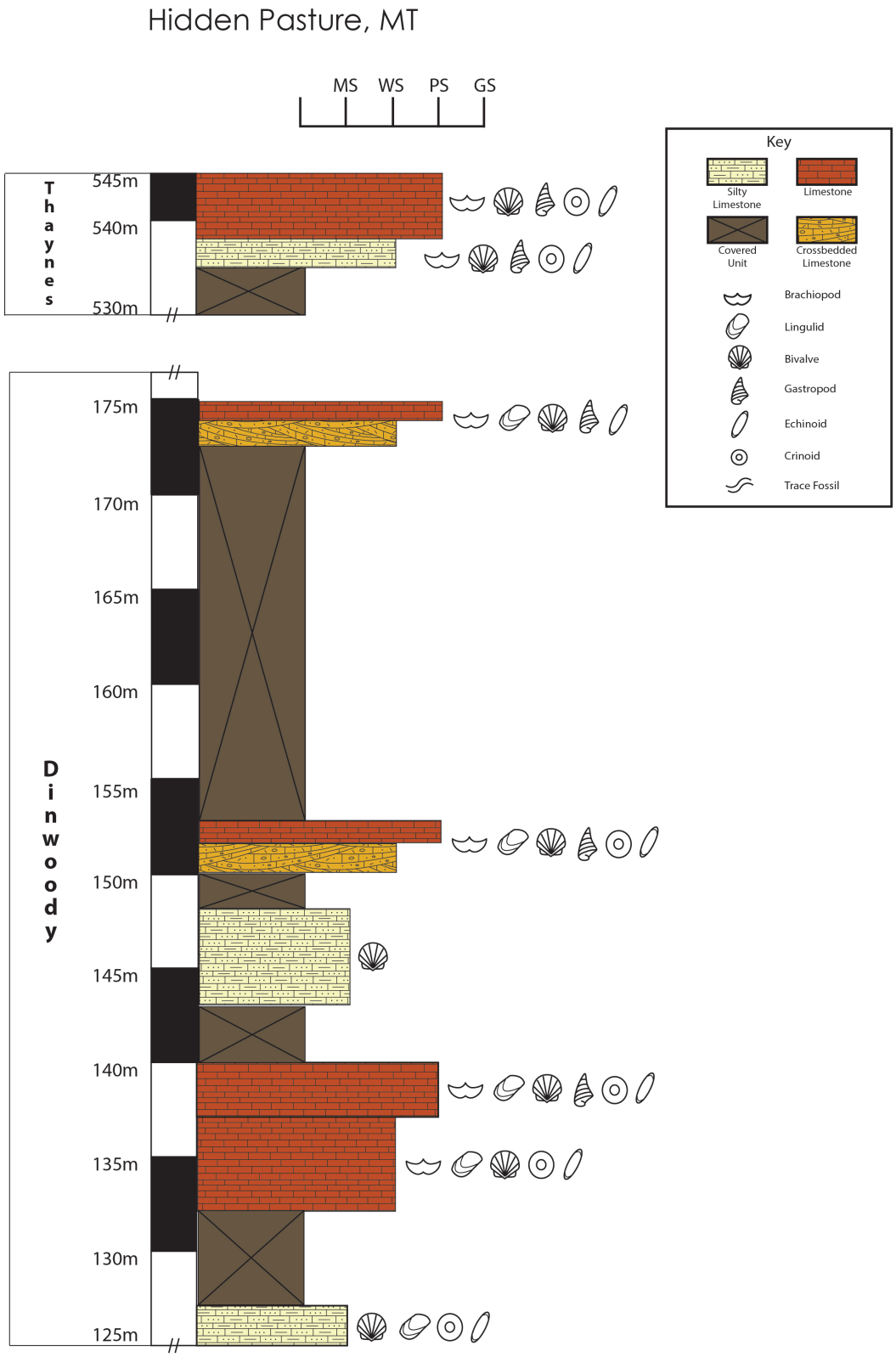

Figure 17 Condensed stratigraphic column of Hidden Pasture, Montana highlighting the faunal composition of beds analyzed in thin section. Paleoecological analysis was performed for all beds containing echinoids.

Figure 18 Bioclastic limestone displaying dense accumulations of echinoid spines and lingulid brachiopods located 137 m from the base of the Dinwoody Formation at Hidden Pasture, Montana. Echinoid spines have been circled in yellow and a lingulid brachiopod in orange.

Figure 19 Alternating beds of silt-rich wackestone and packstone located 147 m from the base of the Dinwoody Formation at Hidden Pasture, Montana.

Figure 20 Hummocky cross-bedded silt-rich wackestone and packstone beds located 147 m from the base of the Dinwoody Formation at Hidden Pasture, Montana.

Approximately 150 m of the Woodside Formation underlies the Thaynes Formation at Hidden Pasture; the base of the Thaynes Formation is identifiable by the appearance of *Meekoceras* -bearing beds 415 m from the base of the section. The *Meekoceras*-bearing packstone continues vertically for 5 m followed by a 2 m interval of silty, lingulid-bearing wackestone. The next limestone bed of the Thaynes, a silt-rich wackestone, appears after a 113 m covered interval 535 m from the base of the measured section (Fig. 21). This wackestone bed is dominated by crinoid ossicles and bivalves clearly visible in the field. Thin section samples of this bed reveal the presence of microgastropods, rhynchonellid brachiopods, and echinoids in low abundance (see Results: Paleoecological Analysis).

Within 1 m, the lithology changes to a dense packstone containing abundant crinoid ossicles, bivalve and rhynchonellid brachiopod shell fragments, microgastropods, and echinoid debris (Fig. 22). The packstone shell bed continues for 9 m marking the end of the measured section at Hidden Pasture.

Figure 21 The two, uppermost limestone outcrops of the Thaynes Formation at Hidden Pasture, Montana both containing echinoid debris.

Figure 22 Dense bioclastic limestone containing clearly visible *Holocrinidae* and *Pentacrinidae* ossicles located 537 m from the base of the Dinwoody Formation at Hidden Pasture, Montana. Camera lens for scale.

3.3 White Hills, Utah

The 20 m-thick section at White Hills, Utah represents one of two sections deposited during the third, Spathian, transgressive event of the Early Triassic. The Spathian transgression resulted in a broad spanning, shallow seaway, depositing the distinct, ledge-forming, limestone beds of the Virgin Limestone Member of the Moenkopi Formation (Fig. 23) (Carr and Paull, 1983; Hofmann *et al.*, 2013b). The base of the measured Virgin Limestone Member section is a 1 m-thick hummocky cross-stratified, calcareous siltstone interfingered with wackestone and packstone shell beds (Fig. 24). The fossilferous wackestones and packstones contain unsorted shell debris of echinoids, crinoids, bivalves, and microgastropods, many of which remained largely intact (Fig. 25).

Figure 23 Complete section of the exposed Virgin Limestone Member at White Hills, Utah. Echinoid debris was found in beds outlined in red.

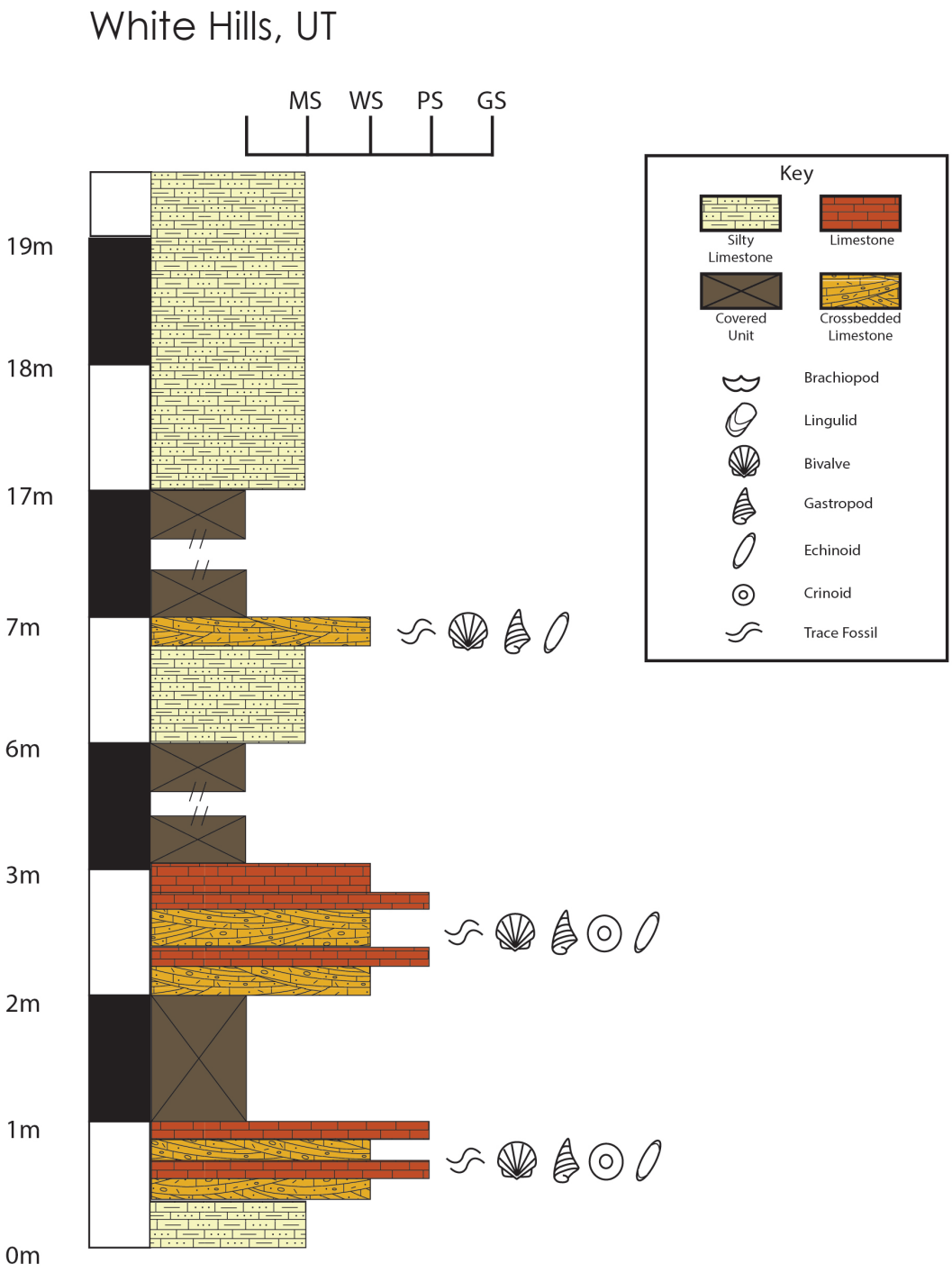

Figure 24 Stratigraphic column for White Hills, Utah highlighting the faunal composition of beds. Paleoecological analysis was performed for the echinoid-bearing beds at 2 m and 6.9 m.

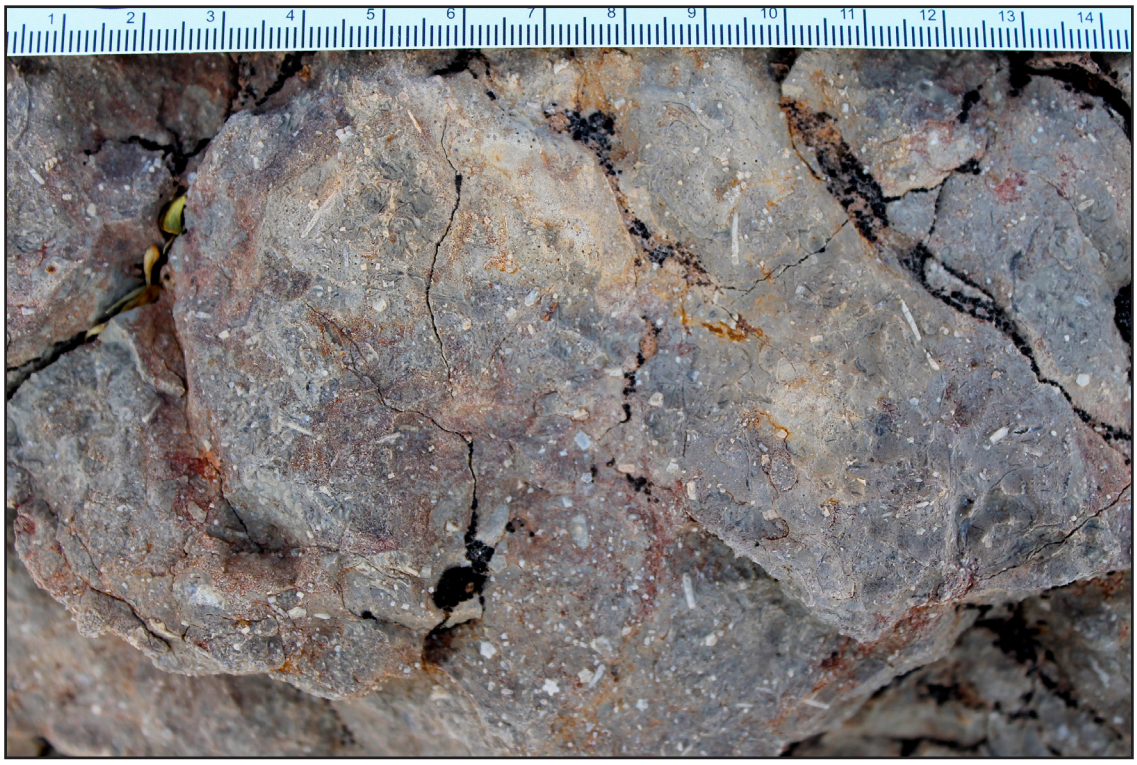

Figure 25 Fossiliferous limestone with distinct echinoid spine debris and crinoid ossicles located 1 m from the base of the Virgin Limestone Member at White Hills, Utah.

Following a thin, 1 m covered interval, a 1 m-thick silt-rich, fossiliferous limestone unit occurs. The limestone unit contains alternating beds of rippled, cross-stratified wackestone and dense packstone (Fig. 26). Bedding planes of the wackestone and packstone beds contain echinoid debris, including fully intact spines, in association with gastropods, crinoid ossicles, and bivalve shell debris (Figs. 27). Trace fossils such as *Planolites* and *Thalassinoides* are also visible upon bedding planes and beds show signs of bioturbation ranging from 3-4 ii. Although echinoid and crinoid debris are readily visible, thin section analysis revealed that bivalves and microgastropods dominate the wackestone and packstone in this interval (see Results: Paleoecological Analysis). These beds are overlain by a 3 m covered interval after which the next limestone ledge appears.

Figure 26 Hummocky cross-stratified wackestone located 2 m from the base of the Virgin Limestone Member at White Hills, Utah.

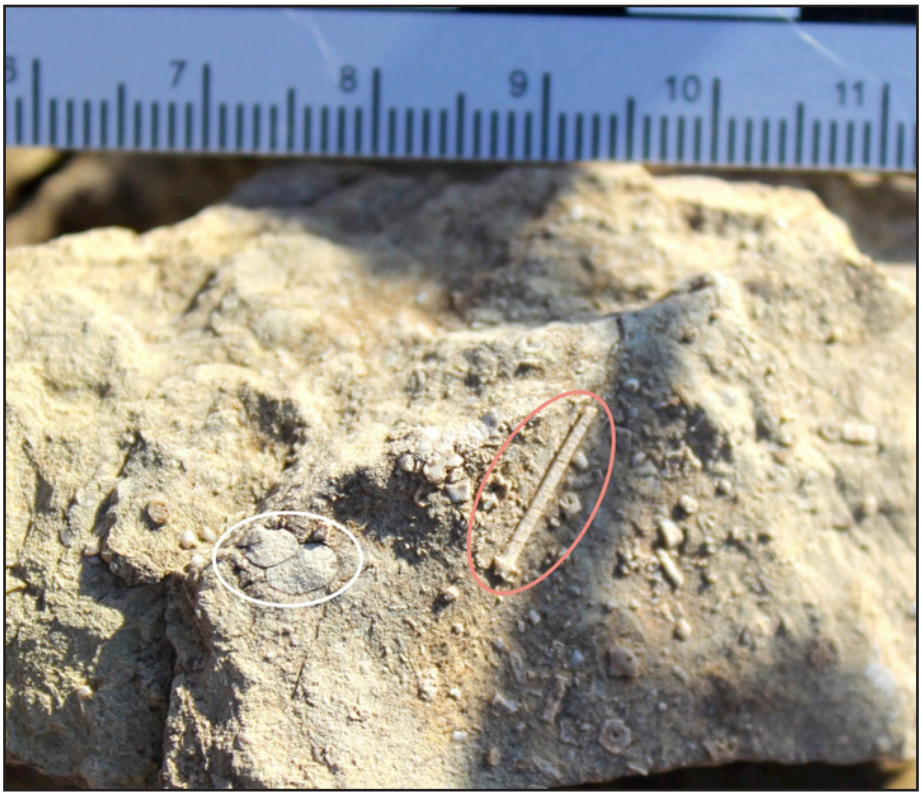

Figure 27 Packstone from the Virgin Limestone Member at White Hills, Utah. Echinoid spine with insertion preserved intact circled in red. Internal mold of a gastropod circled in white.

The next limestone ledge appears 6 m above the base of the measured section and is comprised of a 1 m-thick, silt-rich mudstone that coarsens into a thin bed of wackestone. Ripples are present within the wackestone portion of this bed, but are not visible in the silt-rich mudstone below. In addition to spine fragments, intact echinoid test material was found in association with microgastropods and bivalve shell fragments (Figs. 28 & 29). *Thalassinoides*, *Planolites*, and *Rhizocorralium*, are present on bedding planes and the bed has an overall ii of 3. Unlike the previous beds, crinoid skeletal debris appeared absent in this bed and was later confirmed by thin section analysis.

The top of the Virgin Limestone occurs 17 m above the base of the measured section and is comprised of a 2 m-thick, highly recrystallized mudstone. This unit appears completely devoid of sedimentary structures and the only bioclasts present appears to be rare bivalves. Given the excessive amount of recrystallization and weathering present, no interpretations were made for this bed.

Figure 28 Piece of echinoid test with intact boss from the Virgin Limestone Member at White Hills, Utah.

Figure 29 Three pieces of echinoid test with intact boss and spine fragments from the Virgin Limestone Member at White Hills, Utah. Note microgastropods in the lower, left corner.

3.4 Lost Cabin Springs, Nevada

The measured section at Lost Cabin Springs, Nevada contains mixed carbonate and siliciclastic strata of the Virgin Limestone Member. Unlike the Virgin Limestone observed at the White Hills, UT locality, the Virgin Limestone strata at Lost Cabin Springs were deposited in a more distal portion of the ramp (Larson, 1966; Mata and Bottjer, 2011) and provide an overall more extensive section (Fig. 30). A total of one hundred fifty-five meters were observed at Lost Cabin Springs; however, echinoid debris was not observed above 65 m from the base of the measured section (Figs. 31 & 32). Numerous shallowing-upwards sequences occur throughout the stratigraphic

section and are made apparent by traceable changes in lithology, sedimentary structures, and ichnofabric indices (Mata and Bottjer, 2011). Each parasequence generally coarsens upwards from laminated mudstone to bivalve and crinoid dominated packstone to hummocky, cross-stratified, silt-rich packstone containing dense accumulations of echinoid debris and microgastropods (Mata and Bottjer, 2011).

Figure 30 Photograph of Lost Cabin Springs, Nevada field site showing the measured interval of the Virgin Limestone Member between the base and the top of the section.

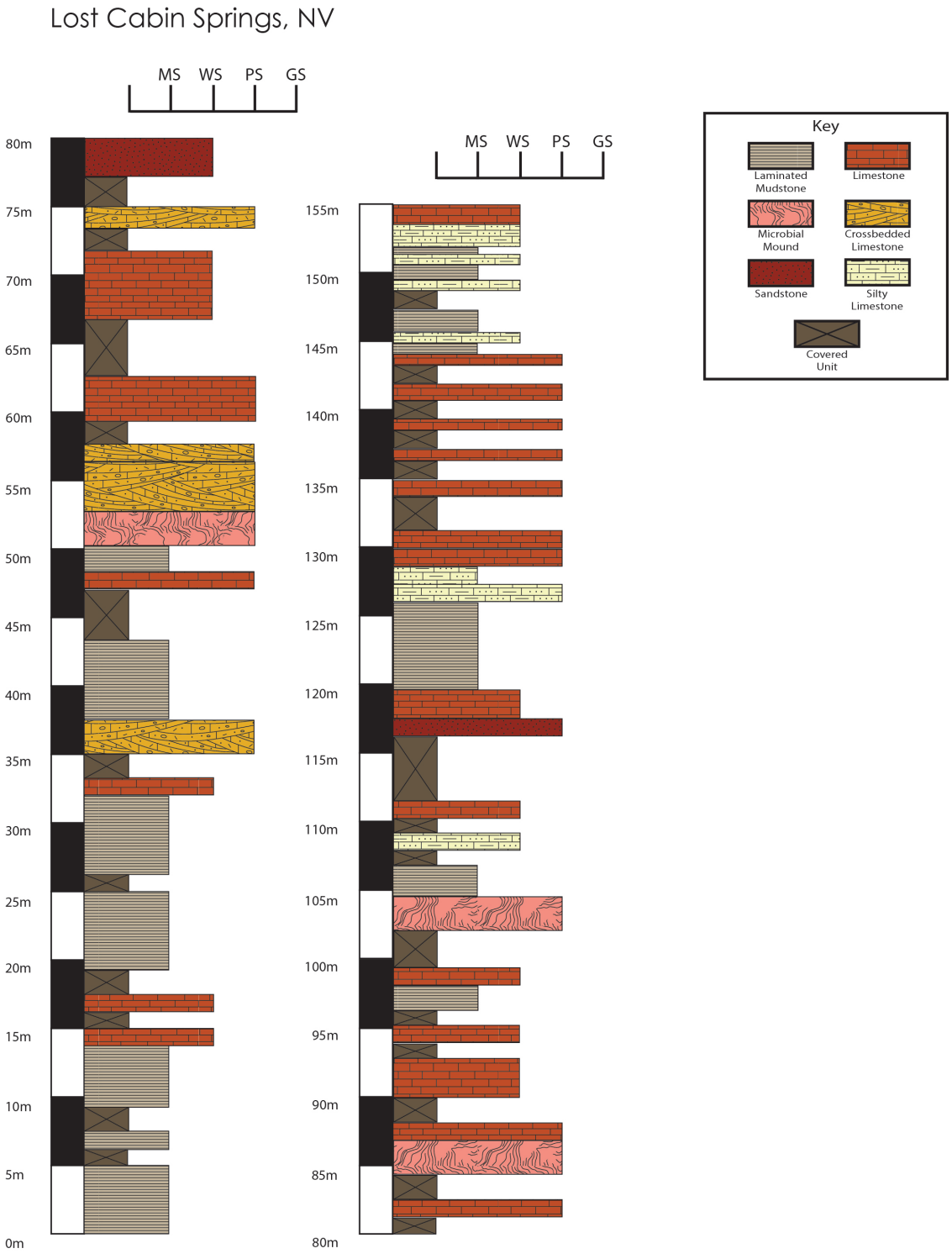

Figure 31 Stratigraphic column for Lost Cabin Springs, Nevada.

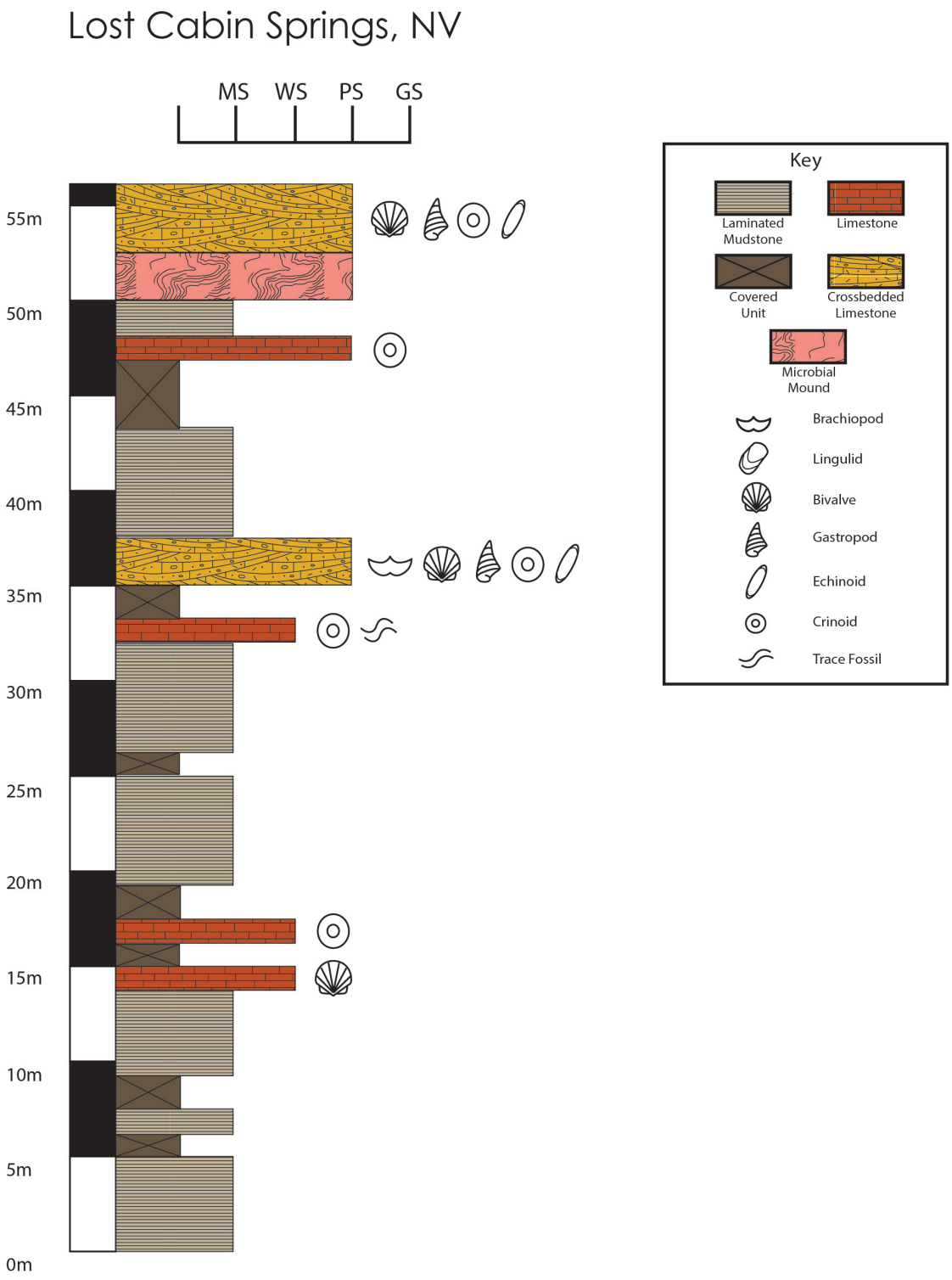

Figure 32 Condensed stratigraphic column of Lost Cabin Springs, Nevada highlighting the faunal composition of beds. Paleoecological analysis was performed for all beds containing echinoids.

The basal 14 m of the measured Virgin Limestone Member at Lost Cabin Springs contains three units of laminated and thin-bedded mudstones that range widely in ii from 1-5. The first bioclasts appear directly above the third mudstone unit in a thin limestone deposit containing bivalves, solely. Above the bivalve-bearing bed lies a 16 m unit composed largely of laminated mudstones again with ii varying from 1-5 capped above and below by crinoid-bearing wackestone beds. The overlying wackestone bed contains trace fossils *Planolites* and *Thalassinoides* in addition to the abundant ossicles of *Holocrinus*. Following a brief, 2 m covered interval the first, echinoid-bearing unit occurs. The 2 m limestone unit contains trough cross-stratified packstones comprised of dense accumulations of echinoids, microgastropods, and crinoid ossicles (Fig. 33). Although crinoids appeared to be the most abundant faunal constituent in field observations, the thin section sample revealed that microgastropods account for more than a quarter of the faunal composition and revealed the presence of both bivalves and rhynchonelliform brachiopods (see Results: Paleoecological Analysis). The echinoid spine debris at Lost Cabin Springs differs morphologically in comparison to the debris observed at all other field sites in this study; the spines in both echinoid-bearing units in this section are squat and rounded, much like the spines of a modern pencil urchin (Fig. 34).

Figure 33 (A) Cross-stratified packstone containing dense accumulations of crinoid, microgastropod and echinoid debris 38 m from the base of the measure section at Lost Cabin Springs. (B) Close-up of outcrop photograph providing a more detailed view of a bioclast accumulation.

Figure 34 Close-up of echinoid-dense packstone outcrop located 38 m above the base of the measured Virgin Limestone Member section at Lost Cabin Springs, Nevada. Notice that the echinoid spines at this location are morphologically dissimilar to those observed at previous field localities.

A thin, crinoid-bearing packstone bed appears 48 m above the base of the measured section topped by a 2 m unit of laminated mudstone. Directly atop the laminated mudstone unit lays the first, 2 m-thick microbial mound which is easily identifiable due to the stacked, domal structures and stromatolitic textures unique to microbial structures (Fig. 35a). The second and final echinoid-bearing unit of the Virgin Limestone Member at Lost Cabin Springs lays directly atop the stromatolitic bed in a dense packstone (Fig. 35b). The 3 m-thick packstone unit displays trough cross-

stratification and contains crinoid ossicles, microgastropods, and bivalves in addition to echinoid debris. Wackestones and packstones composed of crinoids, bivalves, and brachiopods continue upsection intermitted with laminated mudstones as water depths deepen and shallow, as well as two more microbial and sponge mounds which appear 87 m and 106 m above the base of the measured section. Although the stratigraphic section continues beyond the echinoid-bearing bed at 52 m, the remainder of the section will not be described in detail due to the scope of this study.

Figure 35 Photographs of a microbial mound-bearing unit located 50 m from the base of the Virgin Limestone Member at Lost Cabin Springs, Nevada. (A) The mound-bearing unit directly overlays a bed of laminated mudstone (B) and lays directly below a cross-stratified packstone containing echinoid debris.

4. Results: Paleoecological Analysis

Echinoid material was positively identified in 14 of the 25 thin sections corresponding to eight beds of the Dinwoody Formation, two beds of the Thaynes Formation, and four beds of the Virgin Limestone Member. For the purpose of quantifying echinoid abundance in this study, only the 14 beds containing echinoid material have been used for paleoecological analysis (Figs. 36-40). Other identified taxa within the 14 beds include bivalves, gastropods, rhynchonelliform and lingulid brachiopods, and crinoids. Echinoids are found in paleocommunities containing members of the Paleozoic Fauna such as brachiopods and crinoids, paleocommunities with a "mixed fauna", as well as paleocommunities largely dominated by members of the Modern Fauna such as gastropods and bivalves. Mixed fauna is the term that refers to post-extinction communities composed of a mixture of holdover, short-lived Permian survivors and typical Early Triassic taxa, such as opportunistic bivalves (Shen *et al.*, 2011; Clapham *et al.*, 2013).

In addition to varying in proportion, faunal constituents were not consistently present between field localities and, in some cases, dissimilar between beds at a single locality. For example, crinoids were identified in echinoid-bearing beds at Hidden Pasture, MT (Figs. 37& 38); White Hills, UT (Fig. 39); and Lost Cabin Springs, NV (Fig. 40); but were not present in the echinoid-bearing beds at Blacktail Creek, MT (Fig. 36). The faunal constituents of echinoid-bearing beds of the Dinwoody Fm. at Blacktail Creek, MT (Fig. 36) and the Thaynes Fm. at Hidden Pasture, MT (Fig. 38) remain consistently present, but fluctuate in proportion between beds. However, the echinoid-bearing beds of the Virgin Limestone Member at White Hills, UT and

Lost Cabin Springs, NV each lose a faunal constituent (crinoids and rhynchonelliform brachiopods, respectively) upsection in addition to having differing proportions of echinoids and associated fauna between beds (Figs. 39 & 40). Conversely, the echinoid-bearing beds of the Dinwoody Fm. at Hidden Pasture, MT gain a faunal constituent upsection (gastropods), but are similarly variable in constituent proportions between beds (Fig. 37).

Simpson's Index (*1-D*), which accounts for dominance within a community and where a rank of 1.0 indicates infinite diversity, ranges from 0.55–0.79 for the 14 beds in which echinoids appear (Figs. 41–45). Point counts revealed that echinoid-bearing beds with lower *1-D* values (0.55–0.69) were largely dominated by one constituent: Greisbachian age beds are dominated either by bivalves or brachiopods (Figs. 41 & 42); Smithian age beds, crinoids (Fig. 43); and Spathian age beds, gastropods (Fig. 44 &45).

Calculated evenness values (H'/H_{max}) for the 14 beds in which echinoids appear range from 0.7–0.98 (Figs. 41–45), where a rank of 1.0 indicates an ecologically even community. Evenness values for echinoid-bearing beds sampled from Greisbachian age strata range from 0.7–0.98 (Figs. 41 & 42), evenness values of beds sampled from Smithian age strata range from 0.85–0.96 (Fig. 43), and evenness values of beds sampled from Spathian age strata range from 0.76–0.92 (Figs. 44 & 45). Accordingly, the values calculated for Shannon Index (*H'*) shows a similar range and trend to those calculated for evenness (Figs. 41–45). The results obtained from two-sample t-tests produced *p*-values indicating differences in faunal dominance and evenness between successive beds at any given locality are not statistically significant (Appendix L–Q).

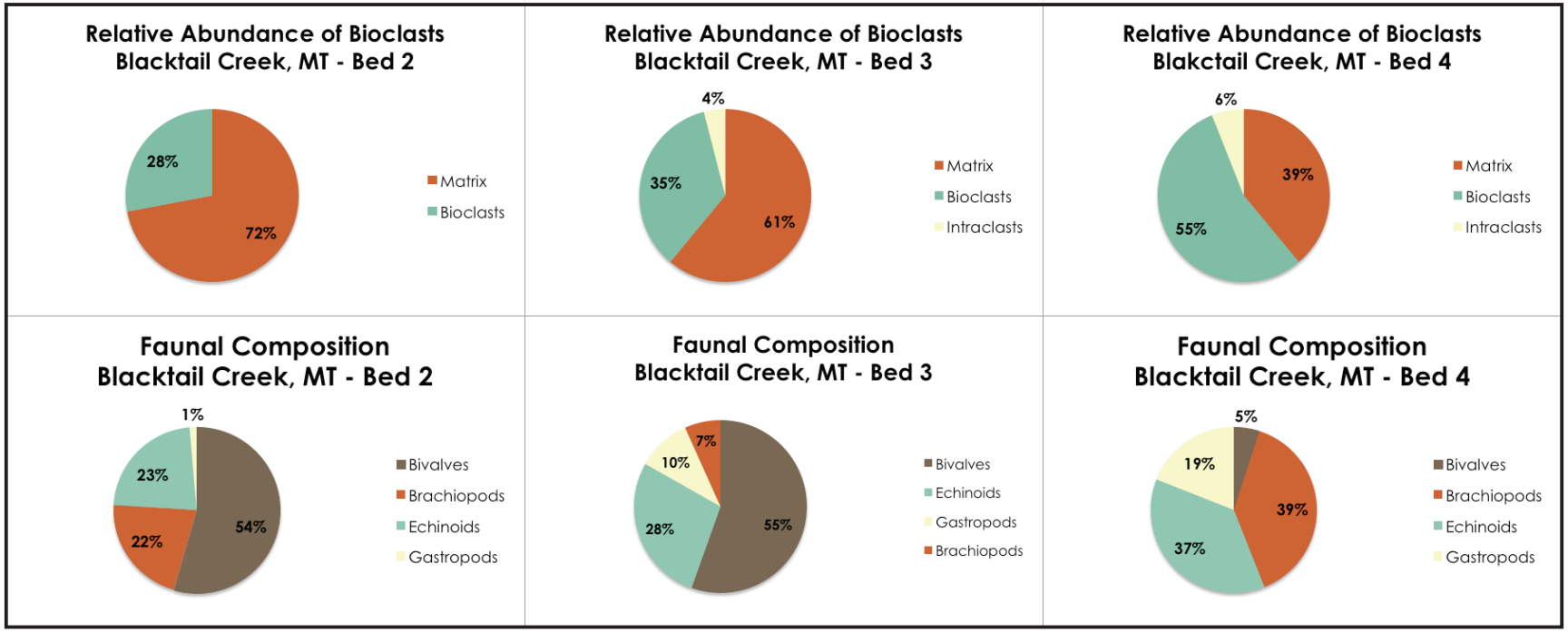

Figure 36 Proportions of benthic marine invertebrate bioclasts by bed for all beds containing echinoid debris in Greisbachian age strata of the Dinwoody Formation at Blacktail Creek, Montana. The proportion of bioclasts has been further resolved into fossil constituents grouped by class for each bed. Intraclasts include unidentifiable, recrystallized clasts and coated grains.

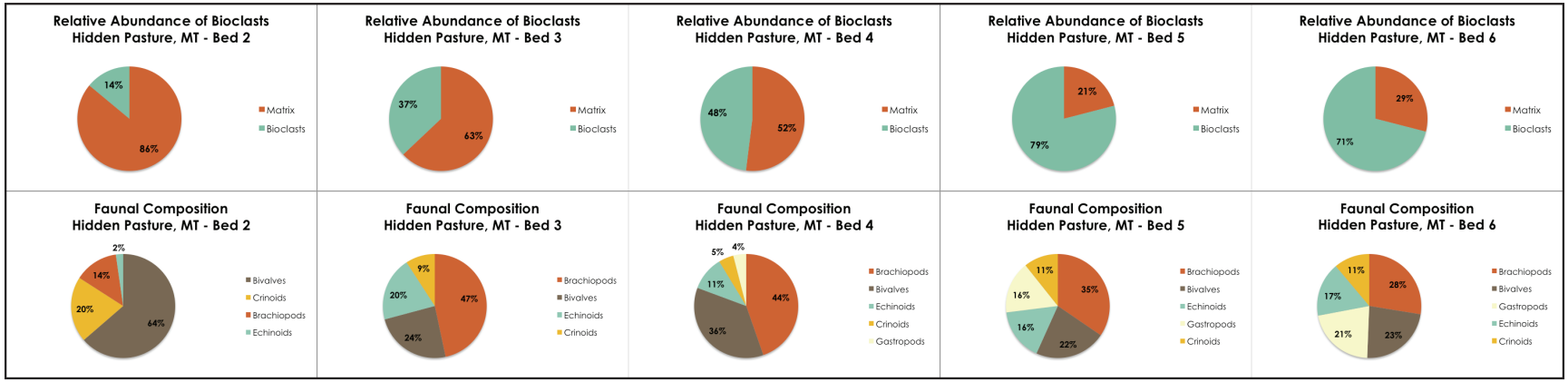

Figure 37 Proportions of benthic marine invertebrate bioclasts by bed for all beds containing echinoid debris in Griesbachian age strata of the Dinwoody Formation at Hidden Pasture, Montana. The percentage of bioclasts has been further resolved into fossil constituents grouped by class for each bed.

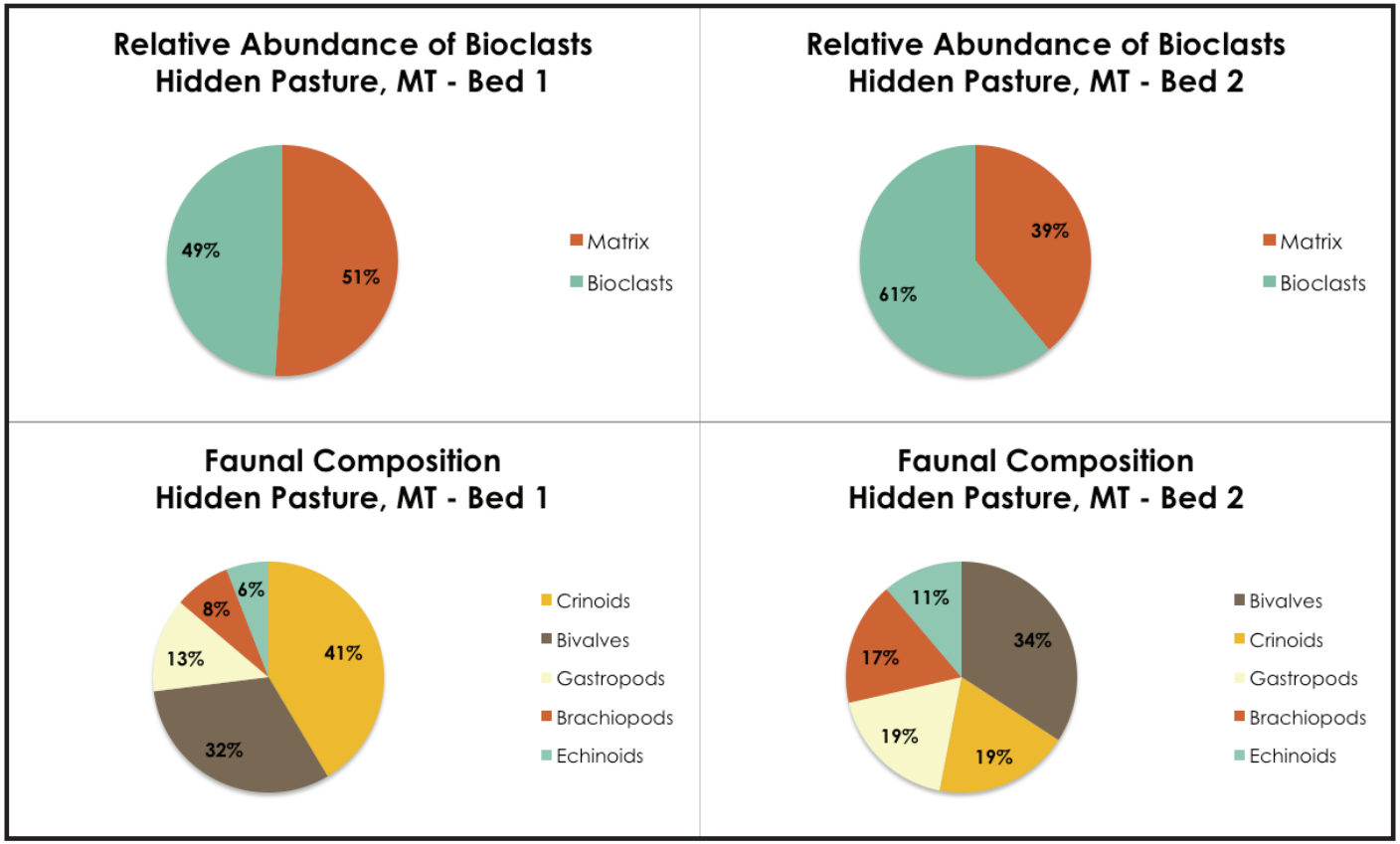

Figure 38 Proportions of benthic marine invertebrate bioclasts by bed for all beds containing echinoid debris in Smithian age strata of the Thaynes Formation at Hidden Pasture, Montana. The percentage of bioclasts has been further resolved into fossil constituents grouped by class for each bed.

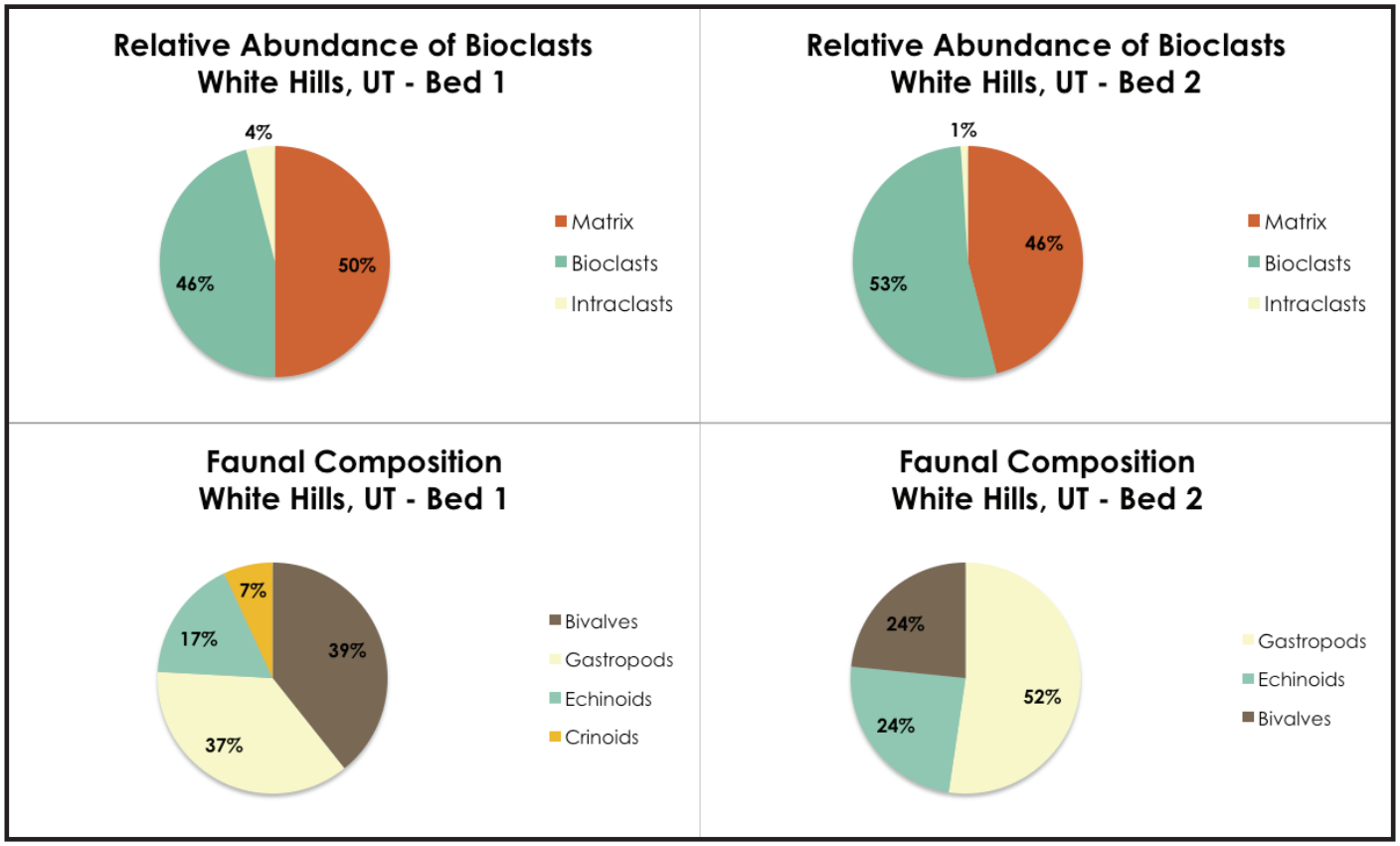

Figure 39 Proportions of benthic marine invertebrate bioclasts by bed for all beds containing echinoid debris Spathian age strata of the Virgin Limestone Member at White Hills, Utah. The percentage of bioclasts has been further resolved into fossil constituents grouped by class for each bed. Intraclasts include unidentifiable, recrystallized clasts and coated grains.

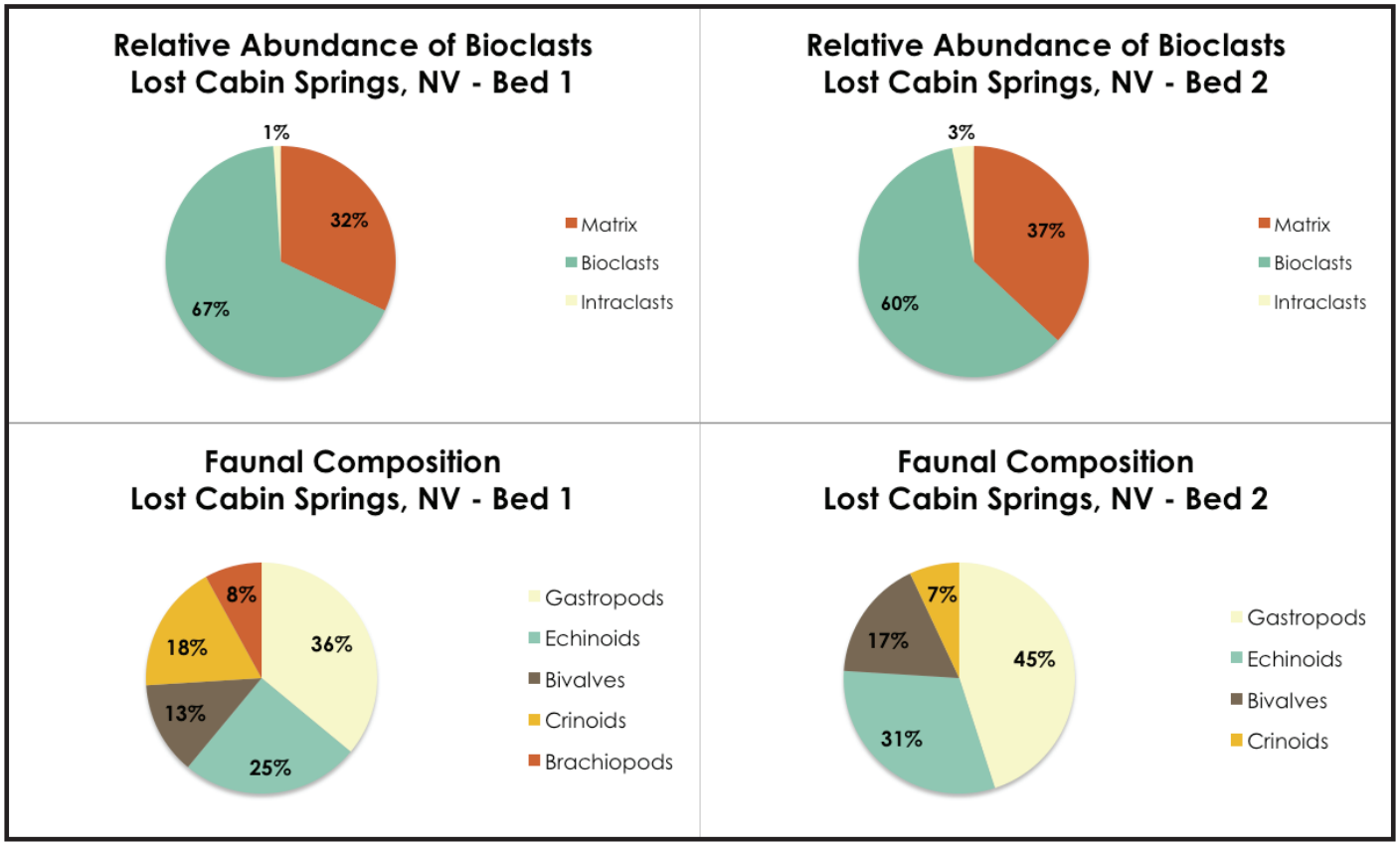

Figure 40 Proportions of benthic marine invertebrate bioclasts by bed for all beds containing echinoid debris in Spathian age strata of the Virgin Limestone Member at Lost Cabin Springs, Nevada. The percentage of bioclasts has been further resolved into fossil constituents grouped by class for each bed. Intraclasts include unidentifiable, recrystallized clasts and coated grains.

At Blacktail Creek, point counts reveal that echinoids constitute 20% to 37% of faunal composition (Fig. 46). Point counts of samples collected from the Greisbachian age strata of the Dinwoody Formation at Hidden Pasture indicate an overall lower abundance of echinoids in comparison to the contemporaneous strata at Blacktail Creek, MT (Fig. 47). Similarly, echinoids appear in low abundance within the Smithian age strata of the overlying Thaynes Formation at Hidden Pasture, MT (Fig. 47). Echinoid abundance varies throughout the Spathian where abundance ranges from 15-30% in the Virgin Limestone Member of the Moenkopi Fm. (Fig. 48 & 49).

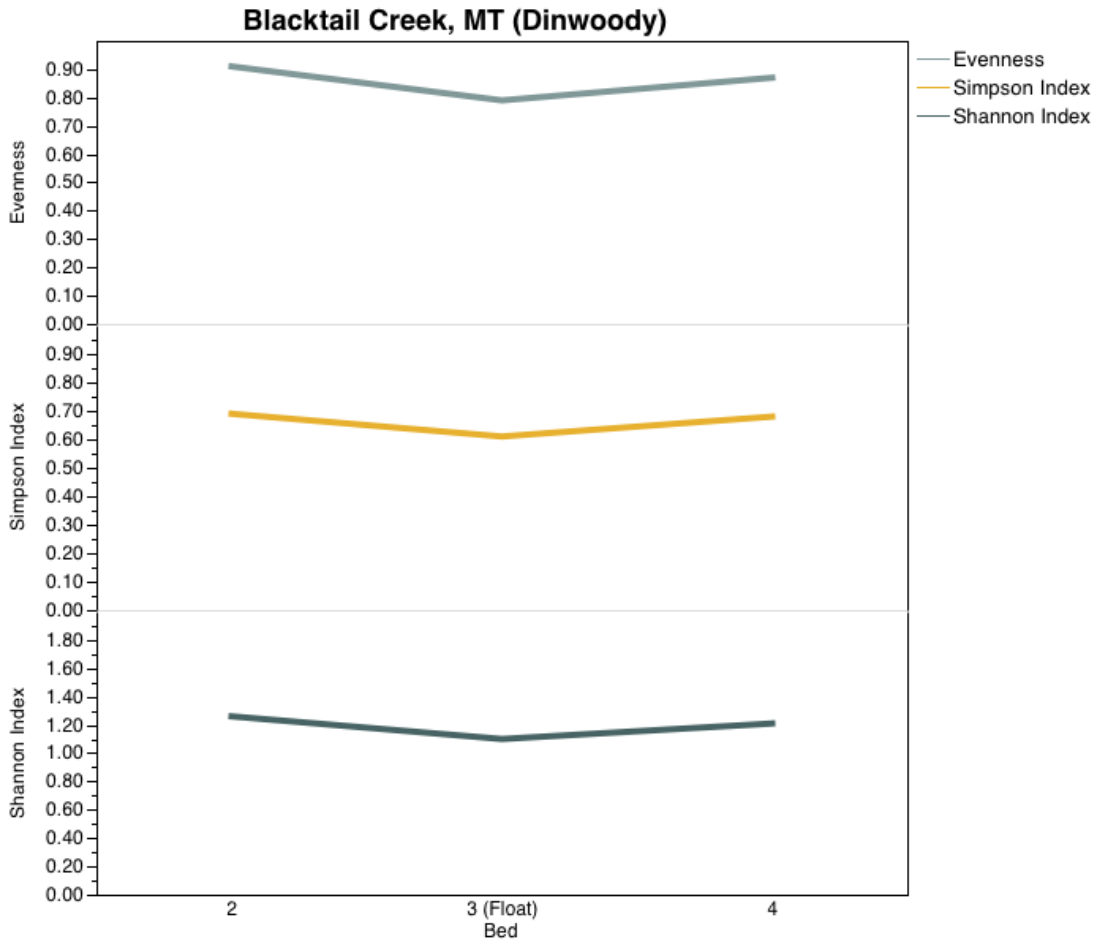

Figure 41 Graphic comparison of diversity indices Shannon Index (*H'*), Simpson Index (*1-D*), and evenness (H'/H_{max}) by bed for the Dinwoody Formation at Blacktail Creek, Montana.

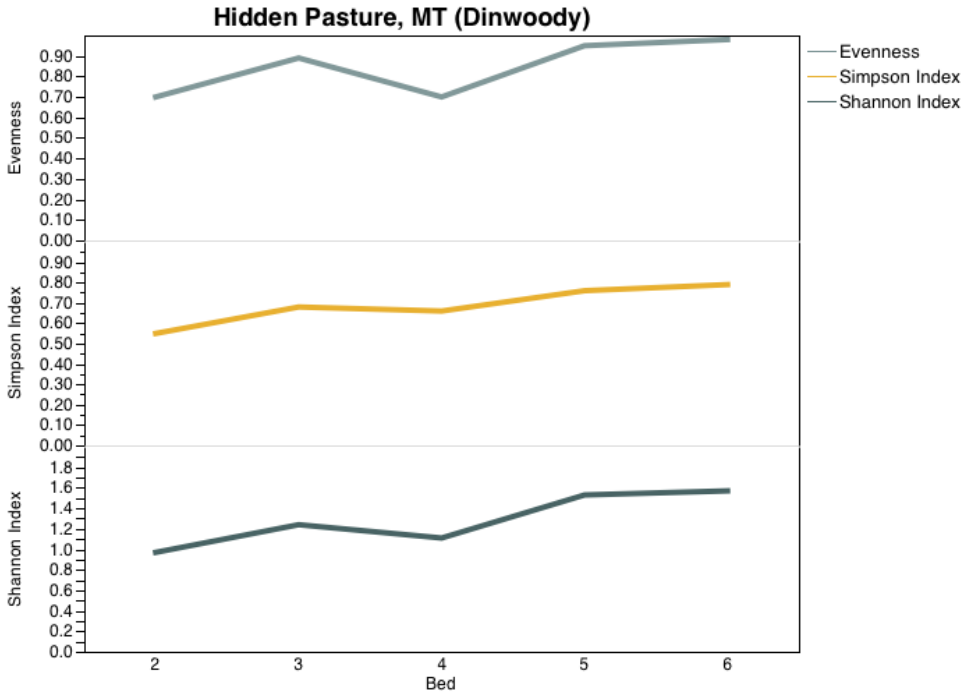

Figure 42 Graphic comparison of diversity indices Shannon Index (*H'*), Simpson Index (*1-D*), and evenness (H'/H_{max}) by bed for the Dinwoody Formation at Hidden Pasture, Montana.

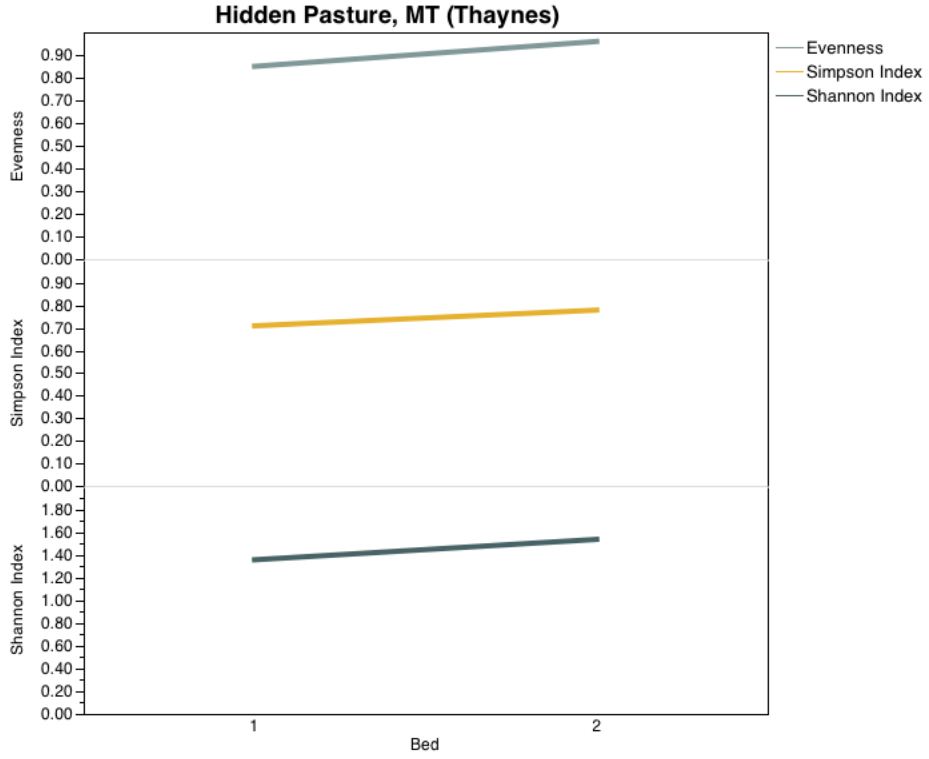

Figure 43 Graphic comparison of diversity indices Shannon Index (*H'*), Simpson Index (*1-D*), and evenness (H'/H_{max}) by bed for the Thaynes Formation at Hidden Pasture, Montana.

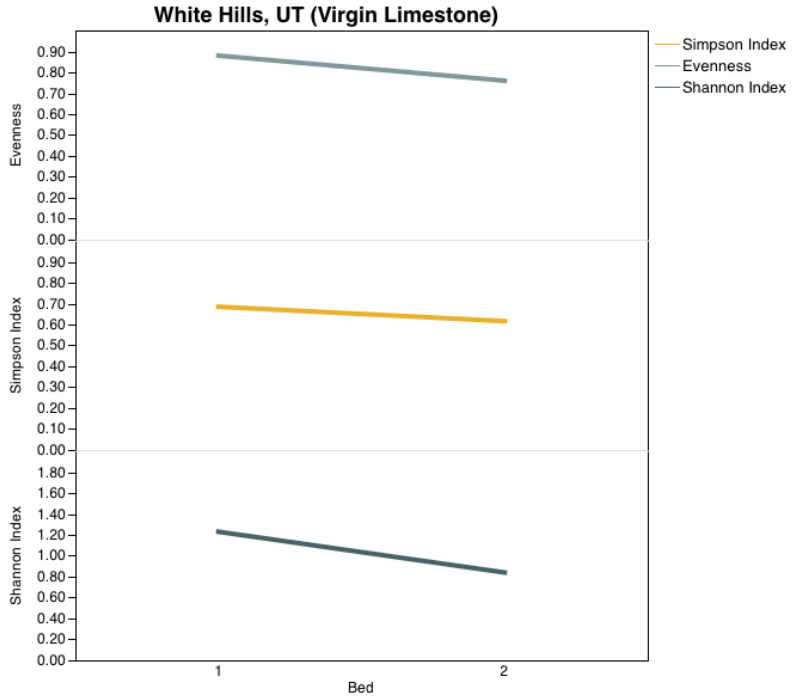

Figure 44 Graphic comparison of diversity indices Shannon Index (*H'*), Simpson Index (*1-D*), and evenness (H'/H_{max}) by bed for the Virgin Limestone Member at White Hills, Utah.

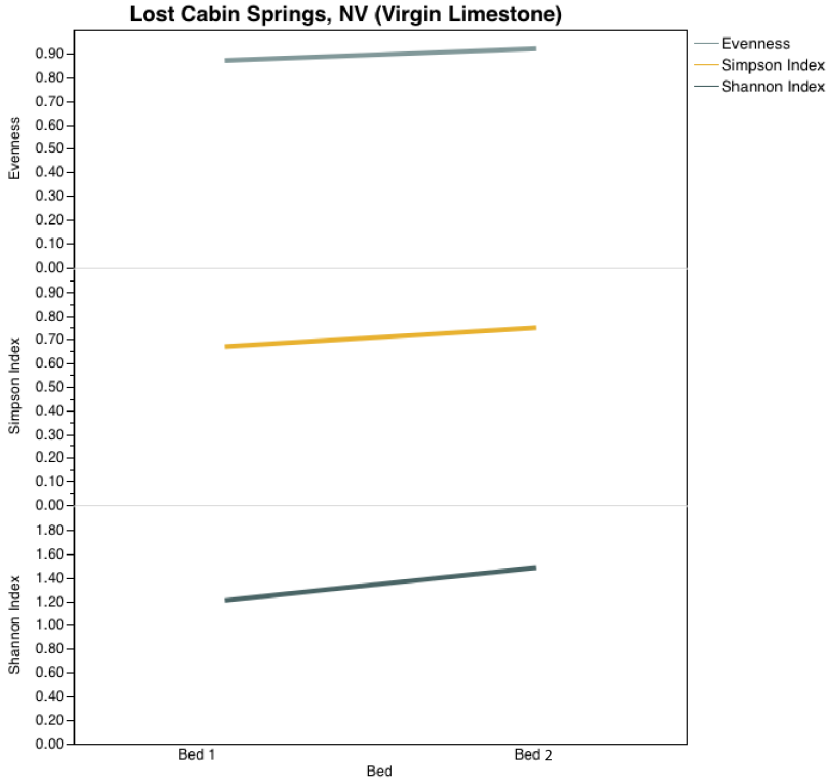

Figure 45 Graphic comparison of diversity indices Shannon Index (*H'*), Simpson Index (*1-D*), and evenness (H'/H_{max}) by bed for the Virgin Limestone Member at Lost Cain Spring, Nevada.

With the exception of the echinoid-bearing beds sampled from the Dinwoody Formation at Hidden Pasture, MT, echinoid abundance appears to have been relatively stable throughout sampled strata. Statistical tests indicate that the positive and negative excursions in echinoid abundance between successive, echinoid-bearing beds at all field localities but one (Fig. 47) were not significant. The abundance of echinoids between beds in the Dinwoody Formation at Hidden Pasture, MT fluctuated quite extensively between beds 2,3, and 4 (Fig. 47). Echinoids comprise only 2% of the faunal composition of Bed 2, but are 10 times more abundant in Bed 3 where they comprise 20% of the faunal composition (Fig. 42). Further, echinoids are nearly half as abundant in Bed 4 as in the previous bed (Bed 3) (Fig. 47). Statistical analysis revealed that the fluctuations in echinoid abundance between these three beds are significant with p-values < 0.05.

Echinoid material observed and collected from all field sites except the Virgin Limestone Member at Lost Cabin Springs, NV, appear to belong to one or two species of *Miocidaris*. Spines belonging to *Miocidaris* range in diameter from 0.6-2.0 mm (Table 1). The echinoid test material observed in the Spathian age strata of White Hills, UT have an average plate width of 4.6 mm, plate height of 2.3 mm, and mamelon diameter of 1.1 mm (Table 2). The measurably small fragments of test material and associated spines suggest that the echinoids preserved at White Hills, UT also belong to the genus *Miocidaris*. The echinoid spines from Lost Cabin Springs, NV appear to belong to a presently undetermined genus or species of echinoid. These spines range in diameter from 1mm-6mm and, where visible, the tips appear to round where spines from all other field localities taper to a sharp point (Table 1). Similar measurements of fossilized

echinoid debris from the western U.S. were obtained by Moffat and Bottjer (1999), Twitchett and Oji (2005), and Mata and Woods (2008). Based on differences in spine morphology, at least two different genera of echinoids are present within observed Lower Triassic strata. The spine debris at Hidden Pasture and Blacktail Creek, MT and White Hills, UT appear quite dissimilar compared to the spine debris found at Lost Cabin Springs, NV. Unfortunately, echinoid test material was neither observed nor recovered from the strata at Lost Cabin Springs, NV, so inferences in regards to genus disparity are only speculative based upon differences in spine morphology. However, thin section analysis shows no morphological disparity in cortex composition between any of the echinoid spines from any field site.

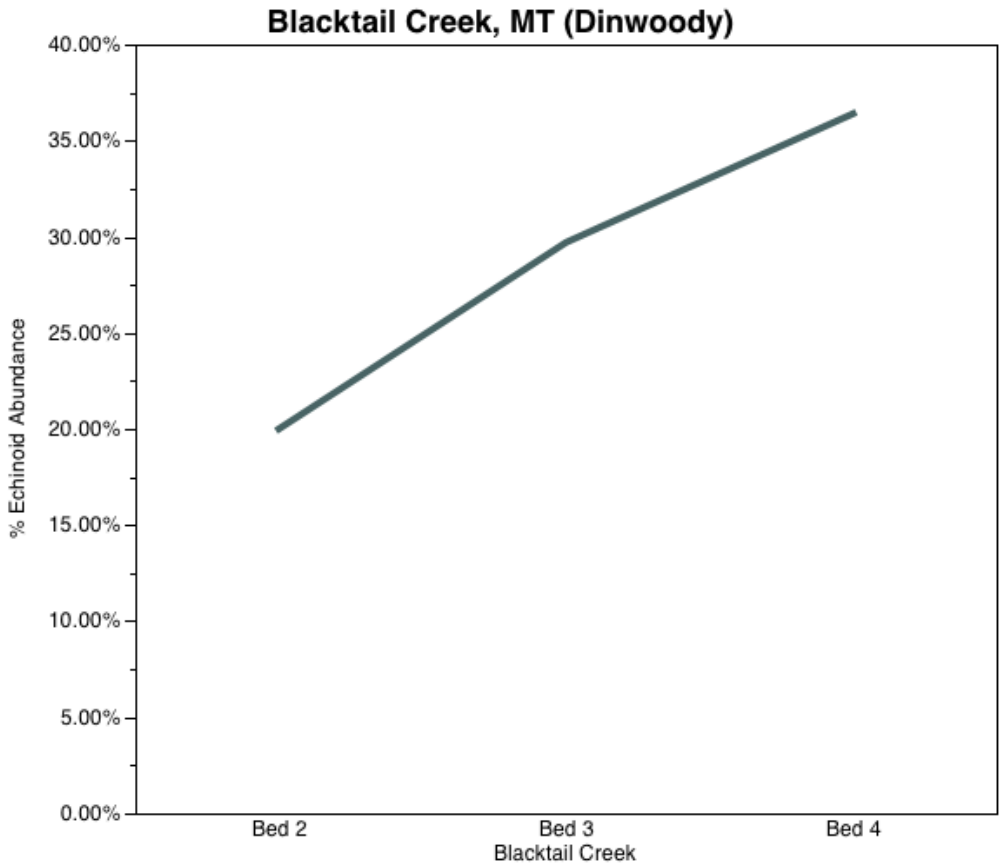

Figure 46 Percent echinoid abundance by bed from the Dinwoody Formation at Blacktail Creek, Montana.

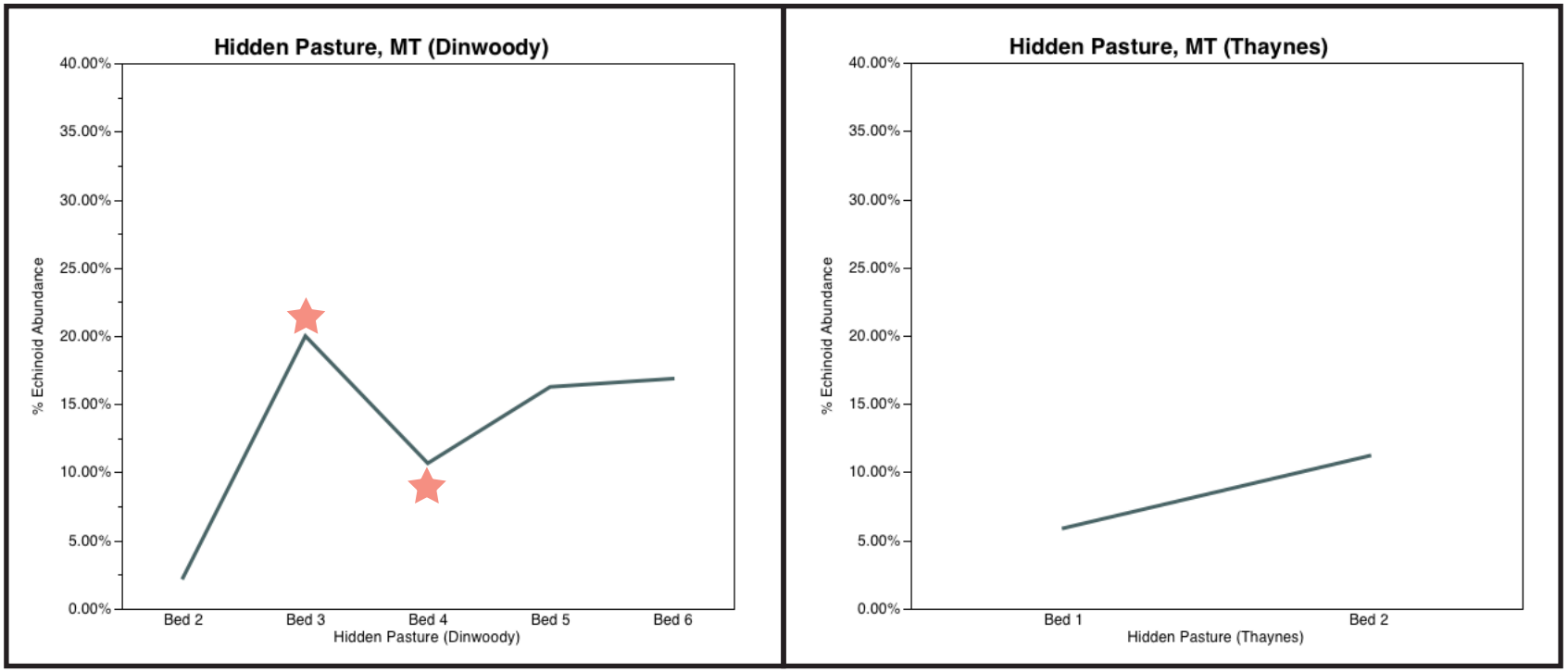

Figure 47 Percent echinoid abundance by bed from the Dinwoody and Thaynes Formations at Hidden Pasture, Montana. The red stars indicate beds with significant shifts in echinoid abundance when compared with the proceeding bed. *P*-values: HP, Bed 3 (0.005); HP, Bed 4 (0.032). *P*-values were obtained via a Z-test with a 95% confidence interval.

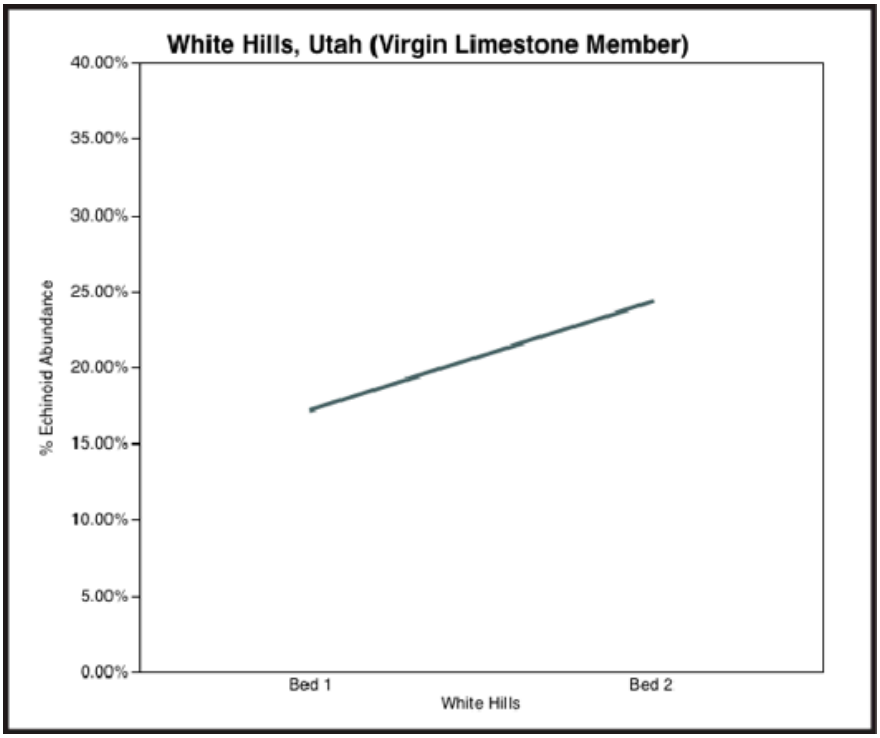

Figure 48 Percent echinoid abundance by bed from the Virgin Limestone Member at White Hills, Utah.

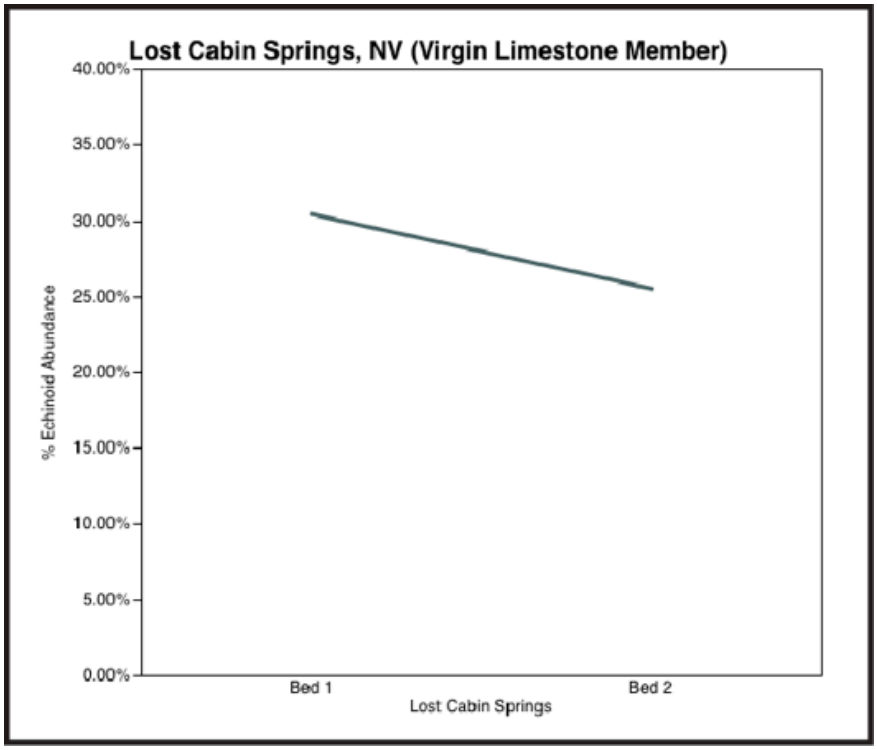

Figure 49 Percent echinoid abundance by bed from the Virgin Limestone Member at Lost Cabin Springs, Nevada.

Field Site	Age	Genus	Spine Diameter (mm)
Blacktail Creek, MT	Greisbachian	*Miocidaris*	0.6-2.0
Hidden Pasture, MT	Greisbachian	*Miocidaris*	0.7-1.6
Hidden Pasture, MT	Smithian	N/A	1.0-2.0
White Hills, UT	Spathian	*Miocidaris*	1.0-1.7
Lost Cabin Springs, NV	Spathian	N/A	1.5-6.3

Table 1 Measured ranges of echinoid spine diameter from each field locality.

Specimen	Plate Width (mm)	Plate Height (mm)	Mamelon Diameter (mm)
1	3.85	1.9	0.63
2	4.57	2.09	1.11
3	5.45	2.33	1.22
4	N/A	2.92	1.42
Average	4.62	2.31	1.1

Table 2 Measured echinoid test material from the Spathian age strata from the Virgin Limestone Member of the Moenkopi Formation at White Hills, Utah.

5. Discussion: Depositional Environment and Paleoecology

Echinoid debris within the Lower Triassic of the western U.S. was found exclusively in strata deposited in shallow marine environments. The packstone and wackestone lithologies in which echinoids were observed; wave-mediated sedimentary structures (ripples, hummocks, and cross-stratification); and evidence of storm events such as fragmented and abraded bioclasts support this interpretation of shallow marine habitable zones within the lower shoreface to offshore transition zone on a shallow marine ramp. Accumulations of bioclasts into shell beds, of which echinoids are included, as well as the disarticulated echinoid tests and spines present within beds of the Spathian age strata of the Virgin Limestone Member and the Greisbachian and Smithian age strata of the Dinwoody and Thaynes Formations indicate deposition within storm wave base (Kidwell and Holland, 1991). These findings are in concurrence with those of Twitchett and Oji (2005) whose qualitative observations of Lower Triassic strata in the western U.S. indicated that all known Early Triassic echinoids inhabited shallow, oxygenated environments within wave base.

5.1 Blacktail Creek, MT

The echinoid bearing beds at Blacktail Creek preserve little to no signs of sedimentary structures; however, many of the echinoid-bearing packstone beds shows some evidence of bioturbation with an estimated ichnofossil index of 3. The disappearance of disaster taxa such as lingulid brachiopods and the bivalve *Claraia* in conjunction with the appearance of echinoid dense packstone beds upsection

indicates deposition in a shallow-shelf habitable zone removed from distal, dysoxic waters, as echinoids require sufficiently greater amounts of oxygen for survival than the disaster taxa typical of the Early Triassic (Webster and Giese, 1975; Korkina *et al.,* 2000). Additionally, the mud-winnowed, packstone lithologies, fragmented skeletal debris, and coated grains identified in thin section suggest deposition within a wave-dominated, nearshore environment.

5.2 Hidden Pasture, MT

Similar to the Dinwoody Formation at Blacktail Creek, the thinly-laminated mudstone lithology, presence of framboidal pyrite, and presence of the disaster taxon *Claraia* that comprise the basal portion of the measured section at Hidden Pasture provide evidence of a distal, dysoxic environment. Much like the section at Blacktail Creek, the strata at Hidden Pasture also display a shallowing-upward sequence. However, the Greisbachian age strata at Hidden Pasture differ from those at Blacktail Creek in that the strata of Hidden Pasture contain varying abundances of crinoids, suggesting deposition in a deeper, possibly basin-ward facing, portion of the Dinwoody Basin. Further, the continuous abundance of lingulid brachiopods, appearance of wrinkle structures, and limited levels of bioturbation upsection suggest that the environments recorded at Hidden Pasture experienced upwelling of dysoxic and, potentially, anoxic waters with some regularity, a phenomenon more likely to affect environments proximal to the basin itself (Rodland and Bottjer, 2001; Pruss and Bottjer, 2004; Mata and Bottjer, 2009). Investigations regarding the evolution of complex organisms by Gingras *et al.* (2011) suggest that shallow marine microbial

mats may have provided a source of food and oxygen, via photosynthetic bacteria, for organisms living within an otherwise low-oxygen setting during the Ediacaran. Further, the microbially hardened substrates of the Ediacaran recorded an abundance of horizontal burrows and traces of the newly mobile organisms (Gingras *et al.,* 2011), not unlike the vertically shallow burrows and traces preserved within the Lower Triassic strata.

Echinoid debris appears exclusively within silt-rich wackestone and packstone beds of the Greisbachian age strata at Hidden Pasture. The wave-ripple cross-bedded wackestone and packstone beds and accumulations of shell hash within the echinoid-bearing units suggest a depositional environment that experienced lengthy periods of relative sea level stability (Paull *et al.*, 1989) punctuated by storm events and, thus, supports deposition on a shallow, wave dominated-shelf somewhere within the offshore transition zone or lower shoreface. Echinoid debris within the Dinwoody of Hidden Pasture appears to cease abruptly once silt input noticeably increases (above 172 m), much like the trend of echinoid disappearance at Blacktail Creek. The disappearance of echinoids throughout both Dinwoody sections appears to coincide with increasing amounts of silt within the deposited beds and, thus, deeper environments. In addition to providing potential life sustaining levels of oxygen and nutrients, the proliferation of microbial mats during the reef gap of the Early Triassic may have provided firm substrates amenable to colonization by grazing gastropods and echinoids. Although gastropods and echinoids have been known to inhabit a range of environments throughout their respective evolutionary histories, many members of each class preferentially inhabit firm or rocky substrates as such substrates often provide optimal

grazing grounds (Schneider, 2008). Thus, the possibility exists that a significant influx of silt onto the shelf could have created an unlivable substrate for echinoid populations.

Echinoids do not reappear within the measured Hidden Pasture section until the wackestone and packstone beds of the Thaynes Formation that were deposited by the second transgression of the Early Triassic. A near identical pattern of benthic faunal colonization appears in the Thaynes Formation as in the underlying Dinwoody Formation. The basal beds of the Thaynes Formation at Hidden Pasture contain lingulid brachiopods and bear no signs of bioturbation or sedimentary structures, suggesting a return to distal, dysoxic waters. The ammonoid, *Meekoceras*, also appears within these basal beds suggesting that pelagic organisms, such as *Meekoceras*, were less affected by dysoxic upwelling perhaps due to their habitation in the nektonic zone. The two, echinoid-bearing, bioclastic wackestone and packstone beds located at the top of the measured, shallowing-upwards section indicate a return to a habitable zone within a proposed lower shoreface environment at least in this area of the basin.

5.3 White Hills, UT

The temporal and environmental trends within the Virgin Limestone Member of the Moenkopi Formation at White Hills, UT are markedly dissimilar to those observed in the Dinwoody Formation. The Virgin Limestone Member appears to have recorded multiple, minute instances of transgression and regression within a single, greater transgressive event. Unlike the strata of the Dinwoody Formation, the strata of the Virgin Limestone Member at White Hills show fewer signs of upwelling, dysoxia, or anoxia and do not contain disaster taxa or mono-specific faunal compositions

(Hofmann *et al.,* 2013b). Additionally, the Spathian age strata of the Virgin Limestone Member displays an overall increase in diversity of trace fossils and bioturbation in comparison to the earlier, Greisbachian age strata (Pruss and Bottjer, 2004; Mata and Bottjer, 2011). This is certainly not to say that the paleocommunities recorded in the Virgin Limestone Member evaded the deleterious environmental conditions of the Early Triassic, nor can the conclusion be made that paleocommunities had fully recovered. Rather, the abundance and evenness of the benthic paleocommunities in this region suggest the presence of a more consistent habitable zone in which organisms found refuge. The sedimentary structures (ripples, hummocks, and cross-stratification), coated grains, alternating beds of silt-rich wackestone and packstone, and relatively well-preserved echinoid fossil material point to a shallow-shelf environment within the lower shoreface to offshore transition zone subject to periodic storm events.

5.4 Lost Cabin Springs, NV

The general, reoccurring trend documented by the parasequences within the Virgin Limestone Member at Lost Cabin Springs suggests shallowing from a low oxygen and, thus, ecologically suppressed, distal setting to a more densely colonized offshore transition zone and, finally, to a wave-dominated, lower to upper shoreface with increased siliciclastic input (Mata and Bottjer, 2011). The stratigraphic section at Lost Cabin Springs also contains at least three distinct microbial and stromatolite-sponge patch reefs, the first of which is bordered above and below by echinoid-bearing units. Geochemical analysis in conjunction with the presence of bivalves and burrows suggest that the microbial mounds within the upper units of the stratigraphic

section indicate an environment with sufficient oxygen to facilitate biotic recovery of benthic organisms (Marenco *et al.*, 2012). In accordance with the documentation of echinoids in all previously discussed field localities, echinoids of the Virgin Limestone Member at Lost Cabin Springs are present only within silt-limited packstone units. Thin section samples from the two echinoid-bearing beds at Lost Cabin Springs reveal matrixes containing micrite and quartz; however, the amount of carbonate cement vastly outweighs any siliciclastic input. The cross-stratification, trough-like bioclast accumulations, fragmented nature of shells, and coated grains within the two echinoid-bearing units suggest deposition within storm-dominated environments. The relatively even faunal compositions of both echinoid-bearing units indicate that the paleoenvironments were oxygenated enough to support benthic colonization. Even though the Virgin Limestone Member at Lost Cabin Springs records an overall deeper marine facies than that at White Hills, UT the dense packstone within the section suggest the presence of numerous, temporality varied habitable zones as environments fluctuated between upper and lower shoreface to offshore transition zones.

5.5 Paleoecology of the Habitable Zone

As defined by Beatty *et al.* (2008), the occurrence of a habitable zone within a paleo-setting relies principally upon: 1) water depth relative to a benthic profile; 2) a regular influx of wave-generated oxygen; and 3) a location some distance away from periodic upwelling of dysoxic/anoxic waters. The multiple transgressive and regressive events throughout the Early Triassic are hypothesized to have facilitated the formation, migration, and local disappearance of habitable zones. The appearance and

disappearance of the habitable zone within the Lower Triassic strata of the western U.S. can be tracked through notation of fluctuations in faunal diversity as it relates to depositional environment. For example, decreases in faunal diversity were often observed in beds at all field localities that displayed an increased deposition of laminar mud or silt, little to no evidence of colonization by benthic fauna, and an increased abundance of disaster taxa such as lingulid brachiopods and bivalves such as *Claraia* (Figs. 37 & 42). These features are indicative of offshore deposition where the habitable zone would have been eliminated due to proximity to dysoxic and anoxic waters.

Further, oxygen stress caused by elevated levels of atmospheric CO_2 is hypothesized to have acted as a key, "top-down", exclusionary factor for shallow benthic paleocommunities during the Early Triassic (Fraiser and Bottjer, 2007a). Because the ocean provides a large sink for increased amounts of atmospheric CO_2, the resulting shift in seawater pH and decline in seawater carbonate ion concentrations would have placed metabolic and physiological restrictions on benthic organism biomineralization, limiting the growth of calcifying marine organisms and potentially triggering their dissolution (Fraiser and Bottjer, 2007a; Ries, 2012). Many marine invertebrates, of which echinoids are included, produce skeletons comprised of high-Mg calcite, a mineral solubility that becomes highly vulnerable in waters with elevated levels of dissolved CO_2 (Ries *et al.*, 2009). As documented by the fluctuations in diversity and evenness throughout the echinoid-bearing beds of the observed Lower Triassic strata, the combined effects of distal noxious waters and elevated levels of atmospheric CO_2 ensured that recovery of benthic marine communities was not linear (Figs. 41-45). However, identifying environments in which echinoids and other vulnerable taxonomic

groups (e.g. bivalves and gastropods) constitute abundant and diverse communities can provide a more precise location of the habitable zone within the lower shorefaces and transition zones, so as to be sufficiently removed from "bottom-up" and "top-down" extinction pressures.

All of the echinoid-bearing beds contain one or more additional taxa indicative of oxygen saturated environments such as gastropods, rhynchonelliform brachiopods, and crinoids. The presence of oxygen sensitive organisms amidst the wave-mediated sedimentary structures in the wackestone and packstone beds suggests regular aeration and mixing of waters by wave interaction and storm events. Further, the diversity and abundance of readily identifiable shell material (e.g. intact echinoid spines and test plates) in the echinoid-bearing beds indicates that oxygen-carrying waves did not create an environment so violent as to be uninhabitable by benthic fauna. Although some of the echinoid-bearing beds within the Dinwoody Formation at Blacktail Creek and Hidden Pasture, MT contain linguilid brachiopods (Figs. 36 & 37), an organism tolerant of low oxygen levels, their presence amongst the larger paleocommunity in these beds likely reflects the opportunistic nature of lingulids rather than an oxygen-depleted environment.

The echinoid-bearing wackestone and packstone beds observed within the Lower Triassic strata contained at least 3 or more, higher taxonomic groups (Figs. 36-40). Alpha diversity indices *H'* and *1-D* suggest that some environments, herein determined to be habitable zones, were able to support relatively diverse paleocommunities with evenness and dominance values ranging from 0.7-0.98 and 0.55-0.79, respectively (Figs. 41-45). Investigations made by Boyer *et al.* (2004) of

the Lower Triassic strata of the western U.S. found that the taxonomic diversity of bioclasts was consistently low throughout the Early Triassic, but appeared to increase through the three Early Triassic time intervals. Their reported values for dominance (*1/D*) and evenness (*H'*) calculated from in-field and hand sample quantifications of the Greisbachian age strata at Hidden Pasture, MT range from 0-0.135 and 0-0.303, respectively (Boyer *et al.,* 2004). Additionally, values are provided from the quantification of Spathian age strata of the Thaynes Fm. and Virgin Limestone Member wherein dominance (*1/D*) and evenness (*H'*) range from 0-0.674 and 0-1.209, respectively (Boyer *et al.*, 2004). The diversity indices calculated by Boyer *et al.* (2004) are drastically lower than the indices calculated in this study and likely reflect dissimilarities in quantification methods and overall objectives between studies. Firstly, the analyses of taxonomic diversity by Boyer *et al.* (2004) are based on semi-quantitative methods that produce quick and accurate estimates of bioclastic fabrics and depositional environments (Kidwell *et al.*, 1986; Kidwell, 1991; Kidwell & Holland, 1991) in the field and require a relatively small sampling of bioclasts in comparison to the sampling requirements of point count analysis conducted in the study herein. Further, the methods used by Boyer *et al.* (2004) exclude quantification of bioclasts less than 2 mm in size, as shell fragments less than 2 mm in size can, in general, prove difficult to accurately identify in the field. Due to the overall miniaturization of organisms in the Early Triassic (Twitchett, 2007), taxonomic diversity estimates based on point counts in thin section may provide a less biased, more inclusive assessment of Early Triassic paleocommunities. Secondly, the purpose of this study was to identify habitable zones, areas with the highest taxonomic diversity, within the Lower Triassic strata of the

western U.S., of which the calculated diversity indices are intended to reflect.

Habitable zones within the studied Lower Triassic strata contain faunal communities with evenness values suggestive of recovered communities (e.g. 0.90–0.98) (Figs. 41–45). Moreover, the calculated evenness values suggest that habitable zones present within the earliest time interval of the Early Triassic, the Greisbachian (H'/H_{max}: 0.7–0.98), were just as likely to contain diverse faunal communities as habitable zones within later time intervals (H'/H_{max}: 0.76–0.96). However, the prevalence of monospecific beds and dark, oxygen-depleted beds of thinly-laminated mudstone throughout the Lower Triassic strata indicate that the habitable zone and its diverse, inhabitant fauna were not sustained for any great length of time during the Early Triassic. Additionally, the lack of temporal discrepancy in the calculated evenness values indicate that evenness may not provide the best indicator of ecological recovery or restructuring in all cases. Instead, the habitable zone seems to have provided a brief, episodic window in which a few otherwise rare or absent benthic organisms could proliferate just enough to maintain their evolutionary progression into later geologic time.

The abundance of echinoids within a particular bed did not always reflect the overall diversity or evenness of paleocommunities within the habitable zone, as some instances in this study show a decoupling of echinoid abundance and faunal diversity. For instance, although echinoid abundance increases upsection from Bed 2 to Bed 3 in the Dinwoody Formation at Blacktail Creek, MT (Fig. 46) and similarly from Bed 1 to Bed 2 in the Virgin Limestone Member at White Hills, UT (Fig. 48), the faunal compositions between the two beds decrease in diversity and evenness, respectively

(Fig. 41 & 44). Similarly, even though echinoids become less abundant upsection in the Virgin Limestone Member at Lost Cabin Springs, NV (Fig. 49), overall faunal diversity and evenness increase from Bed 1 to Bed 2 (Fig. 45). The fluctuating abundances of faunal constituents, including echinoids, suggest that while habitable zones provided refuge from deleterious environmental conditions, organisms within these environments were not removed from the complex, selective pressures of a functioning ecosystem. Such an instance in which selective pressures may have favored members of the Modern Fauna to those of the Paleozoic Fauna can be seen in the echinoid-bearing beds at White Hills, UT where the disappearance of crinoids coincides with an increasing abundances of echinoids and gastropods upsection (Figs. 39 & 48).

Although echinoids do not constitute the dominant fauna in any of the beds sampled, the prevalence of echinoids, as a member of the Modern Fauna, within the Lower Triassic strata of the western U.S. perfectly illustrates the transition from the Paleozoic Fauna to the Modern Fauna following the PTME. Based upon previous paleoecological studies of the Lower Triassic strata of the western U.S. (e.g. Fraiser and Bottjer, 2007b; Clapham *et al.*, 2013; Hofmann, 2013b) as well as the point counts preformed in this study, members of the Modern Fauna, namely bivalves and gastropods, constitute the most abundant and, often, dominant taxon throughout the entirety of the Early Triassic. Although neither bivalves nor gastropods are the specific focus of analysis in this study, their unequivocal abundance further exemplifies the ecological shift between Paleozoic and Modern Faunas.

Fossil records of echinoids indicate that regular echinoids, such as *Miocidaris*, preferred habitation upon firm or rocky substrates (Barnes, 1989). Moreover,

observations of Modern echinoid life habits provide evidence that most regular species preferentially inhabited high-energy environments with hard or firm substrates on which they can graze (Ausich and Webster, 2008; Schneider, 2008). In this study, the limited presence of silt in beds containing echinoids and the occurrence of filter feeding organisms such as crinoids and rhynchonelliform brachiopods further suggests that Early Triassic paleocommunities existed in habitable zones subject to regular mud-winnowing through wave interaction. As such, a large influx of silt would have fouled the waters for filter feeding organisms and produced sediments potentially too soupy for echinoid habitation. The overall restriction of echinoids to the taxonomically diverse, wave-mediated, shallow water deposits of the Lower Triassic strata of the western U.S. deem echinoids a usable, local proxy for identification of the habitable zone.

6. Conclusions

The distribution of echinoids in Early Triassic, benthic paleocommunities appears to have relied largely on the presence or absence of habitable zones. Echinoids within the Lower Triassic strata of the western U.S. appear strictly within lithologies that indicated shallow water deposition, often in association with wave-mediated sedimentary structures. Although oxygen levels constitute the fundamental selective ecological parameter for the habitable zone, field observations and paleoecological analysis suggest that sedimentation patterns as they relate to substrate may have mediated echinoid proliferation as well. Echinoids consistently appeared exclusively within strata that qualify as habitable zones, thus echinoids provide a practical proxy for identification of the habitable zone within Lower Triassic strata of the western United States.

Nearly 950 species of echinoids contribute to the vast biodiversity of invertebrates living within modern marine systems (Kroh, 2010), thus an understanding of echinoid survival during the Permo-Triassic mass extinction and aftermath can provide insight into the evolutionary pressure currently placed upon marine ecosystems and aid in combating the depletion of ecologically essential members of struggling marine environments, like marine invertebrates. In this study, I have shown that even amidst deleterious environmental conditions, simple, yet diverse, ecological communities can persist given the proper conditions for survival.

References

Algeo, T.J., Chen, Z.Q., Fraiser, M.L., Twitchett, R.J., 2011. Terrestrial–marine teleconnections in the collapse and rebuilding of Early Triassic marine ecosystems. Palaeogeogr. , Palaeoclimatol. , Palaeoecol. 308, 1-11.

Algeo, T.J., Hinnov, L., Moser, J., Maynard, J.B., Elswick, E., Kuwahara, K., Sano, H., 2010. Changes in productivity and redox conditions in the Panthalassic Ocean during the latest Permian. Geology 38, 187-190.

Alroy, J., Aberhan, M., Bottjer, D.J., Foote, M., Fursich, F.T., Harries, P.J., Hendy, A.J., Holland, S.M., Ivany, L.C., Kiessling, W., Kosnik, M.A., Marshall, C.R., McGowan, A.J., Miller, A.I., Olszewski, T.D., Patzkowsky, M.E., Peters, S.E., Villier, L., Wagner, P.J., Bonuso, N., Borkow, P.S., Brenneis, B., Clapham, M.E., Fall, L.M., Ferguson, C.A., Hanson, V.L., Krug, A.Z., Layou, K.M., Leckey, E.H., Nurnberg, S., Powers, C.M., Sessa, J.A., Simpson, C., Tomasovych, A., Visaggi, C.C., 2008. Phanerozoic trends in the global diversity of marine invertebrates. Science 321, 97-100.

Ausich, W.I., Webster, G.D., 2008. Echinoderm Paleobiology. Indiana University Press.

Bambach, R.K., Knoll, A.H., Wang, S.C., 2004. Origination, extinction, and mass depletions of marine diversity. Paleobiology 30, 522-542.

Barnes, R., 1989. What, if anything, is a brackish-water fauna. Transactions of the Royal Society of Edinburgh: Earth Sciences 80, 235-240.

Beatty, T.W., Zonneveld, J., Henderson, C.M., 2008. Anomalously diverse Early Triassic ichnofossil assemblages in northwest Pangea: a case for a shallow-marine habitable zone. Geology 36, 771-774.

Bottjer, D.J., Clapham, M.E., Fraiser, M.L., Powers, C.M., 2008. Understanding mechanisms for the end-Permian mass extinction and the protracted Early Triassic aftermath and recovery. GSA Today 18, 4-10.

Bottjer, D.J., Droser, M.L., 1991. Ichnofabric and basin analysis. Palaios , 199-205.

Bottjer, D.J., Schubert, J.K., Droser, M.L., 1996. Comparative evolutionary palaeoecology: assessing the changing ecology of the past. Geological Society, London, Special Publications 102, 1-13.

Boutwell, J.M., 1907. Stratigraphy and structure of the Park City mining district, Utah. J. Geol. 15, 434-458.

Boyer, D.L., Bottjer, D.J., Droser, M.L., 2004. Ecological signature of Lower Triassic shell beds of the western United States. Palaios 19, 372-380.

Brayard, A., Escarguel, G., Bucher, H., Monnet, C., Bruhwiler, T., Goudemand, N., Galfetti, T., Guex, J., 2009. Good genes and good luck: ammonoid diversity and the end-Permian mass extinction. Science 325, 1118-1121.

Brennecka, G.A., Herrmann, A.D., Algeo, T.J., Anbar, A.D., 2011. Rapid expansion of oceanic anoxia immediately before the end-Permian mass extinction. Proceedings of the National Academy of Sciences 108, 17631-17634.

Carr, T.R., Paull, R.K., 1983. Early Triassic stratigraphy and paleogeography of the Cordilleran miogeocline.

Chen, Z., Benton, M.J., 2012. The timing and pattern of biotic recovery following the end-Permian mass extinction. Nature Geoscience 5, 375-383.

Clapham, M.E., Bottjer, D.J., Powers, C.M., Bonuso, N., Fraiser, M.L., Marenco, P.J., Dornbos, S.Q., Pruss, S.B., 2006. Assessing the ecological dominance of Phanerozoic marine invertebrates. Palaios 21, 431-441.

Clapham, M.E., Fraiser, M.L., Marenco, P.J., Shen, S., 2013. Taxonomic composition and environmental distribution of post-extinction rhynchonelliform brachiopod faunas: Constraints on short-term survival and the role of anoxia in the end-Permian mass extinction. Palaeogeogr. , Palaeoclimatol. , Palaeoecol.

Clapham, M.E., Shen, S., Bottjer, D.J., 2009. The double mass extinction revisited: reassessing the severity, selectivity, and causes of the end-Guadalupian biotic crisis (Late Permian).

Dean, J.S., 1981. Carbonate Petrology and Depositional Environments: Of the Sinbad Limestone Member of the Moenkopi Formation in the Teasdale Dome Area, Wayne and Garfield Counties, Utah. . Carbonate Petrology and Depositional Environments: Of the Sinbad Limestone Member of the Moenkopi Formation in the Teasdale Dome Area, Wayne and Garfield Counties, Utah .

De Brun, P. and L. Vedel. 1919. Étude géologique et paléontologique des environs de St.-Ambroix (Gard): Première partie (Houiller, Trias, Infralias). Imprimerie Générale. Nimes. 120.

Döderlein, L., 1887. Die Japanischen Seeigel. E. Schweizerbart'sche Verlagshandlung.

Doney, S.C., Fabry, V.J., Feely, R.A., Kleypas, J.A., 2009. Ocean acidification: the other CO2 problem. Marine Science 1.

Downing, A.L., Leibold, M.A., 2002. Ecosystem consequences of species richness and composition in pond food webs. Nature 416, 837-841.

Droser, M.L., Bottjer, D.J., Sheehan, P.M., McGhee, G.R., 2000. Decoupling of taxonomic and ecologic severity of Phanerozoic marine mass extinctions. Geology 28, 675-678.

Durham, J., Caster, K., Exline, H., Fell, H., Fischer, A., Frizzell, D., Kesling, R., Kier, P., Melville, R., Moore, R., 1966. Part U, Echinodermata 3. Treatise on invertebrate palaeontology.University of Kansas Press, Lawrence , 1-366.

Erwin, D.H., 2000. The permo-triassic extinction. Shaking the Tree: Readings from Nature in the History of Life , 189.

Erwin, D.H., 1996. Understanding biotic recoveries: extinction, survival, and preservation during the end-Permian mass extinction. Evolutionary paleobiology.University of Chicago Press, Chicago , 398-418.

Erwin, D.H., 1994. Early introduction of major morphological innovations. Acta Palaeontol. Pol. 38, 4.

Fagerstrom, J.A., 1987. The Evolution of Reef Communities. Wiley New York.

Flügel, E., 2002. Triassic reef patterns.

Fraiser, M.L., Bottjer, D.J., 2007a. Elevated atmospheric CO< sub> 2 and the delayed biotic recovery from the end-Permian mass extinction. Palaeogeogr. , Palaeoclimatol. , Palaeoecol. 252, 164-175.

Fraiser, M.L., Bottjer, D.J., 2007b. When bivalves took over the world. Paleobiology 33, 397-413.

Fraiser, M.L., Bottjer, D.J., 2005a. Fossil preservation during the aftermath of the end-Permian mass extinction: Taphonomic processes and palaeoecological signals. Developments in Palaeontology and Stratigraphy 20, 299-311.

Fraiser, M.L., Bottjer, D.J., 2005b. Restructuring in benthic level-bottom shallow marine communities due to prolonged environmental stress following the end-Permian mass extinction. Comptes Rendus Palevol 4, 583-591.

Fraiser, M.L., Bottjer, D.J., 2004. The non-actualistic Early Triassic gastropod fauna: a case study of the Lower Triassic SinbadLimestone member. Palaios 19, 259-275.

Fraiser, M., Bottjer, D., 2009a. Opportunistic behaviour of invertebrate marine tracemakers during the Early Triassic aftermath of the end-Permian mass extinction. Aust. J. Earth Sci. 56, 841-857.

Fraiser, M., Bottjer, D., 2009b. Opportunistic behaviour of invertebrate marine tracemakers during the Early Triassic aftermath of the end-Permian mass extinction. Aust. J. Earth Sci. 56, 841-857.

Gingras, M., Hagadorn, J.W., Seilacher, A., Lalonde, S.V., Pecoits, E., Petrash, D., Konhauser, K.O., 2011. Possible evolution of mobile animals in association with microbial mats. Nature Geoscience 4, 372-375.

Grasby, S.E., Beauchamp, B., 2009. Latest Permian to Early Triassic basin-to-shelf anoxia in the Sverdrup Basin, Arctic Canada. Chem. Geol. 264, 232-246.

Grice, K., Cao, C., Love, G.D., Böttcher, M.E., Twitchett, R.J., Grosjean, E., Summons, R.E., Turgeon, S.C., Dunning, W., Jin, Y., 2005. Photic zone euxinia during the Permian-Triassic superanoxic event. Science 307, 706-709.

Grime, J.P., 1997. Biodiversity and ecosystem function: the debate deepens. Science-New York Then Washington, 1260-1261.

Hallam, A., 1991. Why was there a delayed radiation after the end-Palaeozoic extinctions? Hist. Biol. 5, 257-262.

Hallam, A., Wignall, P.B., 1997. Mass Extinctions and their Aftermath. Oxford University Press.

Hammer, Ø, Harper, D.A., 2008. Paleontological Data Analysis. John Wiley & Sons.

Harries, P.J., Knorr, P.O., 2009. What does the 'Lilliput Effect'mean? Palaeogeogr. , Palaeoclimatol. , Palaeoecol. 284, 4-10.

Hofmann, R., Hautmann, M., Bucher, H., 2013a. A New Paleoecological Look at the Dinwoody Formation (Lower Triassic, Western USA): Intrinsic Versus Extrinsic Controls on Ecosystem Recovery After the End-Permian Mass Extinction. J. Paleontol. 87, 854-880.

Hofmann, R., Hautmann, M., Wasmer, M., Bucher, H., 2013b. Palaeoecology of the Spathian Virgin Formation (Utah, USA) and its implications for the Early Triassic recovery. Acta Palaeontol. Pol. 58, 149-173.

Hughes, L., 2000. Biological consequences of global warming: is the signal already apparent? Trends in Ecology & Evolution 15, 56-61.

Jacobsen, N.D., Twitchett, R.J., Krystyn, L., 2011. Palaeoecological methods for assessing marine ecosystem recovery following the Late Permian mass extinction event. Palaeogeogr. , Palaeoclimatol. , Palaeoecol. 308, 200-212.

Joachimski, M.M., Lai, X., Shen, S., Jiang, H., Luo, G., Chen, B., Chen, J., Sun, Y., 2012. Climate warming in the latest Permian and the Permian–Triassic mass extinction. Geology 40, 195-198.

Kidder, D.L., Worsley, T.R., 2004. Causes and consequences of extreme Permo-Triassic warming to globally equable climate and relation to the Permo-Triassic extinction and recovery. Palaeogeogr. , Palaeoclimatol. , Palaeoecol. 203, 207-237.

Kidwell, S.M., Bosence, D.W., 1991. Taphonomy and time-averaging of marine shelly faunas. Taphonomy: releasing the data locked in the fossil record.Plenum, New York , 115-209.

Kidwell, S.M., Flessa, K.W., 1996. The quality of the fossil record: populations, species, and communities 1. Annu. Rev. Earth Planet. Sci. 24, 433-464.

Kidwell, S.M., Fuersich, F.T., Aigner, T., 1986. Conceptual framework for the analysis and classification of fossil concentrations. Palaios 1, 228-238.

Kidwell, S.M., Holland, S.M., 1991. Field description of coarse bioclastic fabrics. Palaios , 426-434.

Kier, P.M., 1968a. Nortonechinus and the ancestry of the cidarid echinoids. J. Paleontol. , 1163-1170.

Kier, P.M., 1968b. The Triassic echinoids of North America. J. Paleontol. , 1000-1006.

Kiessling, W., Roniewicz, E., Villier, L., Léonide, P., Struck, U., 2009. An early Hettangian coral reef in southern France: Implications for the end-Triassic reef crisis. Palaios 24, 657-671.

Knoll, A.H., Bambach, R.K., Payne, J.L., Pruss, S., Fischer, W.W., 2007. Paleophysiology and end-Permian mass extinction. Earth Planet. Sci. Lett. 256, 295-313.

Knoll, A.H., Bambach, R., Canfield, D., Grotzinger, J., 1996. Comparative Earth history and Late Permian mass extinction. Science-New York Then Washington, 452-457.

Korkina, L.G., Deeva, I.B., De Biase, A., Iaccarino, M., Oral, R., Warnau, M., Pagano, G., 2000. Redox-dependent toxicity of diepoxybutane and mitomycin C in sea urchin embryogenesis. Carcinogenesis 21, 213-220.

Kroh, A., 2010. Index of Living and Fossil Echinoids. Annalen des naturhistorischen Museums in Wien, serie A 112, 195-470.

Kummel, B., 1954. Triassic Stratigraphy of Southeastern Idaho and Adjacent Areas. US Government Printing Office.

Kummel, B., 1943. The Thaynes Formation, Bear Lake Valley, Idaho. Am. J. Sci. 241, 316-332.

Kump, L.R., Pavlov, A., Arthur, M.A., 2005. Massive release of hydrogen sulfide to the surface ocean and atmosphere during intervals of oceanic anoxia. Geology 33, 397-400.

Larson, A.R., 1966. Stratigraphy and paleontology of the Moenkopi Formation in southern Nevada .

Lehrmann, D.J., Ramezani, J., Bowring, S.A., Martin, M.W., Montgomery, P., Enos, P., Payne, J.L., Orchard, M.J., Hongmei, W., Jiayong, W., 2006. Timing of recovery from the end-Permian extinction: Geochronologic and biostratigraphic constraints from south China. Geology 34, 1053-1056.

Marenco, P.J., Griffin, J.M., Fraiser, M.L., Clapham, M.E., 2012. Paleoecology and geochemistry of Early Triassic (Spathian) microbial mounds and implications for anoxia following the end-Permian mass extinction. Geology 40, 715-718.

Mata, S.A., Bottjer, D.J., 2011. Origin of Lower Triassic microbialites in mixed carbonate-siliciclastic successions: ichnology, applied stratigraphy, and the end-Permian mass extinction. Palaeogeogr. , Palaeoclimatol. , Palaeoecol. 300, 158-178.

Mata, S.A., Bottjer, D.J., 2009. The paleoenvironmental distribution of Phanerozoic wrinkle structures. Earth-Sci. Rev. 96, 181-195.

Mata, S.A., Woods, A.D., 2008. Sedimentology and paleoecology of the Lower Member of the Lower Triassic (Smithian-Spathian) Union Wash Formation, east-central California. Palaios 23, 514-524.

McKinney, M., 1988. Roles of allometry and ecology in echinoid evolution. Echinoderm Phylogeny and Evolutionary Biology.Clarendon, Oxford , 165-173.

Moffat, H.A., Bottjer, D.J., 1999. Echinoid concentration beds: two examples from the stratigraphic spectrum. Palaeogeogr. , Palaeoclimatol. , Palaeoecol. 149, 329-348.

Newell, N.D., 1952. Periodicity in invertebrate evolution. J. Paleontol. , 371-385.

Newell, N.D., Kummel, B., 1942. Lower Eo-triassic stratigraphy, western Wyoming and southeast Idaho. Geological Society of America Bulletin 53, 937-995.

Paull, R.K., Paull, R.A., 1994a. Lower Triassic transgressive-regressive sequences in the Rocky Mountains, eastern Great Basin, and Colorado Plateau, USA.

Paull, R.K., Paull, R.A., 1994b. Shallow marine sedimentary facies in the earliest Triassic (Griesbachian) Cordilleran miogeocline, USA. Sediment. Geol. 93, 181-191.

Paull, R.K., Paull, R.A., 1983. Revision of type Lower Triassic Dinwoody Formation, Wyoming, and designation of principal reference section. Rocky Mountain Geology 22, 83-90.

Paull, R.A., Paull, R.K., 1986. Depositional history of Lower Triassic Dinwoody Formation, Bighorn Basin, Wyoming and Montana. Am.Assoc.Pet.Geol., Bull.;(United States) 70.

Paull, R.A., Paull, R.K., Kraemer, B.R., 1989. Depositional history of Lower Triassic rocks in southwestern Montana and adjacent parts of Wyoming and Idaho.

Payne, J.L., Lehrmann, D.J., Wei, J., Knoll, A.H., 2006. The pattern and timing of biotic recovery from the end-Permian extinction on the Great Bank of Guizhou, Guizhou Province, China. Palaios 21, 63-85.

Pruss, S.B., Bottjer, D.J., 2005. The reorganization of reef communities following the end-Permian mass extinction. Comptes Rendus Palevol 4, 553-568.

Pruss, S.B., Bottjer, D.J., 2004. Early Triassic trace fossils of the western United States and their implications for prolonged environmental stress from the end-Permian mass extinction. Palaios 19, 551-564.

Pruss, S.B., Bottjer, D.J., Corsetti, F.A., Baud, A., 2006. A global marine sedimentary response to the end-Permian mass extinction: examples from southern Turkey and the western United States. Earth-Sci. Rev. 78, 193-206.

Raup, D.M., 1979. Size of the permo-triassic bottleneck and its evolutionary implications. Science 206, 217-218.

Raup, D.M., Sepkoski, J.J.,Jr, 1982. Mass extinctions in the marine fossil record. Science 215, 1501-1503.

Reif, D.M., Slatt, R.M., 1979. Red bed members of the Lower Triassic Moenkopi Formation, southern Nevada; sedimentology and paleogeography of a muddy tidal flat deposit. Journal of Sedimentary Research 49, 869-889.

Ries, J.B., 2012. Oceanography: A sea butterfly flaps its wings. Nature Geoscience 5, 845-846.

Ries, J.B., Cohen, A.L., McCorkle, D.C., 2009. Marine calcifiers exhibit mixed responses to CO2-induced ocean acidification. Geology 37, 1131-1134.

Rodland, D.L., Bottjer, D.J., 2001. Biotic recovery from the end-Permian mass extinction: behavior of the inarticulate brachiopod Lingula as a disaster taxon. Palaios 16, 95-101.

Schaefer, S. N. 2012. Distribution of Early Triassic rhynchonelliform brachiopods in the Dinwoody Basin of the western United States: A test of the habitable zone hypothesis. M.S. thesis, University of Wisconsin-Milwaukee, Milwaukee, Wisconsin.

Schneider, C.L., 2008. The Importance of echinoids In Late Paleozoic Ecosystems. Echinoderm Paleobiology , 71.

Schock, W.W., 1981. Stratigraphy and paleontology of the Lower Dinwoody Formation and its relation to the Permian-Triassic boundary in western Wyoming, southeastern Idaho and southwestern Montana.

Schubert, J.K., Bottjer, D.J., 1995. Aftermath of the Permian-Triassic mass extinction event: Paleoecology of Lower Triassic carbonates in the western USA. Palaeogeogr. , Palaeoclimatol. , Palaeoecol. 116, 1-39.

Sepkoski, J.J., Bambach, R.K., Raup, D.M., Valentine, J.W., 1981. Phanerozoic marine diversity and the fossil record. Nature 293, 435-437.

Shannon, C.E., Weaver, W., 1949. The mathematical theory of information.

Sheehan, P.M., Harris, M.T., 2004. Microbialite resurgence after the Late Ordovician extinction. Nature 430, 75-78.

Shen, S.Z., Crowley, J.L., Wang, Y., Bowring, S.A., Erwin, D.H., Sadler, P.M., Cao, C.Q., Rothman, D.H., Henderson, C.M., Ramezani, J., Zhang, H., Shen, Y., Wang, X.D., Wang, W., Mu, L., Li, W.Z., Tang, Y.G., Liu, X.L., Liu, L.J., Zeng, Y., Jiang, Y.F., Jin, Y.G., 2011. Calibrating the end-Permian mass extinction. Science 334, 1367-1372.

Simpson, E.H., 1949. Measurement of diversity. Nature .

Smith, A., Hollingworth, N., 1990. Tooth structure and phylogeny of the Upper Permian echinoid *Miocidaris* keyserlingi. 48, 47-60.

Smith, A.B., 1984. Echinoid Palaeobiology. Allen & Unwin London.

Song, H., Tong, J., Xiong, Y., Sun, D., Tian, L., Song, H., 2012a. The large increase of δ 13Ccarb-depth gradient and the end-Permian mass extinction. Science China Earth Sciences 55, 1101-1109.

Song, H., Wignall, P.B., Tong, J., Bond, D.P., Song, H., Lai, X., Zhang, K., Wang, H., Chen, Y., 2012b. Geochemical evidence from bio-apatite for multiple oceanic anoxic events during Permian–Triassic transition and the link with end-Permian extinction and recovery. Earth Planet. Sci. Lett. 353, 12-21.

Song, H., Wignall, P.B., Tong, J., Yin, H., 2013. Two pulses of extinction during the Permian-Triassic crisis. Nature Geoscience 6, 52-56.

Stanley, S.M., 2007. An analysis of the history of marine animal diversity. Paleobiology 33, 1-55.

Sun, Y., Joachimski, M.M., Wignall, P.B., Yan, C., Chen, Y., Jiang, H., Wang, L., Lai, X., 2012. Lethally hot temperatures during the Early Triassic greenhouse. Science 338, 366-370.

Symstad, A.J., Tilman, D., Willson, J., Knops, J.M., 1998. Species loss and ecosystem functioning: effects of species identity and community composition. Oikos , 389-397.

Twitchett, R.J., 2007. The Lilliput effect in the aftermath of the end-Permian extinction event. Palaeogeogr. , Palaeoclimatol. , Palaeoecol. 252, 132-144.

Twitchett, Richard J. Oji, Tatsuo. 2005. Early Triassic recovery of echinoderms. Elsevier SAS. Pp. 1-12.

Tyson, R., Pearson, T., 1991. Modern and ancient continental shelf anoxia: an overview. Geological Society, London, Special Publications 58, 1-24.

Urbanek, A., 1993. Biotic crises in the history of Upper Silurian graptoloids: a palaeobiological model. Hist. Biol. 7, 29-50.

Van der Plas, L., Tobi, A., 1965. A chart for judging the reliability of point counting results. Am. J. Sci. 263, 87-90.

Wagner, P.J., Aberhan, M., Hendy, A., Kiessling, W., 2007. The effects of taxonomic standardization on sampling-standardized estimates of historical diversity. Proc. Biol. Sci. 274, 439-444.

Wallace, D., Wirick, C., 1992. Large air–sea gas fluxes associated with breaking waves.

Webster, S.K., Giese, A.C., 1975. Oxygen consumption of the purple sea urchin with special reference to the reproductive cycle. Biol. Bull. 148, 165-180.

Wignall, P.B., Twitchett, R.J., 2002. Extent, duration, and nature of the Permian-Triassic superanoxic event. Special Papers-Geological Society of America, 395-414.

Wignall, P.B., Sun, Y., Bond, D.P., Izon, G., Newton, R.J., Vedrine, S., Widdowson, M., Ali, J.R., Lai, X., Jiang, H., Cope, H., Bottrell, S.H., 2009. Volcanism, mass extinction, and carbon isotope fluctuations in the Middle Permian of China. Science 324, 1179-1182.

Zonneveld, J., Gingras, M.K., Beatty, T.W., 2010. Diverse ichnofossil assemblages following the PT mass extinction, Lower Triassic, Alberta and British Columbia, Canada: evidence for shallow marine refugia on the northwestern coast of Pangaea. Palaios 25, 368-392.

Appendix A

Blacktail Creek, Montana

Satellite Map

Google satellite map of Blacktail Creek, Montana field site. The yellow star indicates the base of the section located at approximately 44°44’50.91”N 112°17’39.47”W.

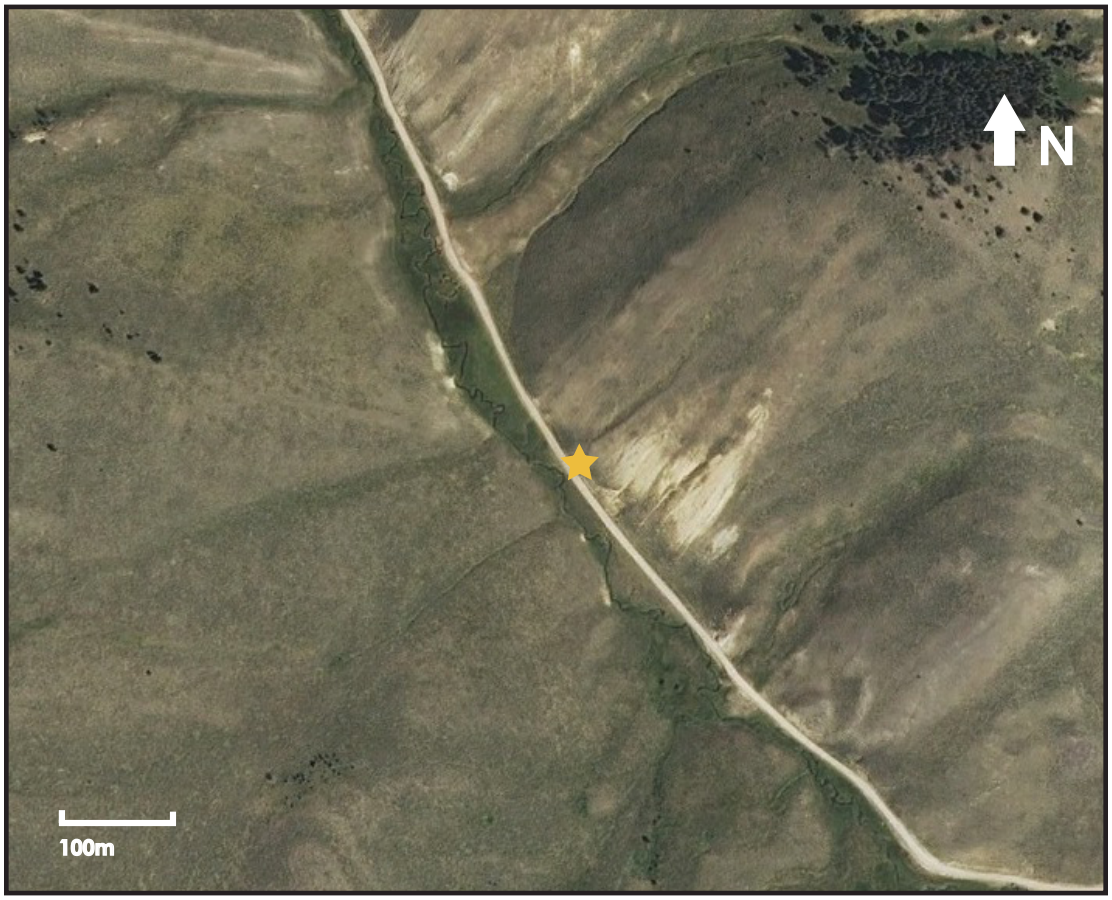

Appendix B
Hidden Pasture, Montana
Satellite Map

Google satellite map of Hidden Pasture, Montana field site. The yellow star indicates the base of the section located at approximately 44°41'15.70"N 112°47'1.00"W.

Appendix C
Bear Lake, Idaho
Satellite Map

Google satellite map of Bear Lake, Idaho field site. The yellow star indicates the base of the section located at approximately 42°6'42.96"N 111°15'24.90"W.

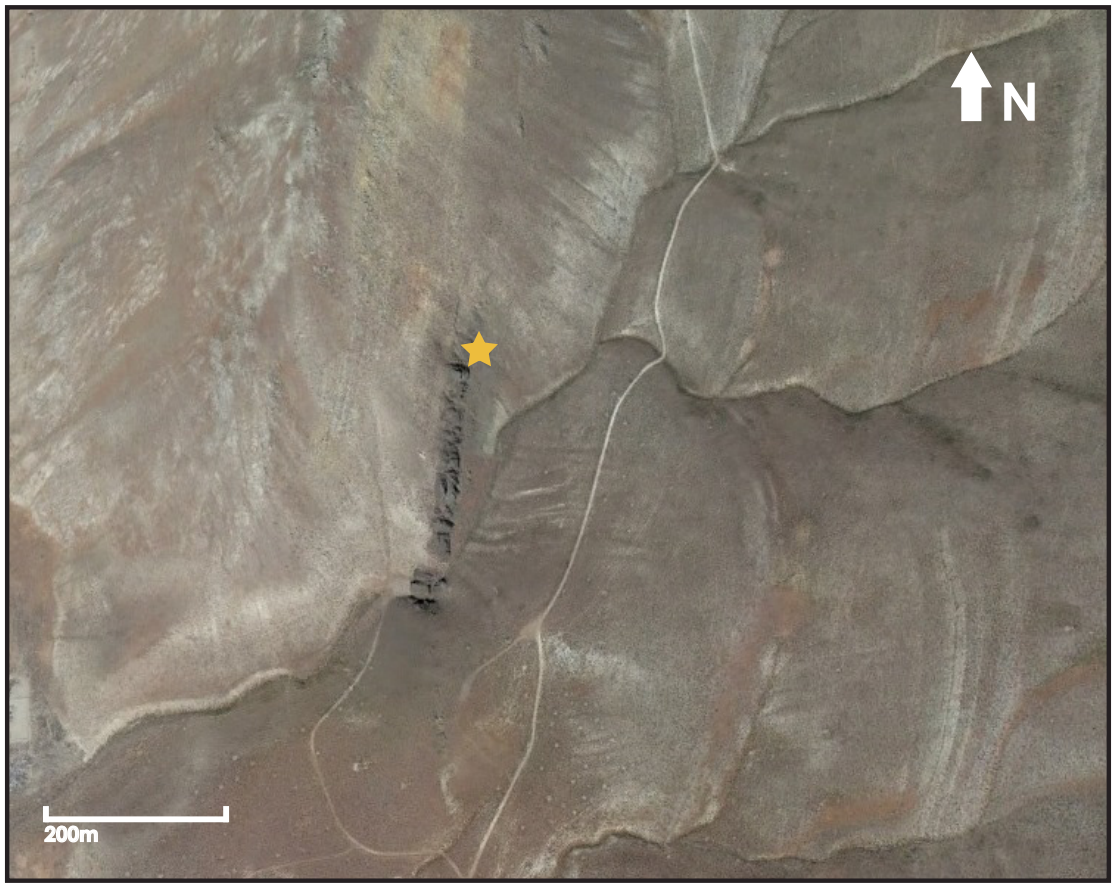

Appendix D
Montpelier Canyon, Idaho
Satellite Map

Google satellite map of Montpelier Canyon, Idaho field site. The yellow star indicates the base of the section located at approximately 42°19'16.04"N 111°15'46.19"W.

Appendix E
White Hills, Utah
Satellite Map

Google satellite map of White Hills, Utah field site. The yellow star indicates the base of the section located at approximately 37° 2'59.46"N 113°41'17.70"W.

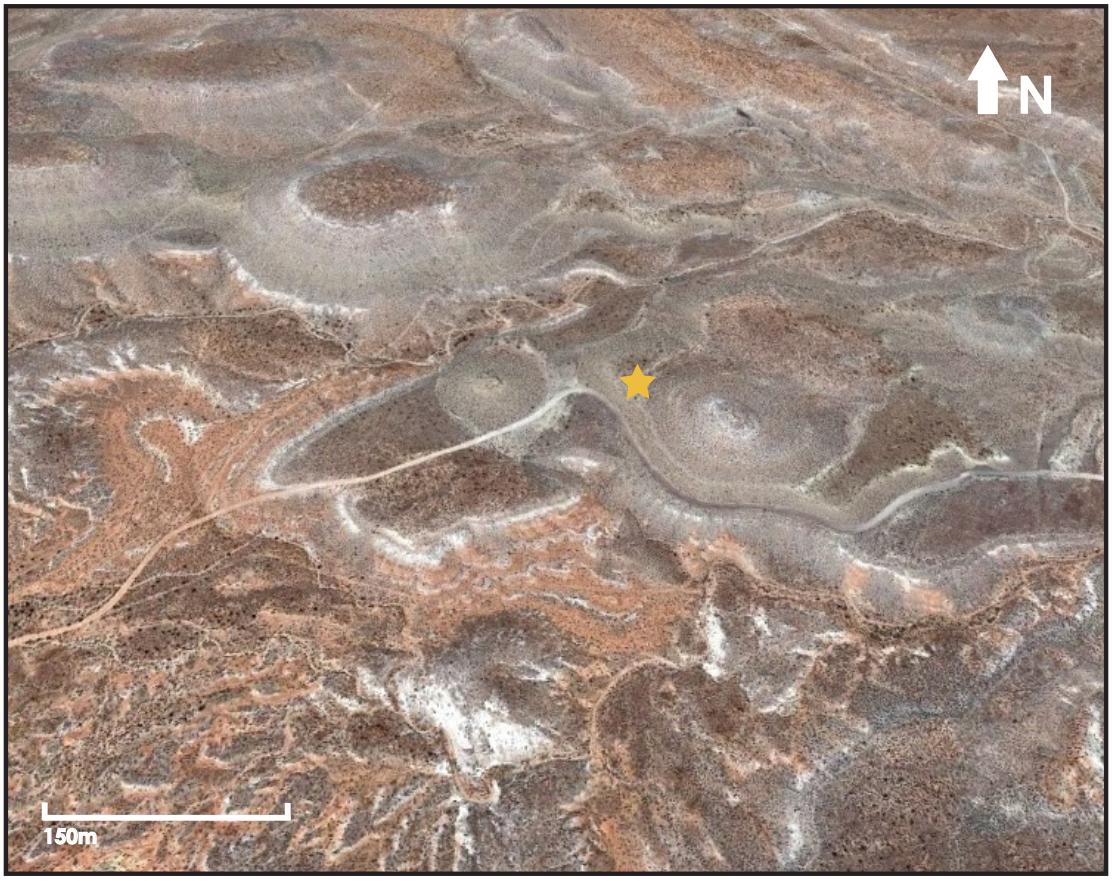

Appendix F
Lost Cabin Springs, Nevada
Satellite Map

Google satellite map of Lost Cabin Springs, Nevada field site. The yellow star indicates the base of the section located at approximately 36° 4'51.25"N 115°39'13.27"W.

Appendix G
Dinwoody Formation
Blacktail Creek, Montana
Point Count Data

Raw abundance of biotic and abiotic components in echinoid-bearing limestones from the Dinwoody Formation at Blacktail Creek, Montana. Abundances were collected through point counts in thin sections, each thin section corresponding to a sampled bed. The abundances of components obtained from each thin section are considered representative of the beds in which they were collected.

Component	Bed 2	Bed 3 (Float)	Bed 4
Sparry Calcite	141	93	53
Quartz	62	18	8
Calcite Cement	71	77	62
Micrite	32	18	9
Intraclasts	0	12	21
Echinoids	24	33	68
Crinoids	0	0	0
Bivalves	23	66	73
Gastropods	16	12	36
Brachiopods	57	8	10
Ostracods	0	0	0
Conodonts	0	0	0
Total	426	337	340

Appendix H
Dinwoody Formation
Hidden Pasture, Montana
Point Count Data

Raw abundance of biotic and abiotic components in echinoid-bearing limestones from the Dinwoody Formation at Hidden Pasture, Montana. Abundances were collected through point counts in thin sections, each thin section corresponding to a sampled bed. The abundances of components obtained from each thin section are considered representative of the beds in which they were collected.

Component	Bed 2	Bed 3	Bed 4	Bed 5	Bed 6
Sparry Calcite	145	69	54	10	19
Quartz	34	35	54	5	10
Calcite Cement	46	74	85	43	63
Micrite	42	27	5	8	5
Intraclasts	0	0	0	0	0
Echinoids	1	24	16	41	41
Crinoids	9	11	7	27	27
Bivalves	28	29	54	56	56
Gastropods	0	0	6	41	52
Brachiopods	6	56	67	87	67
Ostracods	0	0	0	0	0
Conodonts	0	0	0	0	0
Total	311	325	315	318	340

Appendix I
Thaynes Formation
Hidden Pasture, Montana
Point Count Data

Raw abundance of biotic and abiotic components in echinoid-bearing limestones from the Thaynes Formation at Hidden Pasture, Montana. Abundances were collected through point counts in thin sections, each thin section corresponding to a sampled bed. The abundances of components obtained from each thin section are considered representative of the beds in which they were collected.

Component	Bed 1	Bed 2
Sparry Calcite	77	49
Quartz	25	23
Calcite Cement	48	51
Micrite	10	3
Intraclasts	0	0
Echinoids	9	22
Crinoids	63	37
Bivalves	48	67
Gastropods	20	36
Brachiopods	12	34
Ostracods	0	0
Conodonts	0	0
Total	312	322

Appendix J
Virgin Limestone Member
White Hills, Utah
Point Count Data

Raw abundance of biotic and abiotic components in echinoid-bearing limestones from the Virgin Limestone Member of the Moenkopi Formation at White Hills, Utah. Abundances were collected through point counts in thin sections, each thin section corresponding to a sampled bed. The abundances of components obtained from each thin section are considered representative of the beds in which they were collected.

Component	**Bed 1**	**Bed 2**	**Bed 3**
Sparry Calcite	60	60	165
Quartz	0	0	57
Calcite Cement	95	138	92
Micrite	0	5	0
Intraclasts	12	6	0
Echinoids	25	57	0
Crinoids	10	0	0
Bivalves	57	55	7
Gastropods	53	123	0
Brachiopods	0	0	0
Ostracods	0	0	0
Conodonts	0	0	0
Total	312	444	321

Appendix K
Virgin Limestone Member
Lost Cabin Springs, Nevada
Point Count Data

Raw abundance of biotic and abiotic components in echinoid-bearing limestones from the Virgin Limestone Member of the Moenkopi Formation at Lost Cabin Springs, Nevada. Abundances were collected through point counts in thin sections, each thin section corresponding to a sampled bed. The abundances of components obtained from each thin section are considered representative of the beds in which they were collected.

Component	**Bed 1**	**Bed 2**
Sparry Calcite	69	38
Quartz	21	25
Calcite Cement	21	32
Micrite	8	2
Intraclasts	9	4
Echinoids	59	51
Crinoids	14	35
Bivalves	0	15
Gastropods	88	73
Brachiopods	33	26
Ostracods	0	0
Conodonts	0	0
Total	322	301

Appendix L
Dinwoody Formation
Two Sample Z Test

Results from tests of significance for the relative abundance of echinoids by bed. Tables are presented for the Dinwoody Formation at two field localities Blacktail Creek and Hidden Pasture, Montana. Echinoid abundances were obtained through point counting in thin section. All values are *p*-values obtained from Two Sample Z tests. Boldface values indicate statistically significant differences at $\alpha = 0.05$.

Blacktail Creek, MT	***P*-Value**
Bed 2 vs. Bed 3	0.08726
Bed 2 vs. Bed 4	**0.00228**
Bed 3 vs. Bed 4	0.242

Hidden Pasture, MT	***P*-Value**
Bed 2 vs. Bed 3	**0.00512**
Bed 2 vs. Bed 4	0.08364
Bed 2 vs. Bed 5	**0.0139**
Bed 2 vs. Bed 6	**0.01174**
Bed 3 vs. Bed 4	**0.03156**
Bed 3 vs. Bed 5	0.37346
Bed 3 vs. Bed 6	0.4654
Bed 4 vs. Bed 5	0.11876
Bed 4 vs. Bed 6	0.08914
Bed 5 vs. Bed 6	0.85716

Appendix M
Thaynes Formation
Two Sample Z Test

Results from tests of significance for the relative abundance of echinoids by bed. Table is presented for the Thaynes Formation at field localities Hidden Pasture, Montana. Echinoid abundances were obtained through point counting in thin section. All values are *p*-values obtained from Two Sample Z tests. Boldface values indicate statistically significant differences at $\alpha = 0.05$.

Hidden Pasture, MT	***P*-Value**
Bed 1 vs. Bed 2	0.08544

Appendix N
Virgin Limestone Member
Two Sample Z Test

Results from tests of significance for the relative abundance of echinoids by bed. Tables are presented for the Virgin Limestone Member of the Moenkopi Formation at two field localities White Hills, Utah and Lost Cabin Springs, Nevada. Echinoid abundances were obtained through point counting in thin section. All values are *p*-values obtained from Two Sample Z tests. Boldface values indicate statistically significant differences at $\alpha = 0.05$.

White Hill, UT	***P*-Value**
Bed 1 vs. Bed 2	0.1074

Lost Cabin Springs, NV	***P*-Value**
Bed 1 vs. Bed 4	0.27572

Appendix O
Dinwoody Formation
T Test

Results from tests of significance for ecological evenness of faunal composition by bed. Tables are presented for the Dinwoody Formation at two field localities Blacktail Creek and Hidden Pasture, Montana. Faunal compositions were obtained through point counting in thin section. All values are *p*-values obtained from Independent T tests. Boldface values indicate statistically significant differences at $\alpha = 0.05$.

Blacktail Creek, MT	***P*-Value**
Bed 2 vs. Bed 3	0.08726
Bed 2 vs. Bed 4	**0.00228**
Bed 3 vs. Bed 4	0.242

Hidden Pasture, MT	***P*-Value**
Bed 2 vs. Bed 3	0.1949
Bed 2 vs. Bed 4	0.1607
Bed 2 vs. Bed 5	**0.0066**
Bed 2 vs. Bed 6	**0.0016**
Bed 3 vs. Bed 4	0.7153
Bed 3 vs. Bed 5	0.095
Bed 3 vs. Bed 6	0.0681
Bed 4 vs. Bed 5	0.2472
Bed 4 vs. Bed 6	0.234
Bed 5 vs. Bed 6	0.8872

Appendix P
Thaynes Formation
T Test

Results from tests of significance for ecological evenness of faunal composition by bed. Table is presented for the Thaynes Formation at field locality Hidden Pasture, Montana. Faunal compositions were obtained through point counting in thin section. All values are *p*-values obtained from Independent T tests. Boldface values indicate statistically significant differences at $\alpha = 0.05$.

Hidden Pasture, MT	***P*–Value**
Bed 1 vs. Bed 2	0.518

Appendix Q
Virgin Limestone Member
T Test

Results from tests of significance for ecological evenness of faunal composition by bed. Tables are presented for the Virgin Limestone Member of the Moenkopi Formation at two field localities White Hills, Utah and Lost Cabin Springs, Nevada. Faunal compositions were obtained through point counting in thin section. All values are *p*-values obtained from Independent T tests. Boldface values indicate statistically significant differences at $\alpha = 0.05$.

White Hills, UT	***P*-Value**
Bed 1 vs. Bed 2	0.4457

Lost Cabin, NV	***P*-Value**
Bed 1 vs. Bed 4	0.951

Appendix R
Dinwoody Formation
Blacktail Creek, Montana
Rarefaction Curves

Rarefaction curves with 95% confidence intervals for three samples of Early Triassic fauna from the Dinwoody Formation at Blacktail Creek, Montana. Each sample represents a bed in which fossilized echinoid material was identified. The faunal composition of each bed was determined through point counts in thin section. Associations which level off indicate that further counts would not significantly increase the number of taxa found within a particular sample. Conversely, associations which have not yet leveled off indicate that further counts may have reveal additional taxa and are, thus, tentative. In all cases at this locality, sample size, or counted specimen, is greater than the number of taxa.

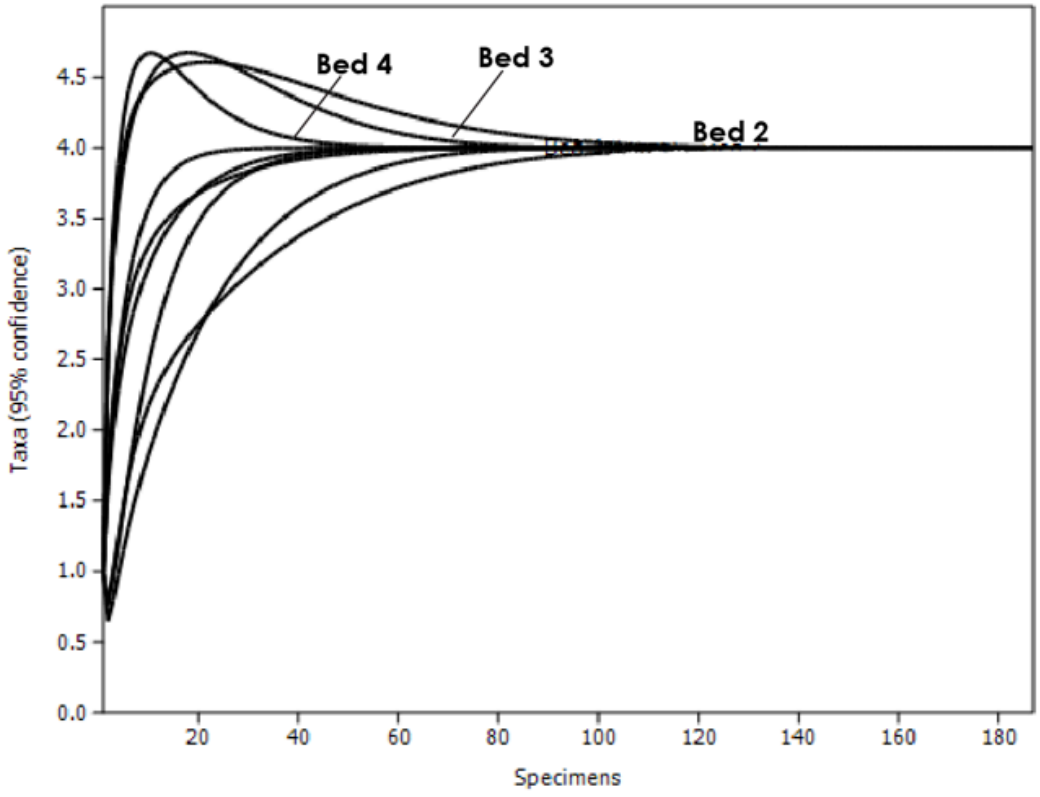

Appendix S
Dinwoody Formation
Hidden Pasture, Montana
Rarefaction Curves

Rarefaction curves with 95% confidence intervals for five samples of Early Triassic fauna from the Dinwoody Formation at Hidden Pasture, Montana. Each sample represents a bed in which fossilized echinoid material was identified. The faunal composition of each bed was determined through point counts in thin section. Associations which level off indicate that further counts would not significantly increase the number of taxa found within a particular sample. Conversely, associations which have not yet leveled off indicate that further counts may have reveal additional taxa and are, thus, tentative. In all cases except Bed 2 at this locality, sample size, or counted specimen, is greater than the number of taxa.

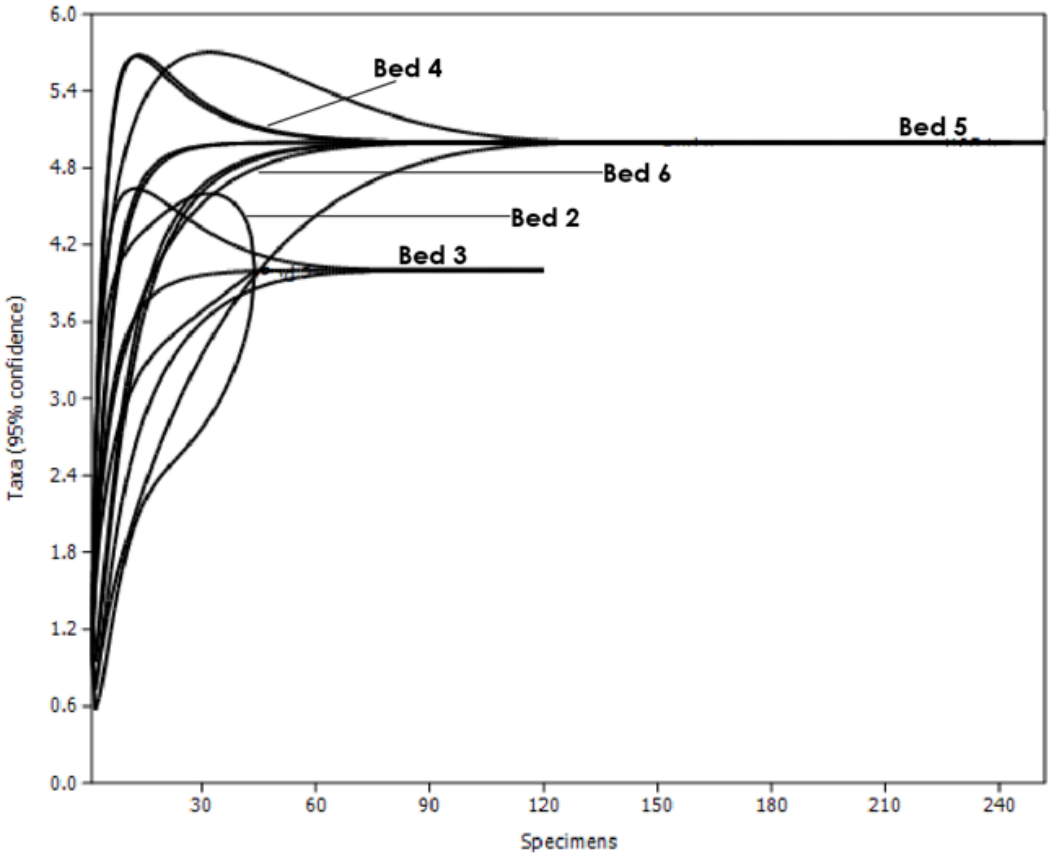

Appendix T
Thaynes Formation
Hidden Pasture, Montana
Rarefaction Curves

Rarefaction curves with 95% confidence intervals for two samples of Early Triassic fauna from the Thaynes Formation at Hidden Pasture, Montana. Each sample represents a bed in which fossilized echinoid material was identified. The faunal composition of each bed was determined through point counts in thin section. Associations which level off indicate that further counts would not significantly increase the number of taxa found within a particular sample. Conversely, associations which have not yet leveled off indicate that further counts may have reveal additional taxa and are, thus, tentative. In all cases at this locality, sample size, or counted specimen, is greater than the number of taxa.

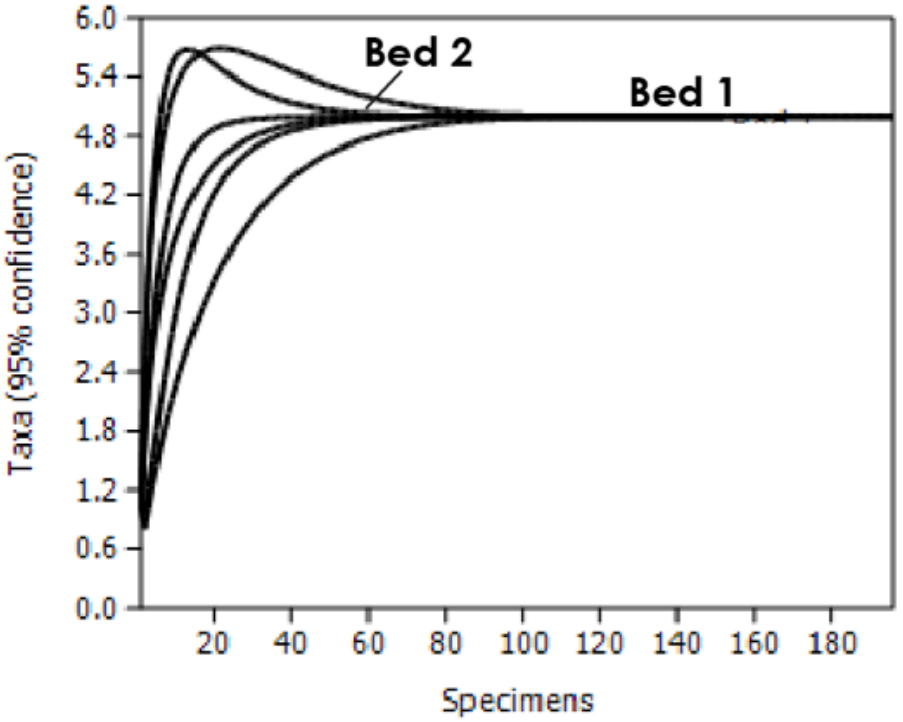

Appendix U
Virgin Limestone Member
White Hills, Utah
Rarefaction Curves

Rarefaction curves with 95% confidence intervals for two samples of Early Triassic fauna from the Virgin Limestone Member of the Moenkopi Formation at White Hills, Utah. Each sample represents a bed in which fossilized echinoid material was identified. The faunal composition of each bed was determined through point counts in thin section. Associations which level off indicate that further counts would not significantly increase the number of taxa found within a particular sample. Conversely, associations which have not yet leveled off indicate that further counts may have reveal additional taxa and are, thus, tentative. In all cases at this locality, sample size, or counted specimen, is greater than the number of taxa.

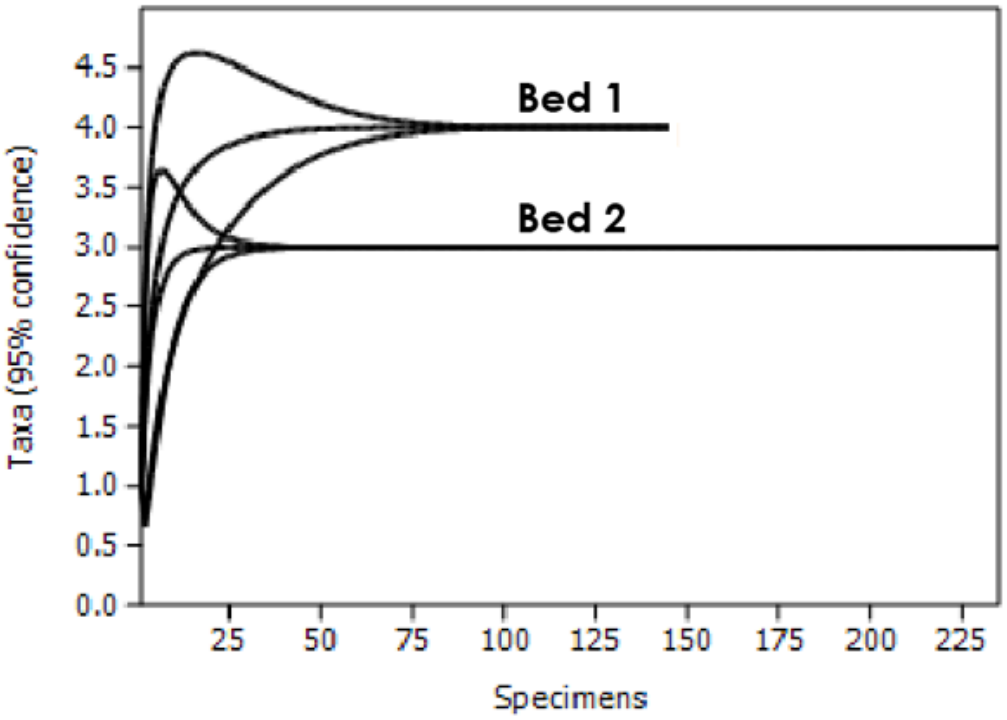

Appendix V
Virgin Limestone Member
Lost Cabin Springs, Nevada
Rarefaction Curves

Rarefaction curves with 95% confidence intervals for two samples of Early Triassic fauna from the Virgin Limestone Member of the Moenkopi Formation at Lost Cabin Springs, Nevada. Each sample represents a bed in which fossilized echinoid material was identified. The faunal composition of each bed was determined through point counts in thin section. Associations which level off indicate that further counts would not significantly increase the number of taxa found within a particular sample. Conversely, associations which have not yet leveled off indicate that further counts may have reveal additional taxa and are, thus, tentative. In all cases at this locality, sample size, or counted specimen, is greater than the number of taxa.